The Phase Inversion-based Coal-CO_2 Slurry (PHICCOS) Feeding System: Design, Coupled Multiscale Analysis, and Technoeconomic Assessment

by

Cristina Botero

Dipl.-Ing., Chemical and Bioengineering,
University of Erlangen-Nuremberg (2007)

Submitted to the Department of Mechanical Engineering
in partial fulfillment of the requirements for the degree of

Doctor of Philosophy

at the

MASSACHUSETTS INSTITUTE OF TECHNOLOGY

February 2014

Author .....
Department of Mechanical Engineering
September 30, 2013

Certified by .....
Ahmed F. Ghoniem
Ronald C. Crane (1972) Professor
Thesis Supervisor

Accepted by .....
David E. Hardt
Chairman, Department Committee on Graduate Studies

The Phase Inversion-based Coal-CO_2 Slurry (PHICCOS) Feeding System: Design, Coupled Multiscale Analysis, and Technoeconomic Assessment

by

Cristina Botero

Submitted to the Department of Mechanical Engineering
on September 30, 2013, in partial fulfillment of the
requirements for the degree of
Doctor of Philosophy

Abstract

The continuous conveying of a solid feedstock like pulverized coal into a pressurized environment is a challenging task required in multiple industrial processes. Plants based on pressurized, entrained-flow gasifiers (EFG) are a good example. EFGs are used to produce synthetic gas for the production of synthetic transportation fuels, chemicals, and for generating electricity in Integrated Gasification Combined Cycle (IGCC) power plants. The latter have also been proposed as an attractive platform for carbon dioxide capture.

Commercially available feeding systems are based on coal-water slurry or lock hoppers. The earlier penalizes the plant efficiency and has feedstock limitations, while the latter is expensive and has pressure limitations. In this work, a coupled multiscale approach is applied, which combines system-level analysis, component-level modeling, and micron-scale particle phenomena, for the development and assessment of a novel coal feeding system.

The proposed Phase Inversion-based Coal-CO_2 Slurry (PHICCOS) feeding system uses supercritical CO_2 with liquid-like density to feed pulverized coal into a high-pressure EFG. The challenge of preparing the coal-CO_2 slurry is addressed using phase inversion: a phenomenon associated with the hydrophobicity of liquid CO_2-coal mixtures. This allows for operation at ambient temperature and without the use of lock hoppers. Furthermore, the PHICCOS feeding system achieves very high feed pressures while reducing the moisture and ash content of the feedstock, which makes it especially attractive for low-rank and high-ash coal.

The merits of the PHICCOS feeding system were demonstrated through techno-economic analysis coupled with particle-level kinetics. The results of this work show the significant advantages of this system over alternative technologies, in particular for low-rank feedstock. Optimization was used to determine the operating conditions

required for the best tradeoff between kinetics, thermodynamics, and costs. The effect of the uncertainty in critical design and operating parameters on the overall economics of a PHICCOS-fed plant were examined using Monte Carlo simulations.

This work shows that the PHICCOS system can efficiently and economically feed pulverized coal into high-pressure reactors in plants equipped with carbon capture. Overall, the economics of the PHICCOS feeding system are better than those of commercial technologies for low-rank coal and are competitive with other solutions for high-rank coal. Furthermore, PHICCOS has unique operational advantages related to the very high feed pressures it can achieve and to its feedstock flexibility: cheap and widely available high-moisture and high-ash coal can be used to produce high value products.

Key words: Coal, CCS, Gasification, Feeding System, Multiscale Analysis

Thesis Committee:

Ahmed F. Ghoniem
Ronald C. Crane (1972) Professor of Mechanical Engineering, MIT

Howard J. Herzog
Senior Research Engineer, MIT Energy Initiative

Randall P. Field
Executive Director of the Conversion Research Program, MIT

John G. Brisson
Professor of Mechanical Engineering, MIT

Paul I. Barton
Lammot du Pont Professor of Chemical Engineering, MIT

Acknowledgments

I am greatly thankful to my Thesis Supervisor, Prof. Ahmed Ghoniem, for his advice, but most importantly for believing in me, for giving me absolute research freedom, and for always questioning my findings and pushing for me to go beyond my comfort zone.

My deepest gratitude to Howard Herzog, my Coadvisor, who supported my work unconditionally and broadened by experience at MIT by exposing me to the world of climate policy and to multiple industrial partners.

This work would not have been possible without the support from Randall Field, whose mentorship, thoroughness, and technical depth were an indispensable component of my PhD. Randy helped me find my way in times of stagnation, gave me recognition with my sponsors, and provided me feedback when I most needed it.

I am very grateful to Prof. John Brisson and Prof. Paul Barton for being part of my PhD Thesis committee and for making this work better through their feedback and interest. Many thanks also to the people at MIT who in one way or another contributed to the technical content of my work, especially Navid Seifkar, Prof. Janos Beer, Simcha Singer, Lei Chen, Rory Monaghan, Srinivas Seethamraju, Andrew Adamczyk, Santosh Shanbhogue and Rob Brasington. I would also like to highlight the fantastic job of MIT Libraries, especially when it came to finding very old and remote documents, that were absolutely crucial to this work. Thanks also to the people external to MIT who helped me make a reality check on my research, especially Neville Holt and Jeff Phillips (EPRI), Temi Linjewile (TECO), Daniel Roberts and David Harris (CSIRO), Dale Simbeck (SFA Pacific), as well as to John Gulen and Gary Leonard (GE) for their valuable career advice.

Special thanks to BP for funding this work, in particular to Mark Sankey and Merion Evans, for the technical discussions, and to George Huff, Andrew Cockerill, and Mark Howard, for their interest in my work and for the professional opportunities they have trusted me with. Thanks also to Aspen Tech for the simulation software and outstanding technical support.

To those who inspired me and pushed me to come to MIT, my eternal admiration and gratitude, as well as to the people without whom I would not have survived here, especially my friends Alex, Erell, Coco, Aziz, Tito, Rodrigo, Nick, Sergio, Xime, and Tony/MIT Women's Volleyball Club. Thanks also to my labmates, especially to those whom I was lucky to get to know a bit better: Kushal, John, Konna, Richie, Christos, Addison, Zhenlong, and Nwike. Many thanks also to Leslie Regan for always helping when needed, as well as to Lorraine and to my friend and motherly figure at MIT, Mary Gallagher.

Finally, I would like to thank my family for their unconditional love and support, and for being an inspiration to work hard, be humble, never stop learning, and value all that life has given me. Lastly, to Jorge, who above everyone else has witnessed my successes and failures and has lifted me in times of crisis and felt proud of me regardless. This work would have never been finalized without his willingness to understand and deal with the more difficult aspects of a PhD and of my personality. My achievements are half his.

Contents

List of Figures

List of Tables

Chapter 1

Introduction

This chapter presents the theoretical background, motivation, and goal of the present work, together with an outline of its structure.

First, the fundamentals of coal gasification for the conversion of carbonaceous fuels into marketable products of higher value is discussed. The importance of coal as a feedstock is highlighted. This is followed by a short overview of the fundamentals of gasification thermochemistry. The main applications of this technology are then presented, together with its synergies with carbon capture.

Pressurized, entrained-flow reactors are introduced as the dominating technology for large-scale applications. The challenge of feeding coal into a high pressure environment is then discussed and the coal-CO_2 slurry feeding system is presented as an alternative to commercial feeding systems in plants with carbon capture. The chapter concludes with an outline of the structure of this thesis.

1.1 Gasification of Coal

Gasification is a thermochemical process used to convert any carbonaceous material into a gaseous product with a usable heating value. It takes place at high temperatures of typically above 800 °C and in the presence of steam and/or CO_2, as schematically illustrated in Figure 1-1.

Unlike combustion, gasification takes place in an oxygen-lean environment. The

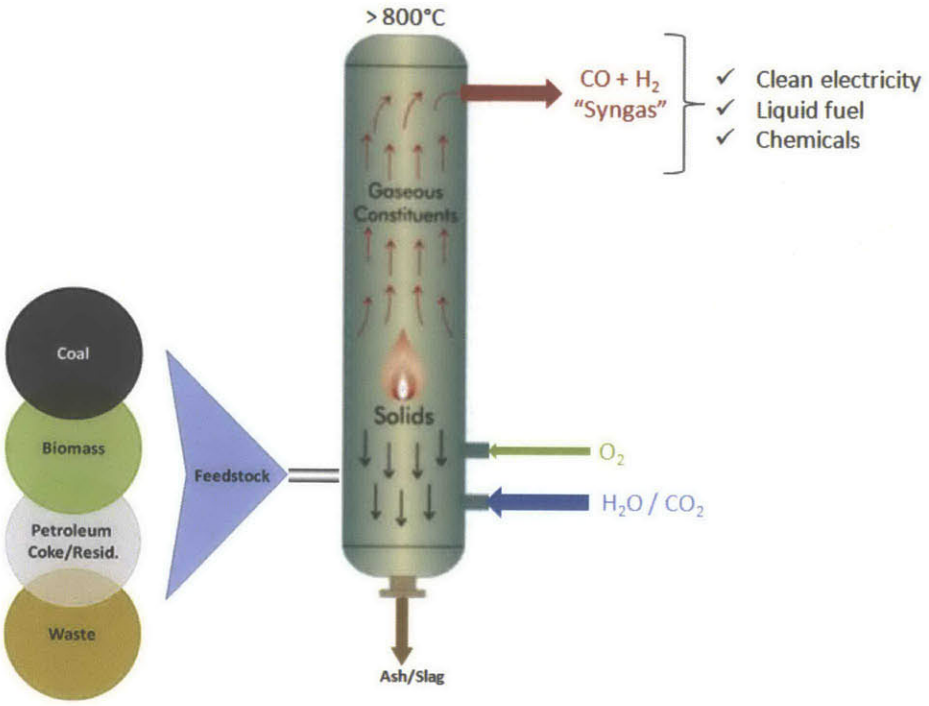

Figure 1-1: Schematic of gasification and its applications.

product, known as synthesis gas (syngas), is composed mainly of CO, H_2, and some minor byproducts. It can be used as fuel to generate electricity or steam, as a basic chemical building block for a large number of uses in the petrochemical and refining industries, and for the production of hydrogen. Gasification adds value to low-value feedstocks by converting them to marketable fuels and products [1].

The applications of gasification can be broadly divided into synthetic fuels, chemicals, and electricity. The latter is produced by feeding syngas to the gas turbine of a combined cycle power plant, an arrangement known as an Integrated Gasification Combined Cycle (IGCC) power plant.

The range of specific products that can be obtained through gasification is illustrated in Figure 1-2. It is is very broad and extends from bulk chemicals like ammonia and methanol to industrial gases. Furthermore, the immediate syngas products can be used as intermediates for higher value products such as acetates and polyurethanes [2].

The conversion of coal into syngas through gasification was first commercialized in the early 19th century by the London Gas, Light and Coke Company for the produc-

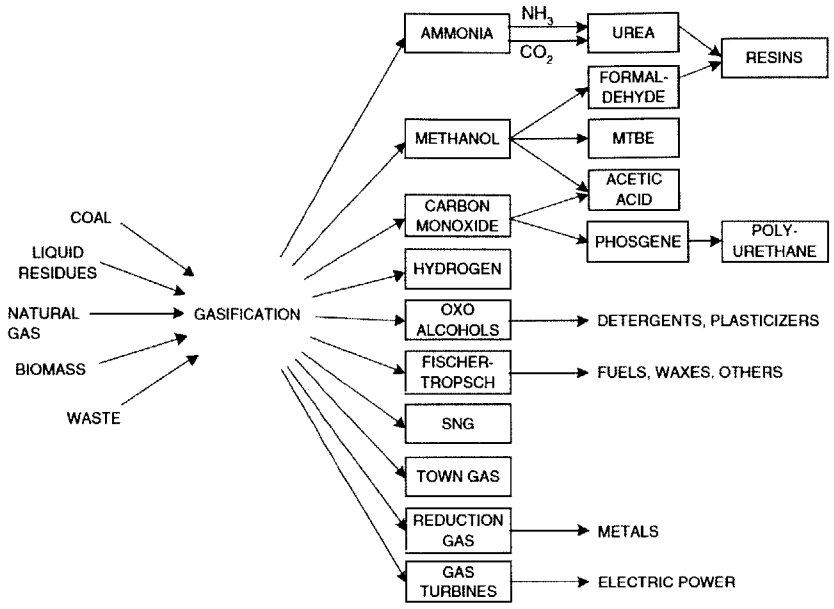

Figure 1-2: Range of products that can be obtained through gasification [3].

tion of town gas for lighting, heating, and cooking. Fully continuous, oxygen-blown processes were only developed after Carl von Linde commercialized the cryonenic separation of air during the 1920s. These were the forerunners of many of the commercial units which exist today. Gasification was used extensively by the Germans during World War II to convert coal into transportation fuels via the Fischer-Tropsch process [1, 3, 4].

The Sasol Corporation in South Africa played a key role in the development of gasification processes for the conversion of coal to hydrocarbon liquids (CTL), i.e. for manufacturing synthetic petroleum products and chemical feedstocks. Today, Sasol is a key supplier of chemicals manufactured from coal. As of 2010, the company operated three plants that produce the equivalent of over 195,000 barrels of fuel and petrochemicals per day (an excess of 40% of South Africa's liquid fuel requirements) and was collaborating with the Shenhua Group in China to develop two CTL plants there, each capable of producing 80,000 barrels per day of synthetic liquid fuel [2].

In the USA, Eastman Chemicals has operated a coal-to-chemicals plant in Kingsport, Tennessee, for over 20 years, producing syngas and converting it to various acetyl chemicals. Similarly, the Great Plains synfuel plant in North Dakota produces more

than 145 billion Nm^3 per year of natural gas, as well as other chemicals, from coal [2]. Furthermore, the 260 MW Tampa Polk IGCC power station has been producing electricity commercially from coal since 2006 [5].

As shown in Figure 1-3, the world syngas generation capacity has been growing steadily in the last century and is expected to continue doing so. Coal is by far the dominating feedstock. As of 2010, there were 412 gasifiers worldwide in 133 plants producing a total syngas output of almost 71 GW_{th} [6].

1.1.1 Coal as Feedstock

Coal not only dominates the gasification landscape but its worldwide consumption is also the fastest-growing of all fossil fuels. Driven predominantly by China, in 2012 coal reached the highest share of global primary energy consumption (29.9%) since 1970 [7].

Coal has by far the largest reserves-to-production ratio of any fossil fuel: world proven reserves in 2012 were sufficient to meet 109 years of global production. Unlike oil, coal reserves are very well distributed worldwide, mostly between Europe & Eurasia (35%), Asia Pacific (31%) and North America (29%) [7]. Furthermore, as shown in Figure 1-4, a large fraction of these reserves consists of cheap, low-quality material with a very high moisture content (low-rank coal) or a very high ash content (low-grade coal).

The importance of low-quality coal has emerged in recent years. High quality coal reserves are are depleting, as these are preferentially mined. Mining operations must be undertaken in increasingly deeper coal seams with greater difficulties and higher costs. Furthermore, the utilization of vast reserves of low-quality coal could be of vital importance to both energy security and economic development in countries where these coals are the only indigenous resource [9].

However, the undesirable properties of low-quality coals make their utilization challenging. Besides a high moisture and/or ash content, these include low calorific value, aggressive ash characteristics, and a low Hardgrove Grindability Index. Processes for drying, cleaning, and upgrading of low-quality coal are of great importance

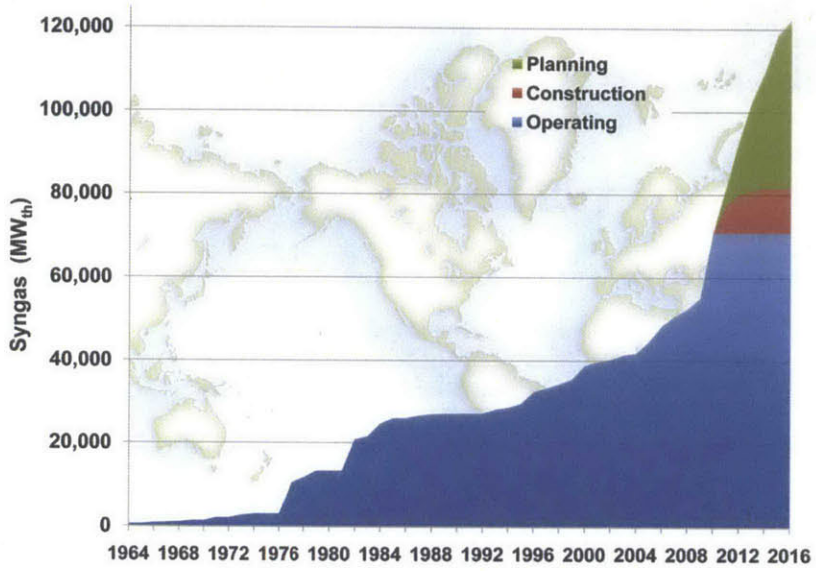

(a) Cumulative by year

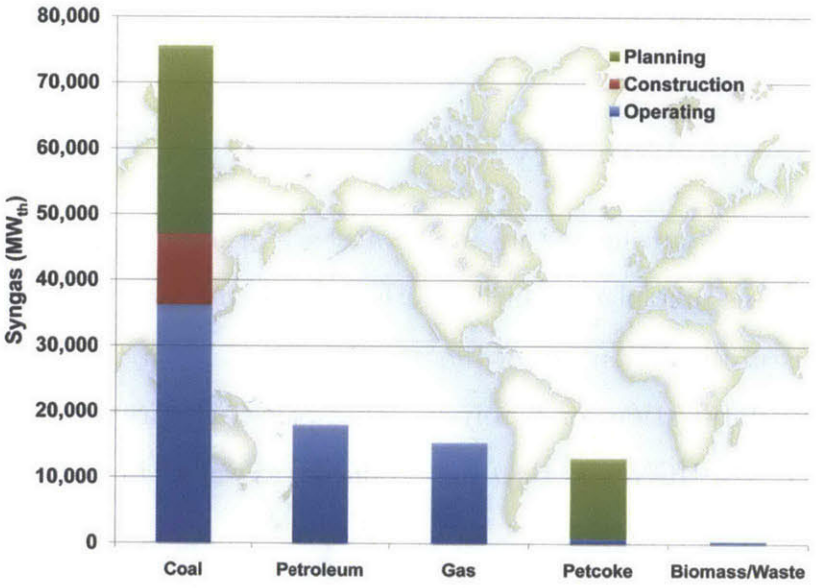

(b) By feedstock

Figure 1-3: World gasification capacity and planned growth [6].

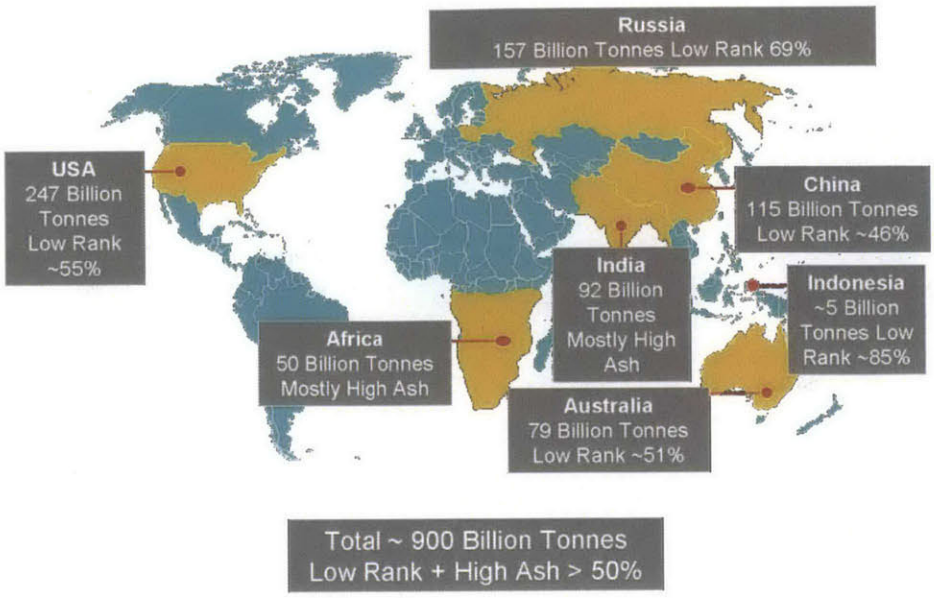

Figure 1-4: Contribution of low-quality coal to large coal reserves worldwide [8].

for increasing its use and making it cleaner, safer for transport and storage, and more valuable as an export fuel. A number of processes of this kind have been developed in Australia, Germany, the USA, and Japan [9].

1.1.2 Thermochemistry

When coal particles are heated up in the absence of oxygen, a number of thermochemical processes take place, which together are often referred to as *gasification.*

First, moisture is driven out of the coal particles and, at temperatures of about 350-800°C, devolatilization, or pyrolysis, takes place. A variety of gases, including CH_4, CO, CO_2, H_2, HCN, and H_2O are produced, as well as hydrocarbon liquids and tars.

The subsidence of tars and hydrocarbon liquids in the gasifier depends on the temperature and heating rate. These products are highly undesirable, since they condense in the low-temperature zones of downstream equipment, clogging gas passages and leading to system disruptions [10].

At temperatures of about 800 °C and higher, the devolatilized coal, referred to as *char*, undergoes the actual gasification reactions. The most important ones are the

steam-gasification and the CO_2-gasification (Boudouard) reaction:

$$C_{(s)} + H_2O \rightleftharpoons CO + H_2 \qquad +131\,\text{MJ/kmol} \qquad \text{(I)}$$

$$C_{(s)} + CO_2 \rightleftharpoons 2CO \qquad +172\,\text{MJ/kmol} \qquad \text{(II)}$$

respectively [3]. The heats of reaction are given above and the positive sign indicates that the reactions are endothermic.

While O_2 is not required for the gasification reactions, in practice oxygen is added to the gasifier in order to cover its thermal energy requirements. Exothermic oxidation reactions such as:

$$C_{(s)} + \tfrac{1}{2}O_2 \rightarrow CO \qquad -111\text{MJ/kmol} \qquad \text{(III)}$$

$$CO + \tfrac{1}{2}O_2 \rightarrow CO_2 \qquad -283\text{MJ/kmol} \qquad \text{(IV)}$$

$$H_2 + \tfrac{1}{2}O_2 \rightarrow H_2O \qquad -242\text{MJ/kmol} \qquad \text{(V)}$$

enable the reactor to operate at autothermal conditions. They provide the thermal energy necessary a) for the endothermic pyrolysis and gasification reactions, b) to heat up the reactants, and c) to make up for any heat losses to the environment. This is schematically illustrated in Figure 1-5.

Apart from the char gasification and oxidation reactions, the water-gas shift (WGS) reaction also plays an important role inside the gasifier [3]:

$$CO + H_2O \rightleftharpoons CO_2 + H_2 \qquad -41\text{MJ/kmol.} \qquad \text{(VI)}$$

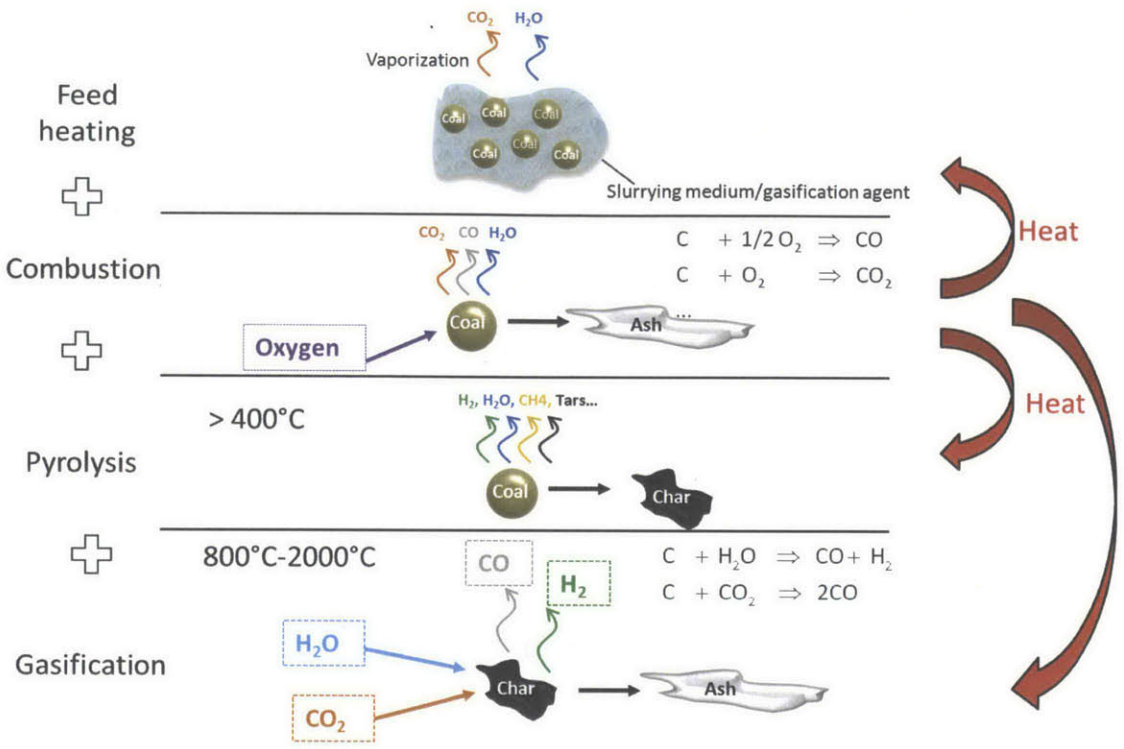

Figure 1-5: Main processes ocurring during autothermal gasification.

Gasifier Cold Gas Efficiency

The cold gas efficiency (CGE) is the most commonly used measure of gasifier performance. It is defined as the fraction of the feedstock's chemical energy that is recovered in the cooled gaseous product. It is calculated from the heating value and mass flow ($\dot{m}$) of the gasifier feed and product gas streams, according to:

$$CGE = \frac{(\dot{m}_{\text{gas}})\,(HHV_{\text{gas}})}{(\dot{m}_{\text{feed}})\,(HHV_{\text{feed}})}, \tag{1.1}$$

where a higher heating value (HHV) basis has been used.

The CGE has a thermal and a kinetic component. The thermal component is an indication of how energy-intensive the reactor is, i.e. how much feedstock must be oxidized -rather than gasified- in order to maintain autothermal operation. In eq. (1.1), the thermal performance is contained in the heating value of the gas, since oxidation products have a negligible heating value.

Feedstock heating is a major loss of thermal performance in an EFG due to its

high operating temperature. This is especially problematic for gasifiers operating with water slurry feed, due to the high heat capacity and vaporization enthalpy of H_2O, see Section 1.2.1.

The kinetic component of gasifier performance is a measure of how fast the chemical reactions are. It can be quantified through the fraction of carbon that is converted to gas, also known as carbon conversion, and is contained in $\dot{m}_{\text{gas}}$ in eq. (1.1).

Note that just like the HHV of the produced gas is not a direct indication of carbon conversion, the latter says nothing about the characteristics of the product: a carbon conversion of 100% could mean that the entire feedstock has been oxidized to CO_2, producing a gas with no heating value. Hence, neither the thermal performance nor the kinetic performance alone is sufficient to characterize gasifier operation. The CGE includes both components and is hence a much more attractive performance measure than carbon conversion or syngas heating value.

A high gasifier CGE leads to a reduction in both the solid fuel consumption and the power consumption of the Air Separation Unit (ASU) delivering O_2. Since both of these directly benefit the plant efficiency, achieving high cold gas efficiencies is key for maximizing overall plant performance. In addition, lower O_2 consumption rates can significantly reduce the capital costs of the plant. The production and supply of oxygen is not only very energy-consuming but also capital-intensive. The ASU alone accounts for about 15% of the total capital cost of an IGCC power plant [11].

1.1.3 Gasification and Carbon Capture

Gasification-based processes add value to heavy carbonaceous feedstocks, such as coal, by increasing their (H/C) atomic ratio to obtain a lighter product with a higher market value, such as hydrogen or synthetic gasoline. H/C ratios of typical carbonaceous materials are presented in Table 1.1.

Because a net removal of carbon from the system is often required, gasification-based processes are an ideal platform for carbon capture. The H/C ratio of the syngas is first adjusted by converting CO to CO_2 and H_2 via the water-gas shift reaction, eq. (VI). This is followed by separation -or capture- of CO_2, for which

Table 1.1: Hydrogen/carbon atomic ratio of typical carbonaceous materials [4].

Material	H/C ratio
Coke	0.13
Anthracite	0.38
Bituminous coal	0.80
Lignite	0.86
Heavy and residual oil	1.41
Wood	1.44
Crude oil	1.71
Methane	4.00
Hydrogen	∞

commercial solvent-based processes such as Selexol or Rectisol can be used. Many other technologies for CO_2 capture are currently being studied and developed [12].

The captured CO_2 can be compressed and stored underground, in which case the process is referred to as carbon capture and storage (CCS). It can also be used for enhanced oil recovery (EOR) or simply vented to the atmosphere. The latter option is environmentally undesirable given the high global warming potential of CO_2. With the low price of CO_2 today, however, CO_2 venting in gasification-based plants is common practice. Rising CO_2 prices due to high demand for EOR and/or environmental regulations may encourage plant operators to deal with the CO_2 differently in the future .

1.1.4 Gasification Technologies

Gasification reactors, or gasifiers, can be broadly classified as moving-bed[1], fluidized-bed, and entrained-flow reactors. These are schematically illustrated in Figure 1-6, together with their corresponding characteristic temperature profile along the gasifier height.

Moving-bed Gasifiers

In moving-bed gasifiers, a bed of coal enters the reactor from the top and slowly moves downward under the influence of gravity. The gas flows counter-currently, as

[1]Also known as fixed-bed to differentiate from fluidized-bed reactors

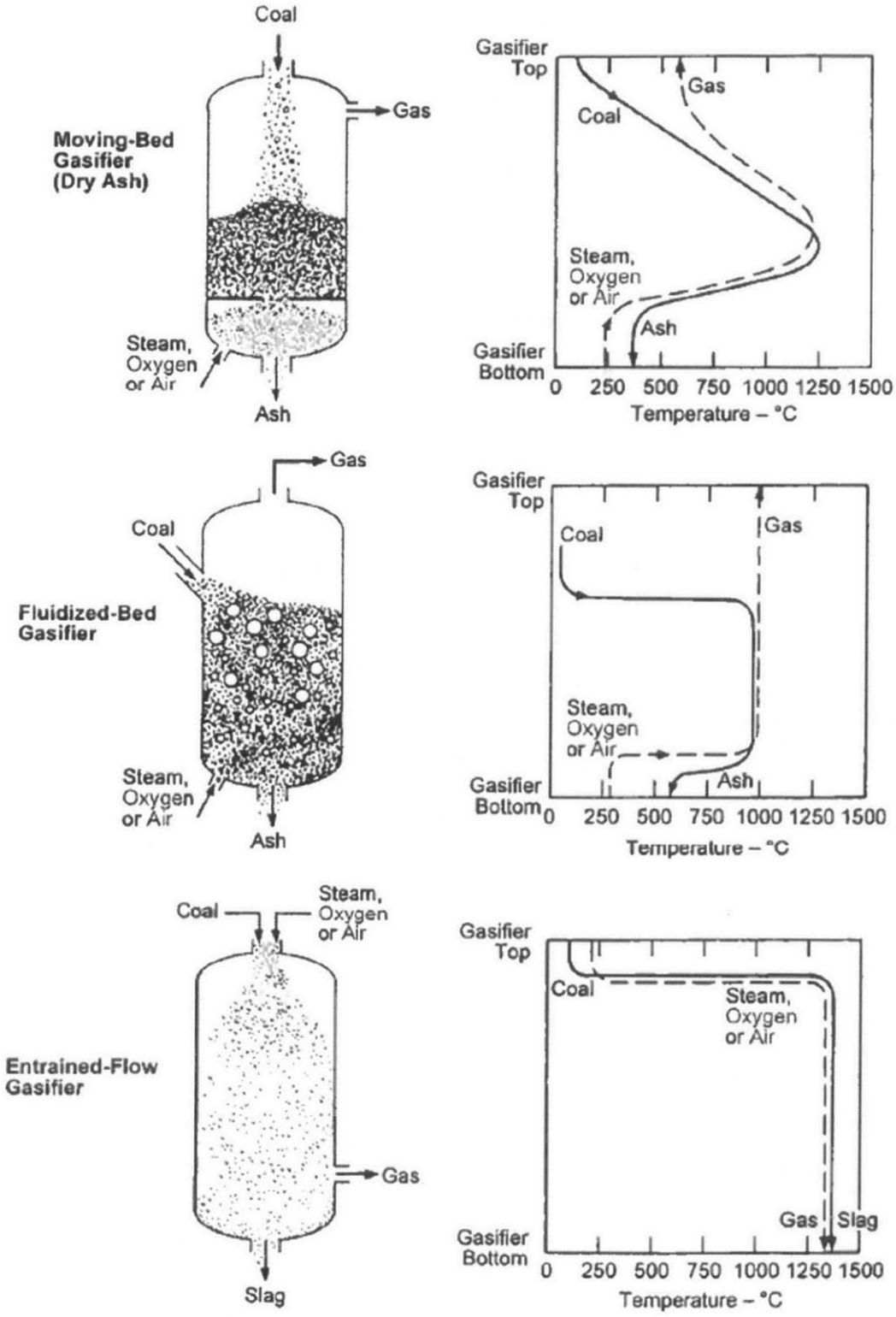

Figure 1-6: The three major types of reactors used for gasification [13].

illustrated in the top section of Figure 1-6.

Oxygen consumption is very low with this flow arrangement since the feedstock is dried and heated up by the hot syngas at the top of the reactor. In turn, the syngas exit temperature is generally low, even if high temperatures are present in the heart of the gasifier. This is particularly true for high-moisture feedstock such as low-rank coal. The gas outlet temperature can vary from an estimated 540°C for bituminous coal feedstock to about 315°C for lignite [14].

Pyrolysis products are still present in the product gas of this reactor type, given the flow arrangement. Direct quenching with recycle water is commonly used to condense the tars and oils as byproducts.

Moving-bed gasifiers pose limitations on the properties and size of the feedstock that can be used. Coal in the size range 5-80 mm is required [15]. In order to avoid blockage, excessive amounts of fines should be avoided, in particular if the coal has relatively strong caking properties. In fact, heavily caking coals cannot be processed in this type of reactor and mildly caking ones require the assistance of a stirrer.

Both slagging (i.e. melted ash) and non-slagging (i.e. solid ash) operation is possible. Excess steam must be added in the latter case to keep the temperature below the ash softening point. Lurgi produces slagging and British Gas Lurgi (BGL) non-slagging versions of this unit type.

Fluidized-bed Gasifiers

Fluidized-bed reactors like that shown in the mid-section of Figure 1-6 provide thorough mixing, thus offering very good heat and mass transfer characteristics. However, this also limits the achievable carbon conversion inside the gasifier, since some of the feedstock that has not fully reacted yet is inevitably mixed with the ash and thus removed prematurely.

Low temperatures typically below 900°C are required inside the reactor, since ash slagging must be avoided for proper bed fluidization. They are accordingly best suited for very reactive feedstocks such as low-rank coals and biomass.

As with any fluidized-bed reactor, particle sizing is critical for the fluidization

behavior of the bed; sizing in the range 6-10 mm is common for this reactor type [3, 14]. Fines introduced with the feed or produced through shrinkage of larger particles during gasification become entrained in the hot syngas and leave the bed overhead. In order to keep carbon conversion high, these are either burnt in a separate combustion unit or partially recovered in a cyclone and recycled to the reactor.

While gasifiers of this type have historically been operated in the stationary fluidized-bed regime, more recent developments have shifted to circulating and transport designs. Fluidized-bed gasification technology has been commercialized by the Gas Technology Institute (GTI), Winkler, Kellog-Rust Westinghouse (KRW), Foster Wheeler, and Kellog, Brown and Root (KBR), among others.

Entrained-flow Gasifiers

In entrained-flow gasifiers (EFG), the feedstock and gas react co-currently, as illustrated in the lower part of Figure 1-6. This type of reactor has a high load capacity since its residence time is only of a few seconds.

The feedstock must be pulverized to less than about 100 μm to ensure adequate mass transfer and entrainment of the solids in the gas. In addition, very high temperatures of about 1300°C and higher are required to ensure proper conversion in such a short residence time. This also guarantees that the reactor operates above the slagging temperature, at which point the ash has a fully liquid behavior and can be removed from the system reliably [3].

Pressurized entrained-flow gasifiers are popular for large-scale applications, since this type of reactor allows for the production of very large flows of gas in a relatively compact vessel. The high operational temperatures lead to nearly complete carbon conversion and a essentially no methane or other hydrocarbons are produced. Entrained flow gasifiers hence have fundamental advantages over fluidized-bed and moving-bed gasifiers: the syngas product contains no hydrocarbon liquids and the only solid waste is an inert slag [14].

Nonetheless, a high oxygen demand is characteristic for this reactor type, given its elevated operating temperature. This is especially true for coals with a high

moisture or ash content, which explains why entrained-flow reactors are not common for processing such feedstocks, which otherwise pose no specific technical limitations in entrained-flow gasifiers [3].

Entrained flow gasifiers are commercialized by Conoco-Phillips, General Electric (GE), Shell, Prenflo, Mitsubishi Heavy Industries (MHI), and Siemens, among others.

1.1.5 Gasification at High Pressure

The gasifier pressure is usually determined by the requirements of downstream processes. For IGCC, syngas at a pressure of 20-30 bar is sufficient with current gas turbine technology. For other processes, such as methanol or ammonia synthesis, much higher pressures of 50-200 bar are necessary [3].

The economic optimum gasifier pressure depends on the application and on the feeding system characteristics. High gasifier pressures favor process economics by reducing the size of the required equipment. The process efficiency also benefits since it costs less energy to compress the feed than to compress the syngas.

The advantages of gasifying at high pressure are such that all modern processes operate at pressures of at least 10 bar and up to 100 bar. According to Higman [3], most of the advantages of high-pressure operation are already obtained when gasifying at a pressure of 15-25 bar. However, this is largely because pressurizing a solid to higher pressure becomes too complicated and expensive with currently available technologies.

The development of efficient, cost-effective feeding systems for high-pressure gasifiers could lead to a significant improvement in the economics of this technology. It is especially important for chemical applications, which operate at very high pressures and currently dominate the gasification market [6, 16].

1.2 Commercial Coal Feeding Systems

Feeding solid fuel feedstock like pulverized coal into a pressurized vessel is a challenging task since, unlike liquids or gases, solids cannot be pressurized. Hence, the

transport of solids to a high-pressure environment can only be achieved with the help of a liquid or gaseous continuous phase.

For large-scale EFGs operating at pressures of 10 bar and above, two commercial feeding systems are available, as shown in Figure 1-7: coal-water slurry (CWS) feed and dry feed based on lock hoppers. The feeding system selected by original equipment manufacturers of high-pressure EFGs differ from manufacturer to manufacturer: GE and Conocco Phillips use water slurry feed, whereas Shell, Prenflo, MHI, and Siemens all utilize dry feed based on lock hoppers.

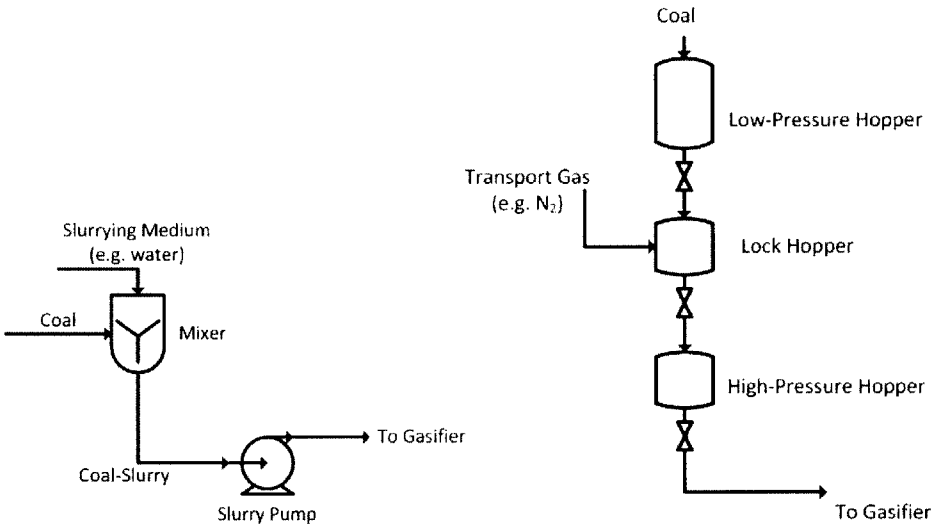

(a) Coal slurry feed (b) Lock hopper system

Figure 1-7: Commercial high-pressure coal feeding systems.

1.2.1 Coal-Water Slurry Feed

In the CWS feeding system, pulverized coal is suspended in water and the suspension, or slurry, is pumped to a high pressure and injected into the gasifier through a slurry atomizer. Very small droplets are desirable, since droplet size has an inverse correlation with carbon conversion [17].

CWS feed is very attractive due to the high pressures it can achieve and, more importantly, because it employs relatively compact and simple equipment. However, CWS-fed gasifiers suffer from a low cold gas efficiency, and hence high oxygen con-

sumption.

The low efficiency can be attributed mostly to the use of water as slurrying medium. The slurry contains significantly more water than that required for the steam gasification reaction [18]. Due to its high high heat capacity and latent enthalpy of vaporization, water is a large thermal load. An estimated 5,600 kJ are required to heat up and vaporize each kilogram of H_2O inside the reactor, as shown in Figure 1-8.

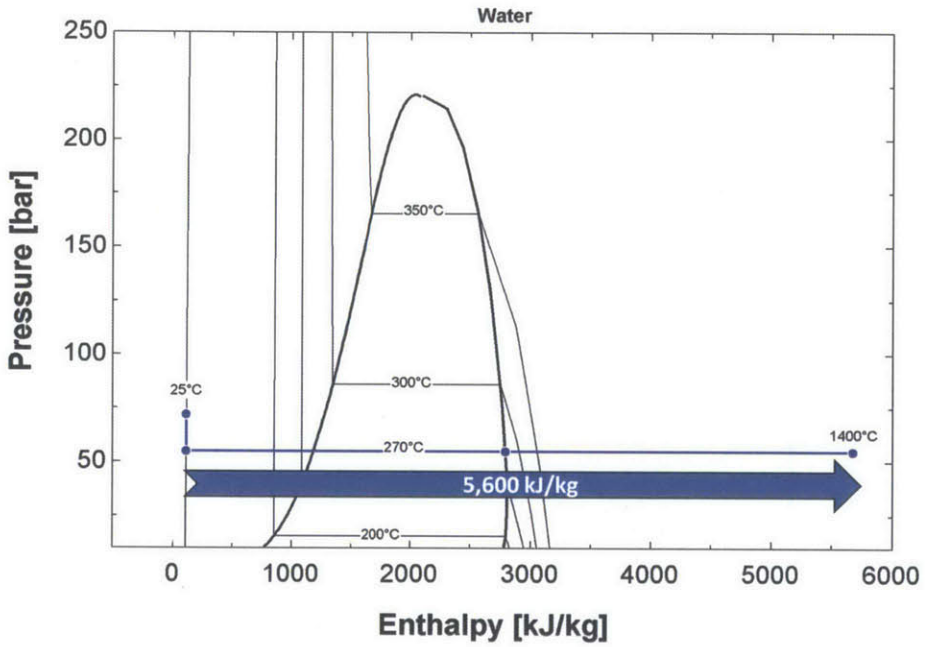

Figure 1-8: Pressure-enthalpy diagram of pure H_2O. State points for the transition from subcooled liquid to superheated vapor at representative gasifier conditions are shown.

Slurrying the feed with water hence comes at the expense of a higher feedstock consumption for a given syngas output, and, most importantly, a larger need for the supply of oxygen. Because oxygen production with current cryogenic technology consumes electricity, recovery of the thermal energy contained in the gasifier products cannot make up for this investment.

Despite its low efficiency, the low capital investment of CWS feed makes it the most economic alternative for feeding high-rank coal such as bituminous coal [19]. For low-rank coal like lignite, whose moisture content can be in excess of 30%, the

system efficiency becomes unbearably low and CWS feed is uneconomical. This is because the feedstock moisture does not contribute to the transport properties of the slurry but only adds to the flow of water entering the gasifier.

Slurry Loading

Among the most important characteristics of coal slurry is its solids loading, X_{sol}, which is used to quantify the percentage of dry solids it contains. It is defined as the weight percent (%-wt.) of moisture-free coal in the slurry and is also referred to as the dry solids content:

$$X_{\mathrm{sol}} = \frac{\dot{m}_{\mathrm{coal}}(1 - X_{\mathrm{m}})}{\dot{m}_{\mathrm{coal}} + \dot{m}_{\mathrm{SM}}}. \tag{1.2}$$

Here, X_{m} is the mass fraction of moisture in the coal and $\dot{m}_{\mathrm{coal}}$ and $\dot{m}_{\mathrm{SM}}$ are the mass flows of as-received coal and of slurrying medium, respectively. The slurrying medium does not include coal moisture.

The slurrying medium provides the lubricating effect necessary for slurry fluidity. Hence, a maximum solids loading exists, which depends on the feedstock and slurrying medium characteristics. It is limited by the maximum viscosity allowable for slurry transportation and pumping, which is about 1000 cp with current technology [20, 21]. The maximum solids loading is an important variable, since it determines the minimum flow of slurrying medium fed to the gasifier and thus the minimum thermal load imposed by the feeding system.

Experimental measurements by Atesok et al. showed that the maximum dry solids loading in coal-water slurry varies strongly with coal rank, but the maximum coal loading does not [21]. The term coal loading, X_{coal}, is used when the coal moisture is included in the loading definition:

$$X_{\mathrm{coal}} = \frac{\dot{m}_{\mathrm{coal}}}{\dot{m}_{\mathrm{coal}} + \dot{m}_{\mathrm{SM}}} = \frac{X_{\mathrm{sol}}}{1 - X_{\mathrm{m}}}. \tag{1.3}$$

Unless otherwise indicated, the terminology *slurry loading* used throughout this work

refers to the definition in (eq. 1.3).

For a given average particle size, it was observed that the maximum X_{coal} remains more or less constant for all coals. For 50 μm particles, for example, Atesok's measurements show that the coal loading is within the narrow range 63-66% for coals ranging from bituminous to lignite and moisture contents from 4% to 16%.

As a first order approximation, thus, the maximum X_{coal} can be considered independent of the rank-specific surface properties of the coal.

1.2.2 Dry Feed based on Lock Hoppers

Lock hopper-based dry feeding systems are sluicing systems that use an inert gas as the continuous phase. They generally consist of three vessels that are situated vertically above one another and separated from each other by valves, see Figure 1-7. The top hopper is at atmospheric pressure, the middle one is the actual lock hopper, and the bottom one can be a storage vessel at an elevated pressure [3].

A gas at pressure, such as N_2 or CO_2, is used to build pressure in the lock hopper and transport the solid to the bottom hopper and to the reactor. Alternated opening and closing of valves is used to assist the process.

The feedstock must be dried to about 5-10% moisture in order to achieve good flow characteristics in the lock hoppers. As a result, this feeding system has a higher efficiency, and hence better feedstock flexibility, than slurry feeding systems. It constitutes the most economic option for feeding low-rank coal [11]. Typical gasifier cold gas efficiencies are in the range 69-77% for the case of single-stage water slurry feed and 78-83% for dry feed, on a higher heating value (HHV) basis [22]. A resulting net IGCC efficiency benefit of an estimated 3%-points has been predicted for dry-fed systems in plants operating on bituminous coal without CO_2 capture [11].

However, dry feeding systems are very costly. The coal preparation and feeding system of a dry-fed gasifier has been estimated to cost about three times that of the corresponding equipment for a slurry-fed design in an IGCC plant of equal electrical output [11]. In addition, dry feeding systems are operationally more complex and become increasingly unreliable and inefficient at pressures beyond 30-40 bar, since

the amount of transport gas becomes very high [3, 16].

The ability of dry feeding systems to economically utilize low-rank coal has, nonetheless, proved to be such a key customer requirement that at least two parallel research projects are currently underway for the design and development of a dry solids pump [23, 24].

This pump, if successfully developed, would benefit from the feedstock flexibility of the dry feed and from the cost and reliability advantage of a pump, relative to a set of lock hoppers. In addition, the dry solids pump would be able to achieve high pressures. Pratt & Whitney Rocketdyne (PWR), whose gasification technology is envisioned to operate at over 80 bar, is funding the largest research effort in this field [25]. However, the mechanical challenges associated with the design of a solids pump are significant. It is yet to be seen whether a reliable, cost effective, scalable solution will become a feasible alternative.

1.3 Coal-CO_2 Slurry Feed

The possibility of using CO_2 as a liquid carrier for slurry-fed gasifiers has been suggested in the past as a means of achieving the efficiency of dry feeding systems with the low cost, reliability, and feedstock flexibility of slurry feeding [3, 26, 27].

Liquid CO_2 -or supercritical CO_2 with liquid-like density- is available in plants with carbon capture and can be used to prepare a coal slurry, which can be pumped to any high-pressure process. This is schematically illustrated in Figure 1-9.

Because coal is a carbon-intensive fuel, large flows of CO_2 are available for preparing coal-CO_2 slurry if the entire carbon content of the fuel is converted to CO_2. This is the case of an IGCC plant with carbon capture, where CO in the syngas is typically shifted completely to CO_2. Figure 1-10 shows that in this case, recirculation of about 20% of the captured CO_2 is, in average, enough to achieve the a coal slurry loading of 70 wt.-%, which is a fairly typical value for CWS.

The numbers in the figure assume that the carbon content of the fuel is converted completely to CO_2 and that 90% of the CO_2 is captured. In practice, depending on

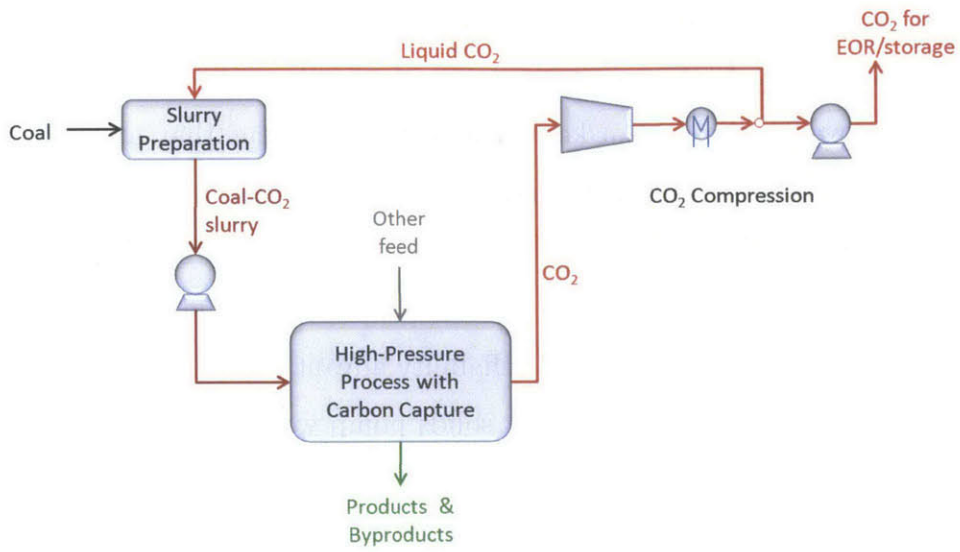

Figure 1-9: Schematic of coal-CO_2 slurry feed for feeding coal to high-pressure reactors in plants with carbon capture.

how the coal-CO_2 slurry is prepared and on the actual flow of CO_2 captured, a larger recirculation of CO_2 may be required.

1.3.1 Properties of CO_2

The properties of CO_2 are compared to those of H_2O in Table 1.2 at conditions representative of pressurized EFG operation. With a 10-times lower vaporization enthalpy and up to 50-times lower viscosity than water, CO_2 has a set of thermophysical properties which appears to be more adequate for coal slurries than water.

Liquid Viscosity

Because CO_2 has an order of magnitude lower viscosity than H_2O, CO_2 slurry is expected to have a lower viscosity than water slurry for the same coal loading and otherwise identical conditions. For lignite dried to 11% moisture, experimental investigations have reported achievable coal loadings of up to 88%-wt. in liquid CO_2 (78% dry solids) [33]. More recent studies have, nevertheless, cast doubts on these findings, concluding that coal loadings of about 80% (71% dry solids) seem more realistic [34].

The low viscosity of coal-CO_2 slurry is also expected to benefit the slurry atom-

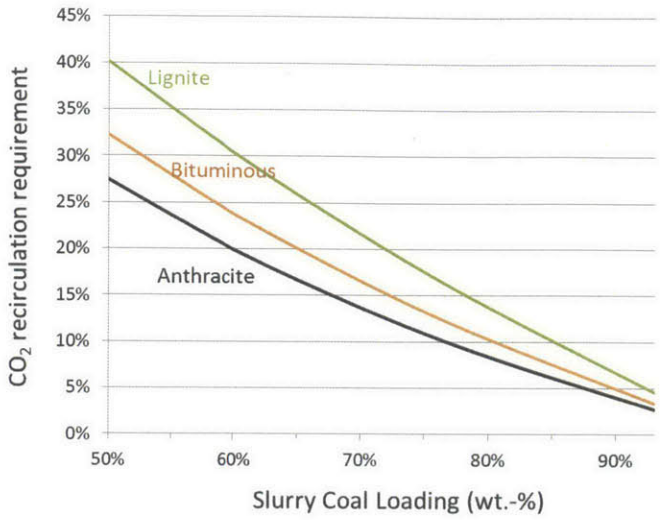

Figure 1-10: Fraction of captured CO_2 that must be recirculated for preparing coal-CO_2 slurry feed, as a function of slurry loading and for different coals. Complete conversion of carbon in the fuel to CO_2 and 90% CO_2 capture were assumed.

Table 1.2: Properties of pure H_2O and CO_2 at representative slurry and gasifier conditions [28–32].

	H_2O	**CO_2**
Critical Temperature	374 °C	31 °C
Critical Pressure	221 bar	74 bar
Slurry *(25°C, 72 bar)*		
Liquid Viscosity	0.89 cP	0.06 cP
Liquid Density	1,000 kg/m^3	752 kg/m^3
Gasifier[a] *(55 bar)*		
Surface Tension	47·10^3 N/m	1.4·10^3 N/m
Heat Capacity of Liquid	4.6 kJ/(kg K)	4.2 kJ/(kg K)
Vaporization Enthalpy	1,605 kJ/kg	146 kJ/kg
Heat Capacity of Vapor	3.6 kJ/(kg K)	2.4 kJ/(kg K)

[a] Properties at average liquid and vapor phase temperatures of 150°C and 840°C for H_2O, and 18°C and 710°C for CO_2, respectively. Isentropic expansion of CO_2 through slurry injector assumed.

ization process directly through the Reynolds' number and indirectly through the critical Weber number for droplet breakup [34].

Enthalpy of Vaporization and Heat Capacity

The enthalpy of vaporization of CO_2 is at least one order of magnitude lower than that of H_2O, which results in a significant reduction of the energy required to vaporize the slurry inside the gasifier. Additionally, the amount of sensible heat that must be provided to the subcooled liquid is negligible, since the CO_2 is either very close to or beyond the saturated liquid line at the gasifier pressure.

This is illustrated in Figure 1-11, where the extreme cases of isentropic and isothermal expansion of the slurry through the injector nozzle are illustrated; in reality, a polytropic change of state is expected. Flash vaporization of the slurry occurs when it enters the gasifier since the pressure inside the reactor is below the saturation value for CO_2 at that temperature.

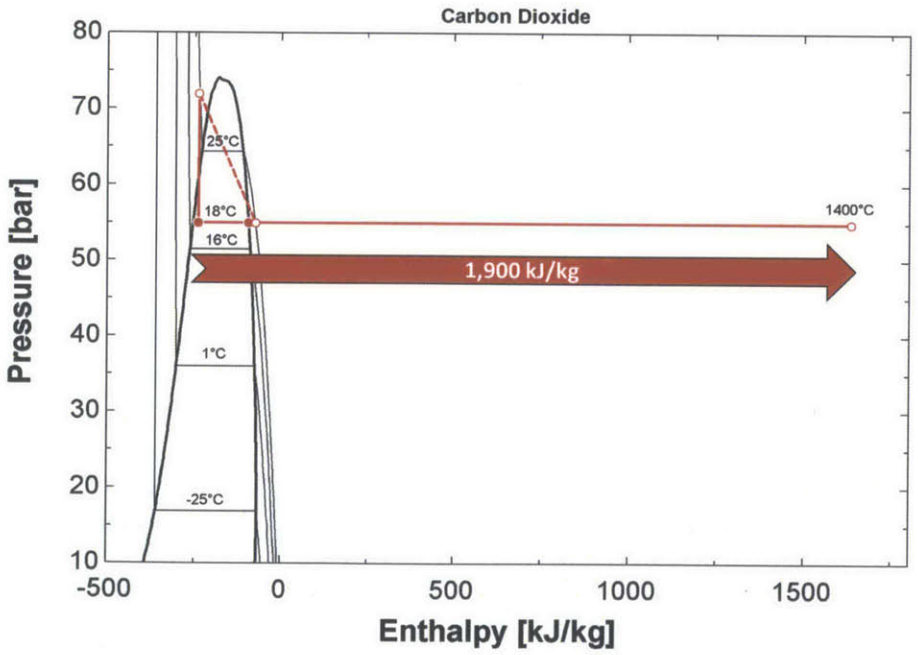

Figure 1-11: Pressure-enthalpy diagram of pure CO_2. State points for the transition from subcooled liquid to superheated vapor at typical gasifier conditions are shown. Both isentropic (—) and isothermal (---) expansion of the slurry during injection to the gasifier are illustrated.

A maximum of 1,900 kJ are necessary to heat up every kg of pure CO_2 to the gasifier temperature; this is about a third of the energy requirement of pure H_2O under identical conditions. This can be attributed to the low vaporization enthalpy of CO_2, but also to the low heat capacity of its vapor phase.

Surface Tension

Surface tension forces at the liquid interface play an important role in both the slurry atomization process and the agglomeration behavior of coal particles at the injector outlet.

The surface tension affects the Weber number directly, which determines the droplet size distribution. The surface tension of CO_2 is over an order of magnitude lower than that of water. It is thus expected that atomizing CO_2 slurry will yield a smaller mean droplet diameter than for water slurry.

In addition, capillary forces between particles are an inverse function of the surface tension. These forces become important when the slurry liquid carrier begins evaporating inside the gasifier and are thought to play a key role in the formation of a self-sustaining agglomerate shell [35]. It is precisely due to this agglomeration that extremely fine grinding of coal is not considered to be beneficial for coal-water slurries, unless the atomizer is capable of producing droplets of about the same size as the coal particles [36]. The effective particle size distribution of coal agglomerates after atomization of the slurry is believed to be determined by the size distribution of the droplets rather than by the initial coal particle size [37].

The low surface tension of CO_2 holds the potential of offering better atomization and agglomeration characteristics for coal slurry, which could increase carbon conversion under otherwise identical conditions. This potentially beneficial aspect of the coal-CO_2 slurry feeding system was not considered in this work.

1.3.2 History of Coal-CO_2 Slurry

Coal-CO_2 slurry was studied extensively in the early 1980's for the transport of pulverized coal through pipelines and as an alternative to oil for firing boilers during a time of high crude prices [38–41]. The study of coal-CO_2 slurry as a way to feed coal to pressurized entrained flow gasifiers was, until very recently, limited to two public studies. Both were conducted in 1986 for the Electric Power Research Institute (EPRI).

The first study was prepared by Arthur D. Little Inc. and focused on the rheology and handling of suspensions of low-rank coal in liquid CO_2. Laboratory and pilot-scale tests showed that coal-CO_2 slurry flow behavior is non-Newtonian and best fits a Bingham plastic model. A maximum solids content of 88 wt.% was achieved for a dried North Dakota lignite at 11 wt. % moisture and 80% minus 170-mesh size consist [33] .

The second study was carried out by Energy Conversion Systems Inc. Here, the thermo-economics of an IGCC plant operating with a lignite-fed GE (formerly Texaco) gasifier were assessed in detail. In view of the high moisture content of lignite coal, alternatives to the coal-water slurry feeding method were studied, among these the coal-CO_2 slurry feed. The study concluded that an IGCC plant with this feeding system has the potential to generate power from lignite more economically than from bituminous coal, given the low cost of the fuel. The study assumed that CO_2 was separated for the sole purpose of preparing the slurry [42].

With global warming now widely accepted as a reality within the scientific community, CCS has been identified as a key technology for significantly reducing CO_2 emissions while allowing fossil fuels such as coal to meet the world's pressing energy needs [43]. Interest in coal-CO_2 slurries has hence been revived, since its economics are favored by the availability of CO_2 in plants with CCS. Recent studies funded by EPRI and conducted jointly with the Dooher Institute of Physics & Energy have revisited and complemented the findings from the 1980's.

The first of these, conducted in 2006, has cast doubts on the ability to achieve the

88 wt. % slurry solids contents reported by Arthur D. Little, claiming 80 wt. % to be a more realistic figure [34, 44]. It also highlights the two orders of magnitude difference in surface tension between liquid CO_2 and water, which is likely to positively affect the atomization properties of coal-CO_2 slurry. Overall, the analysis considers the concept promising, as long as CO_2 capture is an inherent part of the plant operation, and recommends further experimental and computational research work in this area.

Three follow-up studies by the same authors were published in 2009, 2010, and 2012. In the first, rheological test results for a sub-bituminous coal-CO_2 slurry are presented. It concludes that the experiments agree well with theoretical predictions and that suspensions of coal in liquid CO_2 indeed have a lower viscosity than those in water, for the same solids content [45].

In the 2010 study, a flowsheet model was used to simulate an IGCC plant gasifying sub-bituminous coal-CO_2 slurry. Solids loadings of 48% and 55% were assumed in the analyses of water slurry and CO_2 slurry, respectively, based on a combination of rheological testing and modeling using the Dooher Institute Slurry Model (DISM), a physics-based tool developed by the same research group [34, 45]. Furthermore, experiments from a lab-scale drop tube furnace operating with CWS [46] were used to validate the gasifier submodel.

A net plant efficiency increase of 9% (2.8%-points) is reported, relative to a plant with CWS feed, as well as 7%-points higher cold gas efficiency and a 13% lower oxygen-to-coal requirement. The authors recommend experimental testing of CO_2 slurry preparation, rheology, atomization, and gasification to complement existing theoretical findings [46].

In addition to continued rheological testing, EPRI has most recently partnered with Worley Parsons for the design of the coal-CO_2 slurry preparation equipment [47], which has proved to be more complicated than originally thought. Slurry preparation using lock hoppers and cryogenic cooling has been proposed, which could be prohibitively expensive.

1.4 Goal and Structure of this Work

The significant performance improvement reported by EPRI for a plant with CO_2 slurry feed reveals its potential, as well as the need to develop a more fundamental understanding of the differences between water and liquid carbon dioxide as slurrying media and how these may affect individual process units for coals of different rank.

The goal of this work is to conduct a thorough and independent evaluation of the performance and economics of coal-CO_2 slurry for feeding high and low-rank coal to pressurized, entrained-flow gasifiers in plants with carbon capture.

The challenge of mixing coal at ambient pressure with pressurized, liquid CO_2 is addressed by proposing an alternative approach: the Phase Inversion-based Coal CO_2 Slurry (PHICCOS) feeding system. This technology takes advantage of the preferential wetting of the hydrophobic coal surface by CO_2 and the preferential wetting of its mineral impurities by water. It operates at ambient temperature, without the use of lock hoppers, and can achieve very high pressures. Furthermore, PHICCOS inherently reduces the ash and moisture content of the feedstock, which makes it attractive for low-quality coal.

Coupled multiscale analysis is used to study the merits of the PHICCOS feeding system on the plant, component, and particle scales. Its technoeconomics are compared with those of commercial technologies. First, an IGCC plant is used as an example application. The focus then turns to a plant producing clean syngas that can be used for synthetic liquid fuel applications. The study is structured as follows:

- Chapter 2 presents the methodology used for the analysis and introduces the multiscale models on which it is based, together with their coupling strategy.
- In Chapter 3, the preliminary feasibility of coal-CO_2 slurry feed is studied, using an IGCC plant as an example application.
- Chapter 4 studies the impact of finite-rate gasification kinetics on carbon conversion in a coal-CO_2 slurry-fed gasifier.
- Chapter 5 discusses the challenge of mixing coal at ambient pressure with liquid

or supercritical CO_2. The PHICCOS feeding system is presented, together with experimental evidence of phase inversion of coal with CO_2.

- Chapter 6 presents the overall technoeconomics of an IGCC plant with carbon capture and PHICCOS feed and compares them with those of commercial technologies. Thermodynamic, kinetic, economic, and slurry preparation aspects are all considered in the analysis.

- In Chapter 7, CO_2 slurry skimming and steam injection are introduced as ways to address the tradeoff between kinetic and thermal performance in a gasifier with PHICCOS feed. Optimization of the feeding system and gasifier operating conditions is conducted in order to achieve the most attractive plant economics. The focus turns from IGCC to a clean syngas production plant for synthetic fuel applications.

- In Chapter 8, the main uncertain variables of PHICCOS are discussed and quantified. Monte Carlo simulations are conducted to study their effect on the overall cost of producing clean syngas in a PHICCOS-fed plant.

- Chapter 9 presents the conclusions from this study and discusses recommended future work.

Chapter 2

Methodology and Tools

This chapter describes the methodology used to conduct a multiscale analysis of the coal-CO_2 slurry feeding system. First, the main components of the overall analysis are presented, together with their corresponding scales. The general evaluation basis is subsequently defined. Finally, the multiscale models used for the analysis are described in detail, together with the coupling strategy used.

2.1 Methodology

The different aspects of the CO_2 slurry feeding system considered in this work are schematically illustrated in Figure 2-1, together with the corresponding range of scales involved. Plant-level and component-level modeling, together with particle-scale phenomena were used for the analysis. The models were used individually and/or coupled with each other and with a cost model of the plant.

First, a system-level model of an IGCC plant with carbon capture and coal-CO_2 slurry feed was used to evaluate the preliminary feasibility of this feeding system and identify its main merits and challenges.

The effect of CO_2 in the feed on carbon conversion in a gasifier with CO_2 slurry feed was subsequently studied. For this, a reduced order model of the gasifier was used, which includes a high-pressure kinetic submodel and accounts for pore-scale diffusion limitations.

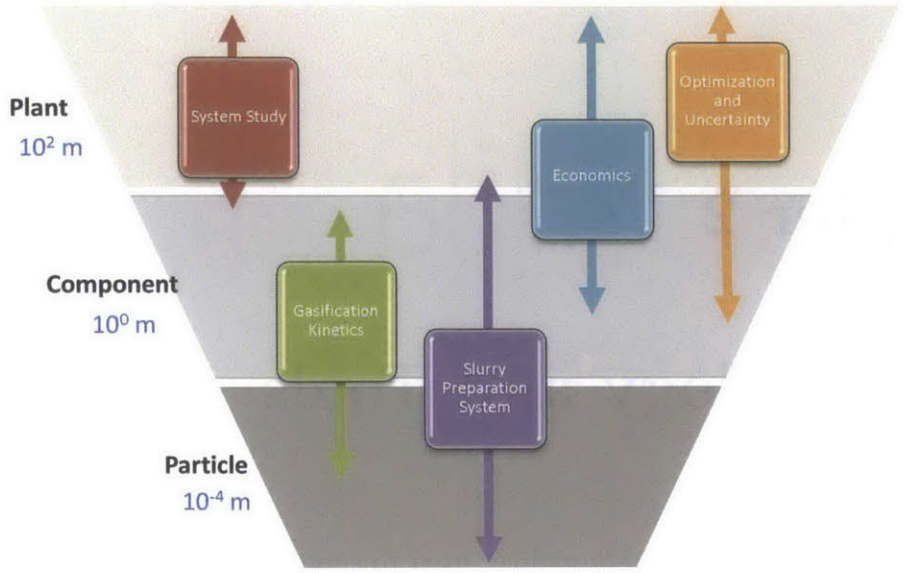

Figure 2-1: Aspects of coal-CO_2 slurry feeding system considered and scales involved.

Next, the coal-CO_2 slurry preparation step of the process was considered in more detail. Particle-scale observations were used to design the PHICCOS preparation and feeding system and integrate this unit it into the plant.

The overall performance and economics of an IGCC plant with carbon capture and PHICCOS feed were subsequently quantified under consideration of the kinetic and slurry preparation aspects identified earlier. For this, the gasifier model was coupled with the IGCC plant model and with a component-by-component cost model of the system.

Finally, the operating conditions of the gasifier and feeding system were optimized, using overall plant economics in a syngas production plant as a target. Furthermore, the uncertainty in the cost and performance estimates was evaluated through Monte Carlo simulations.

2.2 General Evaluation Basis

Multiscale modeling and simulation was used to generate material and energy balances for each case studied. These provide a design basis for estimating the capital costs of the major pieces of equipment in the plant, as well as of the operating costs of the system.

The general evaluation basis common to all cases studied is described here. Any differences to the assumptions listed in this section are documented in the corresponding section of this thesis.

2.2.1 Coal Characteristics

CWS feeding of low-rank coal would result in an extremely high oxygen consumption in a single-stage EFG due to the high moisture content of this feedstock. In the case of CO_2 slurry feed, however, the thermal burden of slurry water has been eliminated so more moisture can be tolerated. Low-rank coals are thus expected to benefit the most from a CO_2 slurry feed. Furthermore, low-rank coal is, in general, very appealing due to its low cost, availability and, in the case of Powder River Basin (PRB) coal, low sulfur content.

In order to cover a wide range of coal ranks, both high-rank and low-rank coals are considered throughout the entire study. Their proximate and ultimate analyses are presented in Table 2.1. Lignite and sub-bituminous coal have a high moisture content of up to 36%, relative to that of bituminous coal, which is only 11%. The possibility of feeding these low-rank coals with their as-received (ar) moisture content (i.e. without drying) is one of the merits of the coal-CO_2 slurry feeding system. This has been achieved in the past with CWS only in two-stage gasifiers [19, 22].

For all slurry-fed cases considered, hence, as-received moisture is assumed. Retaining the coal moisture not only simplifies the feedstock preparation system, but can be beneficial in the case of CO_2 slurry, where coal moisture is the only source of H_2O entering the gasifier. The moisture helps increase the content of H_2 in the syngas and also carbon conversion. The effect of H_2O on the kinetics of a coal-CO_2

Table 2.1: Proximate and ultimate analyses of coals studied (dry basis) [11, 19, 48].

Rank	**Bituminous**	**Sub-bituminous**	**Lignite**	
Seam	*Illinois # 6*	*PRB*	*Beulah-Zap*	*North Dakota*
	Proximate Analyses (weight %)			
Moisture (ar)	11.12	28.09	32.24	36.08
Ash	10.91	8.77	9.72	15.43
Volatile Matter	39.37	44.73	44.94	41.49
Fixed Carbon	49.72	45.87	44.54	43.09
HHV, kJ/kg	30,506	27,254	25,588	24,254
	Ultimate Analyses (weight %)			
Carbon	71.72	68.43	65.85	61.88
Hydrogen	5.06	4.88	4.36	4.29
Nitrogen	1.41	1.02	1.04	0.98
Chlorine	0.33	0.03	0.04	0.00
Sulfur	2.82	0.63	0.80	0.98
Ash	10.91	8.77	9.72	15.43
Oxygen	7.75	16.24	18.19	16.44

slurry-fed gasifier are discussed in Chapters 4 and 7.

2.2.2 Slurry Loading

A constant coal loading of 71% was used for CWS for all coals. This value corresponds to that reported by NETL for bituminous coal-water slurry [19] and was assumed to be independent of coal rank, see Section 1.2.1. The corresponding dry solids loading for coals of different ranks is presented in Table 2.2. They agree well with those observed in the Polk IGCC Power Station for bituminous coal slurry as well as those reported by ConocoPhillips for bituminous, PRB, and lignite coals [19, 49–51].

Table 2.2: Dry solids loading (wt.-%) of CWS and coal-CO_2 slurry. The as-received coal-loadings are 71% and 80%, respectively. All coals contain their as-received moisture content.

	Bituminous	Sub-bituminous	Lignite
Coal-water slurry	63%	51%	48%
Coal-CO_2 slurry	71%	58%	54%

For liquid CO_2 slurry, the maximum coal loading was assumed to be a nominal 80% for all coals. The corresponding dry solids content in CO_2 slurry is presented

in Table 2.2 for the as-received coals considered in this study. The assumed loading is based on recent assessments [34, 44] and is considered more realistic than the 88% (78% dry solids) reported by Peirson et al. in their experimental measurements of coal-CO_2 slurries [33].

2.2.3 Gasifier Characteristics

A pressurized entrained-flow gasifier resembling GE design was used throughout this study as a platform to evaluate the coal-CO_2 slurry feeding system. The GE design is schematically illustrated in Figure 2-2 in its two variants. The term gasifier is often used to include the vessel that contains both the actual gasifier (i.e. the reactor) and the syngas cooler, as shown in the figure.

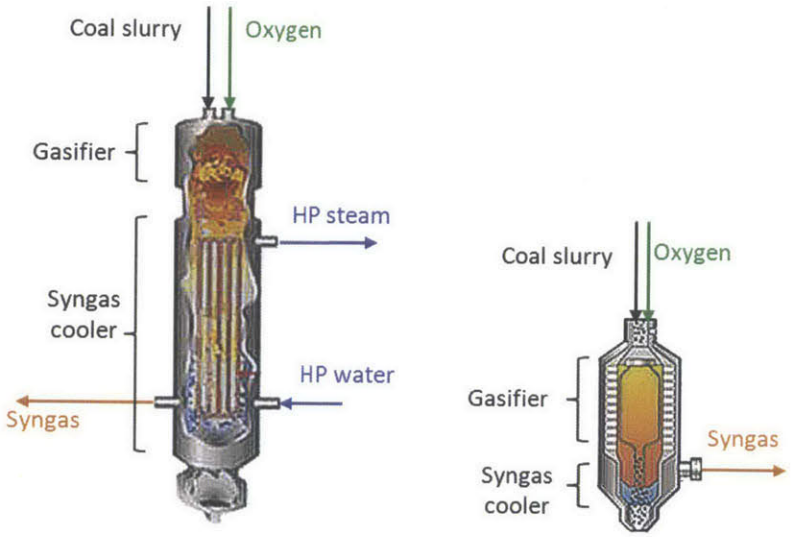

(a) Radiant-quench cooling (b) Full-quench cooling

Figure 2-2: GE gasifier with radiant or full-quench cooling.

Gasifier

The gasifier is a slurry-fed, downflow, single-stage entrained-flow reactor. It is oxygen-blown and the reactor shell is an uncooled refractory-lined vessel. The slurry feed is introduced, together with the oxygen, through the feed injector (burner), which is located centrally at the top.

The main characteristics of the gasifiers considered are summarized in Table 2.3. They resemble the 900 ft^3 and 1,800 ft^3 reactors used in the Cool Water IGCC demonstration project [52] and in the Tampa Polk IGCC power station [19, 49], respectively.

Table 2.3: Characteristics of gasifiers studied [19, 49, 52–54].

	Cool Water Gasifier	**Tampa Polk Gasifier**
Feeding system	Slurry feed	Slurry feed
Volume	26 m^3 (900 ft^3)	51 m^3 (1,800 ft^3)
Diameter	2.4 m	3.0 m
Pressure	30 bar	56 bar
Throughput (HHV)	320 MW_{th}	850 MW_{th}
Reference outlet temperature		
Bituminous coal	1,443°C	1,397°C
Lignite	–	1,300°C
Reference carbon conversion		
Bituminous coal	96.5%	98.0%
Lignite	–	99.9%

It is important to note that the reactor volume in Table 2.3 refers to the reaction zone only, i.e. it does not include syngas cooling. Furthermore, it refers to the tangent-to-tangent section, as indicated in Figure 2-3. The nominal volume does not include the top and bottom hemispherical sections of the gasifier, in agreement with pressure vessels sizing conventions [55].

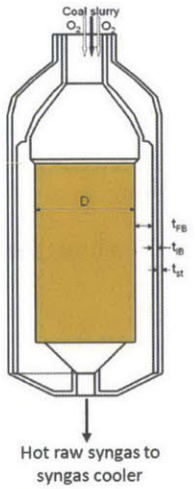

Figure 2-3: Gasifier nominal volume. The hemispherical sections are not included, per convention.

The reference gasifier outlet temperature and outlet conversion in the table cor-

respond to operation with conventional CWS feed and were estimated based on a combination of literature data and reactor modeling. The temperature is that at the outlet of the reaction zone, i.e. entering the syngas cooler.

For bituminous coal, the reference conversion for each gasifier size originates from data for a CWS-fed GE reactor of the same size [19, 49, 52]. The reference temperature is reported for the 1,800 ft^3 reactor and was estimated from the reported oxygen flow rate for the 900 ft^3 one [52]. The gasifier model described in Section 2.3.3 was used for this purpose. The estimated temperature of 1,443°C is somewhat higher than the refractory skin temperature of 1,150-1,400°C near the outlet reported for this reactor [52] and is thus consistent with the expectations.

Lignite was only studied in the 1,800 ft^3 gasifier and no reference conversion data was available for this feedstock in the context of CWS feed. Full conversion was assumed, since reactor modeling with detailed kinetics shows that a conversion of 99.96% is achieved when the gasifier is operated at the minimum outlet temperature of 1,300°C [54] and CWS feed. This temperature is above the minimum required to guarantee proper slag flow and is dictated by the maximum allowable concentration of CH_4 in the syngas [3].

Syngas Cooler

As shown in Figure 2-2, two versions of the GE gasifier are currently offered, one with combined radiant-quench (rad-quench) cooling and one with full-quench (FQ) gas cooling. The earlier includes a radiant heat exchanger, which produces steam that can be exported e.g. for the bottoming cycle of an IGCC plant. In the full-quench design, the hot syngas is cooled down through direct contact with water in a water bath.

The GE full-quench gasifier is the simplest and most inexpensive design on the market [3]. It has taken precedence over the more expensive radiant-quench configuration [1]: the radiant cooler alone has been reported to represent as much as 10% of the total capital cost in an IGCC plant [13]. Furthermore, FQ cooling produces syngas which is fully saturated with water, which makes it especially attractive in

plants with carbon capture, where high concentrations of water are desirable for the water-gas shift reaction.

Hence, a full-quench cooled reactor was considered throughout the majority of this study. Combined radiant-quench cooling was only considered in the feasibility stage.

2.2.4 Main Cases Studied

Table 2.4 presents a summary of the main cases studied throughout this work. The table does not include cases that were considered only during the feasibility stage, i.e. sub-bituminous coal feed and radiant-quench syngas cooling.

Table 2.4: Main cases studied. The performance and costs were estimated through modeling and simulation (✓) or from the literature sources indicated. The asterisk (*) indicates the most economic commercial technology for each feedstock [11, 19].

	Coal	Feeding system	Gasifier	Performance model	Capital costs	Cost model
*	Bituminous	CWS	GE-FQ	✓	[19]	✓
	Bituminous	PHICCOS	GE-FQ	✓	[19, 56]	✓
	Bituminous	Dry	Shell	[19]	[19]	✓
	Lignite	CWS	GE-FQ	✓	[11]	✓
	Lignite	PHICCOS	GE-FQ	✓	[11, 56]	✓
*	Lignite	Dry	Shell	[11]	[11]	✓

Rad-quench cooling was not studied in more details since it is too expensive, in particular for applications with carbon capture [18]. The properties of sub-bituminous coal, on the other hand, lie between those of bituminous coal and lignite. It was considered sufficient to study the latter two in order to cover the entire range of coal ranks of interest.

State-of-the-art technologies with which the proposed feeding system competes are also considered in this work for comparison. The selected alternatives are those which yield the lowest cost of electricity in an IGCC plant with carbon capture according to NETL's assessments of commercial gasification technologies for IGCC [11, 19]. These were used extensively as a reference throughout this study. For bituminous coal, a

GE gasifier with CWS feed is currently the cheapest option, whereas a Shell gasifier with dry feed is the most attractive one for lignite [11, 19].

As indicated in Table 2.4, the performance of all slurry-fed cases (CWS, PHICOS) was estimated through modeling and simulation. This allows for a fair comparison between both slurry feeding systems. Dry-fed cases were not modeled and have been included in the results, where appropriate, for comparison purposes only. The performance of these was taken from the literature. Note, however, that the same capital cost source as well as the same cost model were used for all cases in order to guarantee consistency in the economic assumptions.

2.2.5 Applications Considered

This work studies coal-CO_2 slurry feed as applied to gasification-based plants with carbon capture. Both an IGCC plant and a plant producing clean syngas ready for synthetic fuel production via Fischer Tropsch (FT) are considered. The main characteristics of these two plants are listed in Table 2.5.

The coal-CO_2 slurry feeding system is, nonetheless, applicable to any plant in which pulverized coal must be fed to a high-pressure environment and where CO_2 is, or can be made, available. High-pressure oxyfuel combustion plants, for example, could also benefit from this technology.

IGCC Plant with Carbon Capture

A schematic of an IGCC power plant with carbon capture and coal-CO_2 slurry feed or conventional CWS feed is presented in Figure 2-4. The characteristics of the plant correspond to a large extent to those in *Cases 2/2a* of NETL's assessment of commercial gasification technologies for IGCC [11, 19].

Pressurized coal slurry is injected into the gasifier, together with O_2 produced in an air separation unit. The hot syngas generated in the gasifier is cooled down and cleaned of particulates and other minor species. Its CO content is subsequently converted to CO_2 through reaction with H_2O in a WGS reactor. Next, CO_2 and H_2S

Table 2.5: Main characteristics of gasification-based plants studied.

	IGCC	Clean Syngas Production
Feedstock		
Coal composition	as-received (see Table 2.1)	
Feeding system	Coal slurry at 72 bar	
Solids loading	See Table 2.2	
Gasifier		
Type	Entrained-flow	
Stages	1	
Outlet temperature	1,300-1,700°C	
Pressure	56 bar	
Oxidant	95 %-vol. O_2 at 68 bar	
Oxidant supply	ASU: 1,370 kJ_{el}/kg	
Heat losses	1% of HHV	
Syngas cooling	Radiant-quench ($\Delta T_{eq.}$ = -200K)	
	Full-quench ($\Delta T_{eq.}$ = -10K)	
WGS Reactor		
Number of stages	2	1
Shift steam	H_2O:CO = 2:1	30% excess (molar)
Product composition	H_2:CO ≈ 60	H_2:CO = 2
AGR Unit		
Solvent	Selexol	Selexol
H_2S removal	99.6%	99.6%
CO_2 capture	90% (overall)	90% (local)
Power Island		
Steam turbine	12.4 MPa/538 °C/538 °C	–
Condenser pressure	51 mm Hg	–
Syngas diluent	N_2	–
Gas Turbine	Advanced F-class	–
Fuel Gas HHV	4.8 MJ/Nm^3	–
ASU integration	none	
CO_2 compression		
Compressor		
Number of stages	7	
Stage pressure ratio	1.5-2.5	
Intercooler temperature	30 °C	
Outlet pressure	80 bar	
Isentropic efficiency	η_s = 85%	
Pump		
Outlet pressure	153 bar	
Isentropic efficiency	η_s = 75%	

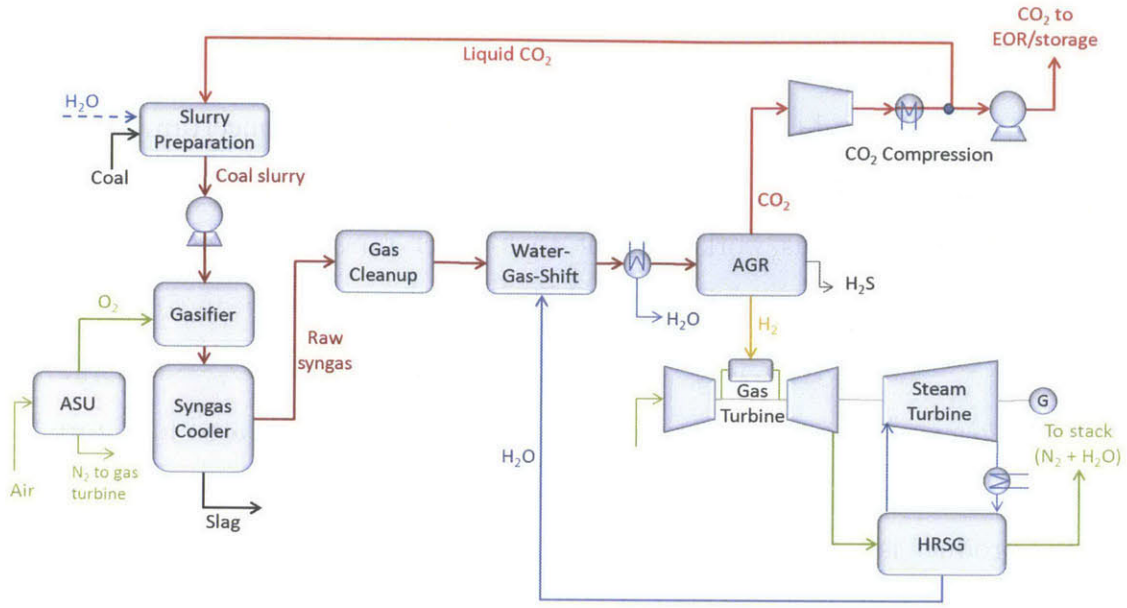

Figure 2-4: Schematic of IGCC power plant with coal-CO_2 slurry feed. Conventional coal-water slurry feed is also shown.

are separated from the gas in an Acid Gas Removal (AGR) unit.

The decarbonized syngas is diluted with N_2 from the ASU before being combusted in a gas turbine (GT), which produces most of the power in the IGCC plant. The gas turbine exhaust is used to produce steam in a heat recovery steam generator (HRSG) and is subsequently released to the atmosphere. Steam is delivered to process units which require it, such as the WGS reactor, and to a steam turbine (ST), which produces additional electric power in the plant.

The CO_2 captured in the AGR unit is brought to a pressure of 153 bar through a combination of intercooled compression and pumping. If the plant has a CO_2 slurry feed system, a fraction of the dense-phase CO_2 is recirculated back to the slurry preparation unit. For plants operating with water slurry, the entire CO_2 stream is sent for storage.

The CO_2 used for the slurry has liquid-like density and is close to its critical point; the exact conditions of the recirculated stream determine whether it is in its liquid or supercritical phase. The term liquid carbon dioxide is used here to denote dense-phase carbon dioxide at a pressure close to or above the critical pressure and a temperature below the critical point.

Clean Syngas Production Plant

During the final stages of this work, i.e. for the optimization and uncertainty analysis, the focus turns from IGCC to a more general clean syngas production plant. This makes the findings of this work relevant to a wider range of applications, i.e. to any plant that requires clean syngas, including IGCC, chemicals, or synthetic fuel production.

The syngas production plant considered is schematically illustrated in Figure 2-5. It is almost identical to the IGCC plant, except that it contains no power island, since the product is clean syngas, rather than electricity. Furthermore, as indicated in Table 2.5, the raw syngas is shifted to a H_2:CO ratio of only 2.0. A single-stage WGS reactor is hence sufficient.

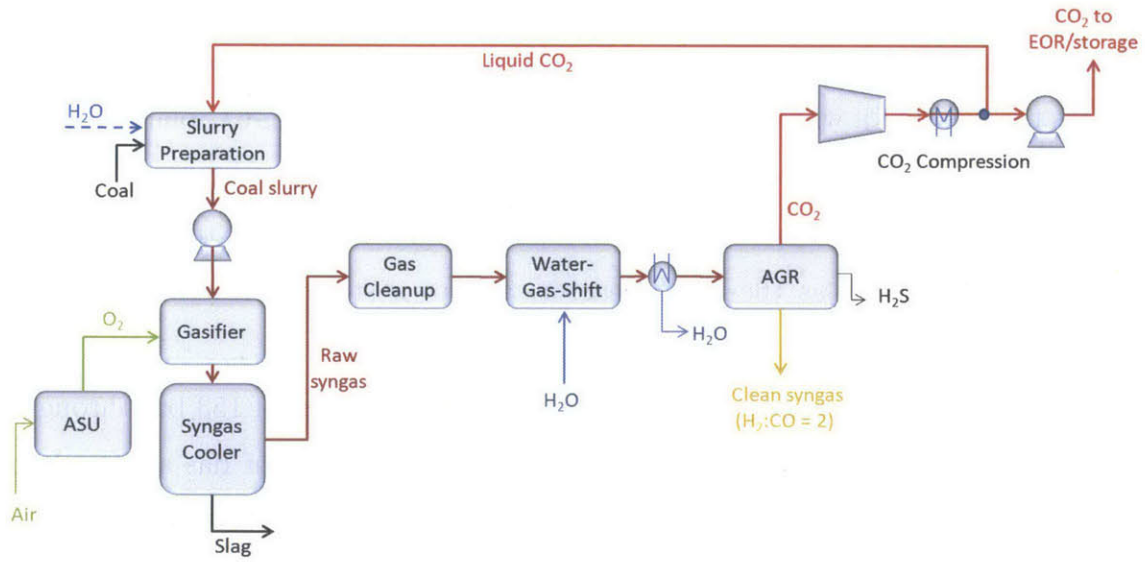

Figure 2-5: Schematic of syngas production plant with coal-CO_2 slurry feed. Conventional coal-water slurry feed is also shown.

Note that clean syngas for other applications, such as chemicals, could also be produced in this plant by adjusting the WGS operation to yield a different H_2:CO ratio.

2.3 Multiscale Models

Two detailed plant-level models, one surrogate plant model, one component-level model including particle-scale phenomena, and one cost model were developed and/or co-developed within the scope of this work. The model hierarchy is schematically illustrated in Figure 2-6.

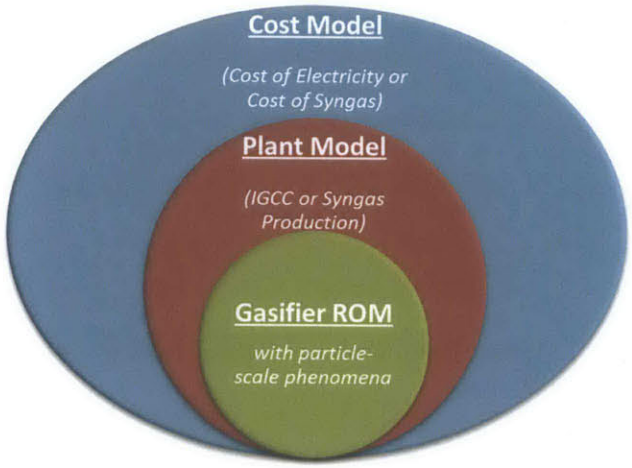

Figure 2-6: Hierarchy of multiscale models.

Some of the models were used on a standalone basis during the initial part of this study. This is the case of the IGCC plant model and the gasifier reduced-order model, which were used by themselves for the feasibility study (Chapter 3) and for the evaluation of gasification kinetics (Chapter 4), respectively.

For the overall economic assessment in an IGCC plant (Chapter 6), as well as for optimization (Chapter 7) and uncertainty quantification (Chapter 8), the multiscale models were coupled in order to capture all the aspects of the feeding system, i.e. gasification kinetics, slurry preparation, plant performance and integration, and costs.

2.3.1 System-level Model of IGCC Plant

The steady-state, system-level model of the IGCC plant was implemented in the process simulation software Aspen Plus (A+) [57]. A screenshot of the model is presented in Figure 2-7. Each of the boxes in the figure corresponds to a hierarchy, or process area, i.e. an A+ submodel consisting of individual unit operations not shown

in the figure. The model is based on that developed by Field and Brasington and has been described in detail elsewhere [58].

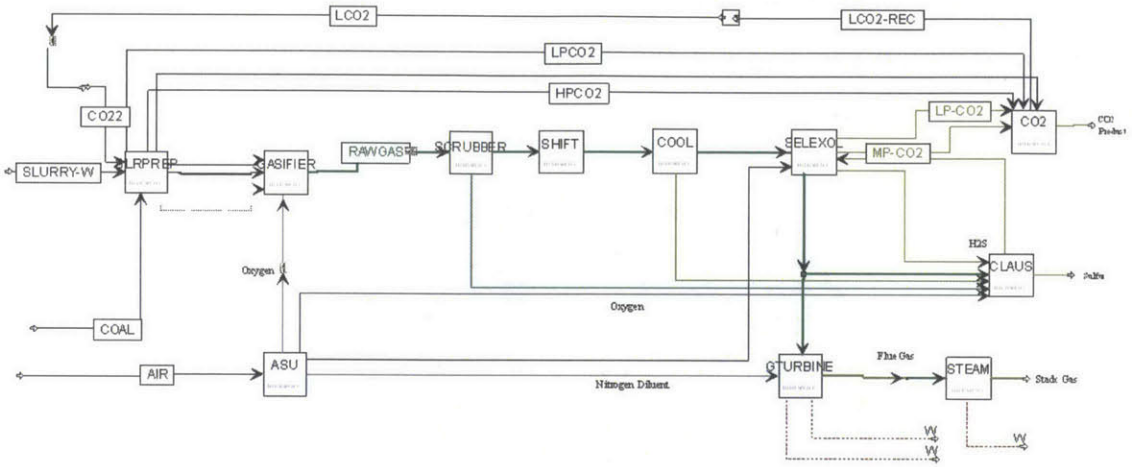

Figure 2-7: Screenshot of system-level model of IGCC plant in Aspen Plus. Only high-level hierarchies are shown.

The original model contains a CWS-fed gasifier. It was first expanded to include the option of feeding coal-CO_2 slurry, though the challenge of mixing coal and liquid CO_2 was initially not considered [18]. This was later addressed by including a submodel for coal-CO_2 slurry preparation based on the PHICCOS process [59].

The key assumptions and process variables of the IGCC plants simulated in this study are summarized in Table 2.5 and are briefly described in what follows. For further details, the reader is referred to the original contribution by Field and Brasington.

Feeding System

Both CWS and coal-CO_2 slurry feed to the gasifier are considered and modeled in this work. The CWS feed submodel resembles real operation of this feeding system: as-received pulverized coal is mixed with water at ambient pressure and subsequently pumped to the gasifier pressure.

The coal-CO_2 slurry feeding system was modeled in a similar way during the feasibility stages of this work (see Chapter 3): it is initially assumed that coal at

ambient pressure can be mixed with liquid CO_2 near ambient temperature in the same way that it can be mixed with water [18].

Given the challenges associated with the coal-CO_2 slurry preparation step, the IGCC plant model was later expanded to include a submodel of coal-CO_2 slurry preparation via the PHICCOS process, see Section 5.5. The updated IGCC model was used in the overall technoeconomic assessment presented in Chapter 6.

Gasification

The original IGCC model by Field and Brasington includes a 0-D representation of the CWS-fed gasifier, which was modeled in A+ using an equilibrium reactor (RGIBBS) with a fixed carbon conversion of 98% and an outlet temperature of 1,370°C [58]. This approach was used in the feasibility phase of this work presented in Chapter 3.

The A+ submodel of the gasifier was modified after the feasibility stage in order to study the gasification kinetics in more detail. Instead of performing chemical equilibrium calculations for a given carbon conversion, the gasifier submodel was replaced by a black box which imports syngas, slag, and oxygen conditions from a detailed, 1-D component-level model of the gasifier implemented in the software Aspen Custom Modeler.

The detailed gasifier model, which is described in Section 2.3.3, includes a predictive description of the heterogeneous gasification kinetics at high pressures and is able to estimate carbon conversion.

Air Separation Unit

O_2 is produced in an ASU, compressed, and delivered to the gasifier, together with the coal slurry feed. The flow of O_2 is controlled in order to achieve a given gasifier outlet temperature.

Nitrogen from the ASU is delivered as syngas diluent to the gas turbine and also to the Selexol unit. Modeling of the ASU focuses on the compression power requirement; rigorous modeling of the cryogenic process was not carried out.

Syngas Cooling

The syngas produced in the gasifier is made up primarily of CO, H_2, CO_2, and H_2O, plus minor concentrations of other species such as HCl, NH_3, H_2S, and COS.

The gas is cooled either by a combination of radiant and quench cooling or through quench cooling alone, see Figure 2-2. In the former case, the gas is first brought to a temperature of about 600 °C in the radiant cooler, which raises intermediate pressure steam for the bottoming cycle with the recovered heat. In both cases, the quench cooler section uses liquid water to cool down the gas through evaporative cooling, bringing it to saturation conditions; no steam is generated in the process.

The gasification reactions freeze at the syngas cooler conditions. The WGS reaction, however, must be considered in the cooler since is favored by low temperatures and proceeds until the gas is quenched.

The WGS reaction was modeled by using a *temperature approach to equilibrium* in A+. This is a simple method which allows for the use of equilibrium constants to estimate product composition in cases where equilibrium is not achieved. The equilibrium constant is calculated at a temperature which deviates from the actual temperature by a given value $\Delta T_{eq.}$. In the gasifier, the exact value of this approach depends on the cooling rate, see Table 2.5, and was chosen for each of the syngas cooling configurations through comparison of the syngas composition with experimental data for a gasifier of similar characteristics [58, 60].

Gas Scrubbing

A water wash is used to remove chlorides and particulates from the gas in a real IGCC plant. The model represents only the removal of the chlorides, since all particulates are assumed to leave with the slag. The temperature of the gas drops by a few Kelvin in the process.

Water-Gas Shift Reactor

A 2-stage catalytic reactor is used to convert most of the CO content of the syngas into CO_2 and more H_2 according to the water-gas shift reaction (VI). The H_2O:CO molar ratio is adjusted to 2:1 prior to the first reactor; steam extraction from the power plant's bottoming cycle is used for this purpose, where necessary, resulting in a reduction of the steam turbine power output. The humidity content of the gas before the shift determines whether steam extraction must be carried out or not.

The product of the WGS reactor consists primarily of H_2, CO_2, and H_2O. It then passes through a series of heat exchangers and is cooled down until a temperature of about 40 °C is reached, as required by the acid gas removal unit. Steam for the steam turbine is generated in the process.

Acid Gas Removal

CO_2 and H_2S are separated from the synthesis gas in the AGR unit. The physical solvent Selexol is used for this purpose.

Note that in order to achieve an overall CO_2 capture level of 90%, more than 90% of this gas must be separated locally in the Selexol unit; unconverted CO is oxidized to CO_2 in the gas turbine and released to the atmosphere, thus reducing the overall capture level.

The two-stage Selexol process used for acid gas removal was modeled rigorously in Aspen Plus. The H_2S-loaded solvent from the first absorption stage is regenerated thermally in a stripper; the CO_2-loaded solvent from the second stage is regenerated through pressure drop in multiple subsequent flash drums at high pressure (HP), intermediate pressure (IP), and low pressure (LP).

High pressure CO_2 is compressed and recycled to the CO_2 absorber in order to minimize the amount of H_2 losses in the AGR unit. CO_2 from the IP and LP drums is delivered to the CO_2 compressor and brought to the conditions required for transportation to the storage site.

The Selexol unit consumes thermal and electrical energy. Steam is required for

solvent regeneration in the stripper, whereas electricity is required to drive the solvent recirculation pumps and chiller. The later is used in order to increase the CO_2 and H_2S solubility in the absorbers.

Sulfur Recovery (Claus Unit)

H_2S is separated from the syngas in the AGR process and delivered to the Claus unit, where it is converted to elemental sulfur, which can be sold as a byproduct.

The reactions taking place in the Claus process can be represented by the overall expression

$$2H_2S + \tfrac{3}{2}SO_2 \rightleftharpoons 3H_2O + 3S, \tag{2.1}$$

which is exothermic and thus makes this process area a net exporter of steam.

Power Island

The power island consists of a syngas expander, one or more gas turbines, and a Rankine cycle.

Syngas Expander Decarbonized syngas from the AGR unit is reheated and expanded to about 30 bar before being delivered to one or more gas turbines, which were modeled as a single gas turbine for simplicity. The gasifier studied produces gas at a pressure higher than that required by the gas turbine combustor and the use of an expander thus allows for additional power production in the plant.

Gas Turbine The expanded syngas is diluted with N_2 from the ASU, to the extent required to achieve the heating value indicated in Table 2.5, before it is fed to the gas turbine combustor. Dilution is necessary in diffusion-flame gas turbines, such as those burning H_2, in order to avoid excessively high peak temperatures and keep NO_x emissions at acceptable levels. Steam extracted from the bottoming cycle of the power plant is used as diluent if the ASU cannot provide enough N_2. Since this

reduces the power generated in the steam turbine, N_2 dilution is preferred, wherever possible.

Bottoming Cycle The energy contained in the gas turbine exhaust, together with that available from other streams, is used for additional power generation in a bottoming Rankine cycle. An HRSG produces steam for the steam turbine generator. Steam is also provided to process units that require it, such as the WGS reactor.

CO_2 Compression

A multiple-stage intercooled compression process brings CO_2 separated in the Selexol unit to 80 bar, which is the pressure required for the formation of a dense phase at the intercooler temperature of 30°C. The CO_2 has a liquid-like density and is at a subcritical temperature but its pressure is supercritical. It is subsequently pumped to the final pressure required for transportation to the storage site. A fraction of the CO_2 flow is recirculated if the plant operates with coal-CO_2 slurry feed.

Heat Integration

Heat integration is a trade-off between capital costs and plant efficiency. In the IGCC model used, the heat integration degree is fairly typical. Hot water and steam for the power island are produced from the heat available in the syngas at different temperature levels. Heat from the radiant syngas cooler and from the coolers prior to the shift reactors are typical examples of such. Heat from lower temperature sources, such as the CO_2 compressor intercoolers, is not recovered but rejected to the cooling water.

2.3.2 System-level Model of Syngas Production Plant

A screenshot of the the A+ model of the syngas production plant studied in the later phases of this work is presented in Figure 2-8. Only high-level hierarchies are shown.

The model is almost identical to the IGCC plant model, except:

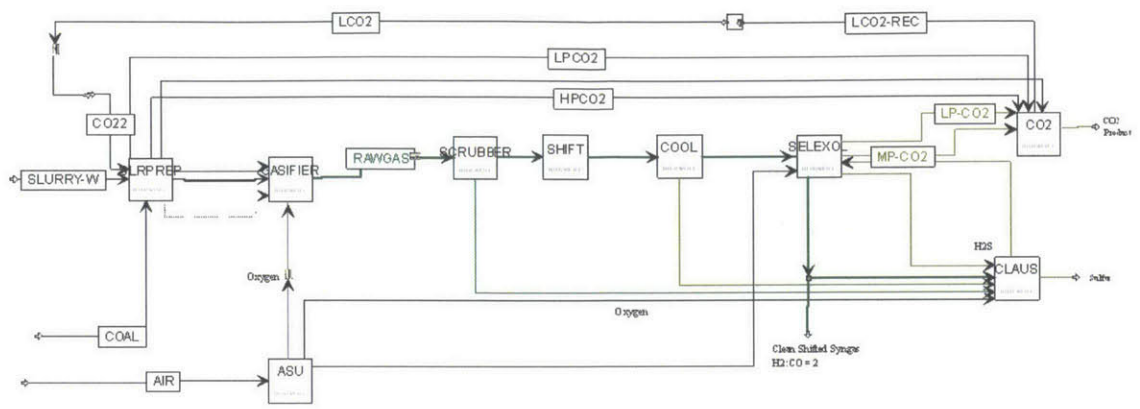

Figure 2-8: Screenshot of syngas production plant model in Aspen Plus. Only high-level hierarchies are shown.

a) It contains no power island since the product is syngas and not electricity

b) The clean, shifted syngas product has a H_2:CO ratio of 2.0.

Other than this, this plant contains the same process units as the IGCC plant, see Section 2.3.1.

The H_2:CO ratio of 2.0 is significantly lower than that in an IGCC plant with carbon capture, where the CO_2 is shifted almost completely to H_2. As a result, the WGS reactor requires little shift steam, if any.

Finally, unlike the highly integrated IGCC, the syngas production plant considered contains no heat integration and imports steam and electricity, rather than producing them locally.

2.3.3 Reduced Order Model of Gasifier

A detailed 1-D, steady-state reduced order model (ROM) of a high-pressure EFG resembling GE design was used to simulate the gasifier operation in all stages of the project after the feasibility stage.

The ROM incorporates multiple submodels including fluid mixing and recirculation, particle properties, drying and devolatilization, chemical kinetics, heat transfer, and slagging. It was originally developed by Monaghan and Ghoniem and has been described in detail elsewhere. It was validated extensively through comparison of the

predicted syngas composition, carbon conversion, and temperature profile, with that of multiple laboratory and pilot-scale reactors [61–64].

An idealized reactor network model is used in the ROM to represent the fluid mixing and recirculation between different regions inside the gasifier. For the axially-fired, swirling, single stage reactor studied here, which resembles a GE design, the network consists of four zones, as schematically illustrated in Figure 2-9.

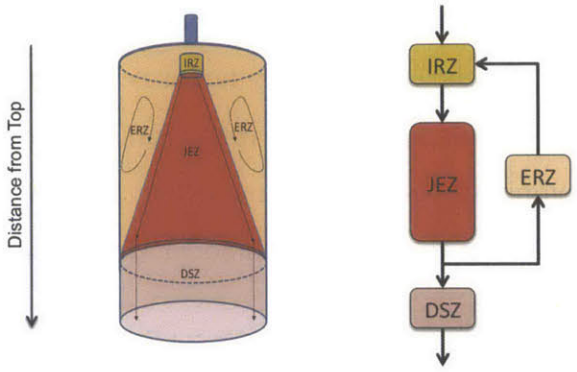

Figure 2-9: Representation of gasifier through a network of idealized reactors in reduced order model.

In the internal recirculation zone (IRZ), which is modeled as a well-stirred reactor (WSR), the coal slurry and oxygen streams are injected and mix with each other as well as with hot, recirculated gas and particles from the external recirculation zone (ERZ). The gasifier feedstock is rapidly heated up by the hot stream and through heat release by partial oxidation in the presence of oxygen. The slurrying medium evaporates and the coal particles are fully dried and devolatilized in this zone. The model assumes that the oxygen is fully depleted within the IRZ so that the maximum gasifier temperature is reached at the IRZ outlet.

The two-phase flow leaving the IRZ expands like a free jet in the jet expansion zone (JEZ), which is modeled as a truncated conical, 1-D plug flow reactor (PFR). Once the jet reaches the reactor wall, most of the flow is modeled as a 1-D PFR in the downstream zone (DSZ). However, a fraction of the flow in the expanding jet is detrained and flows back to the IRZ through the ERZ. The latter is modeled as a WSR. Note that syngas cooling is considered to be outside to scope of the ROM. It is included in the system-level model, see Section 2.3.1.

Char gasification with H_2O and CO_2 takes place in the JEZ and DSZ, where the temperature is high and no oxygen is present. Other reactions, such as the homogeneous water-gas shift reaction, however, also play an important role here.

The heterogeneous gasification kinetics submodel of the original ROM was modified as part of this work in order to improve its fidelity under the high-pressure conditions of interest. The modified submodel uses a Langmuir-Hinshelwood expression with kinetic parameters based on experimental measurements at high pressure from the literature [65]. A relative reactivity factor is introduced to account for reactivity differences between coals of different ranks. Furthermore, internal mass transfer limitations at high temperatures are accounted for through the effectiveness factor approach [66]. The details of the kinetic submodel are presented in Chapter 4.

2.3.4 Surrogate Model of Syngas Production Plant

The sensitivity, optimization, and uncertainty analyses conducted in the later phases of this work and presented in Chapters 7 and 8 require a very large number of simulations. This places special requirements on the modeling strategy used. Most importantly, the models must be able to run quickly and robustly without user intervention.

The A+ plant model described in Section 2.3.2 does not comply with the requirements above, given its detailed nature. Hence, a simplified plant model was constructed in Excel and is schematically represented in Figure 2-10. It is a surrogate of the more detailed A+ model and runs quickly and robustly. The simplicity of the surrogate model, together with its native Excel interface, make it more appropriate when a large number of simulations is required.

The model is a collection of mass and energy balances implemented in Excel with the purpose of predicting the syngas flow and composition, as well as the flow of CO_2 to the compressor. It uses Aspen Excel Properties Calculator [67] for estimating the thermophysical properties of the syngas.

The surrogate includes all syngas processing units, except for the gasifier, whose performance (syngas conditions, oxygen consumption, etc.) is imported from the

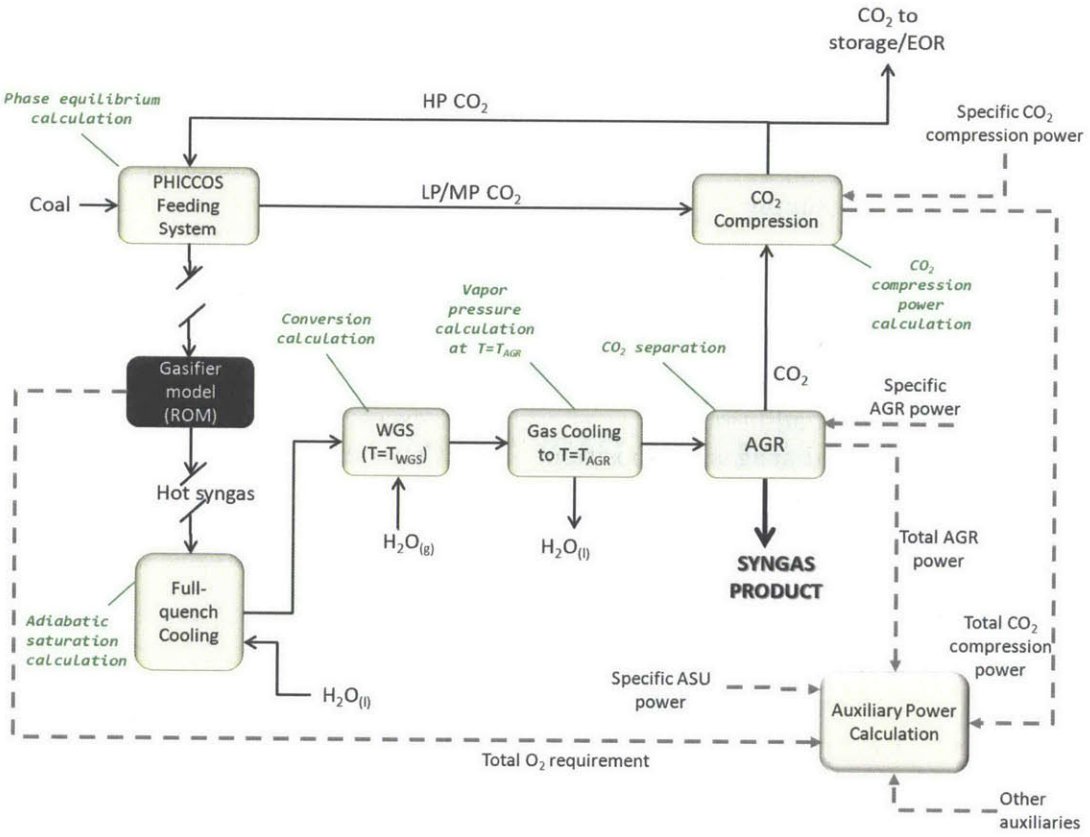

Figure 2-10: Overview of main calculations performed in surrogate model of syngas production plant in Excel. The dashed lines indicate information, rather than material streams.

ROM. Only CO, H_2, H_2O, and CO are considered. Furthermore, the auxiliary power consumption in the plant is calculated from specific power consumption numbers extracted from the A+ model. The main syngas production plant characteristics and modeling assumptions used are listed in Table 2.6 and are described in what follows.

Table 2.6: Key data for surrogate model of syngas production plant.

Feeding system	
Feeding system	CWS or PHICCOS
Solubility of CO_2 in H_2O	2.55% (molar) at 80 bar
	0.05% (molar) at 1 bar
Gasifier	
Thermal input	1,700 MJ/s (2 x 850 MJ/s)
Oxygen supply	
ASU	1,370 kJ_e/kg O_2 [18, 58]
O_2 compressor	208 kJ_e/kg O_2
Syngas cooling	Full-quench to 224°C
Gas Conditioning	
Water-gas shift reactor	
Steam addition	30% excess (molar)
Shifted syngas composition	H_2:CO = 2:1 (molar)
AGR & Claus unit	230 kJ_e/kg CO_2
Carbon capture	90% (local)
Auxiliary power consumption	
CO_2 compression	
CO_2 captured in AGR	896 kJ_e/kg CO_2
MP CO_2 from PHICCOS	173 kJ_e/kg CO_2
LP CO_2 from PHICCOS	1,517 kJ_c/kg CO_2
Coal handling, BOP, and others	144 kJ_e/kg coal (ar) [19]
Additional for dry-fed plant	
Syngas compression	140 kJ_e/kg syngas (H_2:CO=2)

Feeding System

The surrogate model can operate with CWS or with coal-CO_2 slurry feed based on the PHICCOS feeding system. The details and main operational parameters of the latter are presented in chapter 5.

The PHICCOS feeding system submodel only considers its fluid phase. Its main role is to calculate the flow of HP CO_2 recirculated from the CO_2 compressor to the

PHICCOS feeding system, $\dot{m}_{CO_2,HP}$:

$$\dot{m}_{CO_2,HP} = \frac{\dot{m}_{coal}}{X_{CWS}}\left(\frac{\dot{m}_{CO_2}}{\dot{m}_{CWS}}\right), \tag{2.2}$$

$$\tag{2.3}$$

where X_{CWS} and $\left(\dot{m}_{CO_2}/\dot{m}_{CWS}\right)$ are operational parameters of the PHICCOS feeding system, see Chapter 5, and represent the coal loading in the CWS and the mass flow ratio of CO_2 to CWS, respectively.

The flows of MP CO_2, $\dot{m}_{CO_2,MP}$, and LP CO_2, $\dot{m}_{CO_2,LP}$, from PHICCOS that must be recompressed in the CO_2 compressor are also calculated here:

$$\dot{m}_{CO_2,MP} = \dot{m}_{coal}\left[\frac{1}{X_{CWS}}\left(\frac{\dot{m}_{CO_2}}{\dot{m}_{CWS}}\right) - \frac{1 - X_{CCO2S}}{X_{CCO2S}}\right] \tag{2.4}$$

$$\dot{m}_{CO_2,LP} = \left[y_{CO_2(80bar)} - y_{CO_2(1bar)}\right]\dot{n}_{H_2O}M_{CO_2}. \tag{2.5}$$

Here, X_{CCO2S} is the coal loading of the final coal-CO_2 slurry delivered to the gasifier, M_{CO_2} is the molecular weight of CO_2 and y_{CO_2} is the solubility of CO_2 in water at the PHICCOS operating temperature, in moles of CO_2 per mole of H_2O, and $\dot{n}_{H_2O}$ is the molar flow of water recirculated in the PHICCOS feeding system.

Gasifier and Raw Syngas Cooling

The gasifier is not modeled in the surrogate. The syngas conditions and the oxygen demand are inputs to the Excel model and originate from the ROM results.

The hot syngas from the gasifier is cooled to a temperature of 220°C in the full-quench cooler. This temperature is a representative value taken from the A+ model. The total flow of water vapor in the cooled syngas is calculated from the saturation vapor pressure of water at the stream conditions.

WGS Reactor

The molar conversion in the WGS reactor, $\Delta\dot{n}$, is calculated through a mass balance:

$$\Delta\dot{n} = \frac{\left(\frac{\dot{n}_{H_2}}{\dot{n}_{CO}}\right)\dot{n}_{CO,in} - \dot{n}_{H_2,in}}{1 + \left(\frac{\dot{n}_{H_2}}{\dot{n}_{CO}}\right)}, \tag{2.6}$$

where the specified H_2:CO ratio in the product, $(\frac{\dot{n}_{H_2}}{\dot{n}_{CO}})$, is 2.0, see Table 2.6. A 30% excess molar flow of H_2O is assumed, which is provided through steam addition, if required. This excess corresponds to that in the IGCC plant model.

Shifted Syngas Cooling

The molar flow of water condensed out of the syngas prior to the AGR, $\Delta\dot{n}_{H_2O}$, is estimated using the saturation pressure of water, p_{sat}, at the AGR temperature. Assuming ideal gas behavior:

$$\Delta\dot{n}_{H_2O} = \dot{n}_{H_2O,in} - \frac{p_{sat}}{p - p_{sat}}\left(\dot{n}_{H_2} + \dot{n}_{CO} + \dot{n}_{CO_2}\right) \tag{2.7}$$

The flows of CO_2, H_2, and CO are assumed to remain unchanged, i.e. their solubility in H_2O is neglected.

AGR

The AGR separates 90% of the CO_2 flow. Its power consumption is estimated from the flow of CO_2 separated and from the specific power consumption number in Table 2.6. The latter was calculated from the results of the A+ model and includes the Claus unit's power requirements.

CO_2 Compression

The total power consumed by the CO_2 compressor is estimated from the flow of CO_2 captured in the AGR and from the LP and MP CO_2 that must be recompressed as part of the PHICCOS feeding system (see Chapter 5). The specific power required for

each of these three streams was calculated from the A+ CO_2 compressor submodel.

Surrogate Model Validation

The gas flows and compositions estimated with the surrogate model at different locations are presented in Figure 2-11, together with the auxiliary power consumption in the plant. The results are compared with the corresponding values from the detailed A+ model, using bituminous coal feed as an example, in order to verify the validity of the surrogate model.

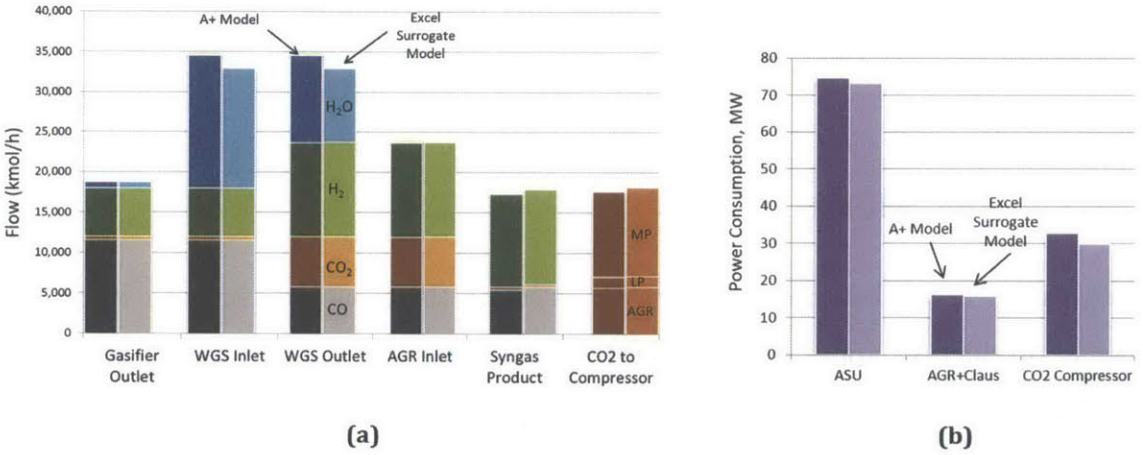

Figure 2-11: Validation of surrogate model with A+ model: (a) Gas flow and composition, and (b) Auxiliary power consumption. The results are for a plant with bituminous coal, PHICCOS feed with a coal-CO_2 slurry loading of 80% and a gasifier outlet temperature of 1,600°C. The gasifier outlet conditions are imported from the ROM.

The results in the figure show that there is very good agreement between the predictions by the detailed and the surrogate model. A maximum deviation of 5% and 7% is observed for the gas flow and auxiliary power consumption predictions, respectively.

Considerations for Dry-fed Plant

Modeling and simulation of the dry-fed Shell gasifier used for comparison throughout this work is outside its scope and its performance was taken from the literature [11, 19].

However, the dry-fed Shell gasifier considered for comparison throughout this study operates at a lower pressure of about 35 bar due to limitations in the lock-hopper feeding system. Hence, syngas compression to the final pressure of 52 bar is required and was accounted for in the analysis. The capital costs and energy consumption of a syngas compressor were estimated using Aspen Process Economic Analyzer and Aspen Plus.

Furthermore, unlike the full-quench gasifiers considered for the PHICCOS and CWS feeding systems, the Shell gasifier is a net producer of steam from its radiant syngas cooler. The negative steam costs (i.e. profit from steam production) were included in the cost estimates for this reactor.

2.3.5 Cost Model

A cost model was developed in Excel to estimate the economics in both IGCC and syngas production applications. The figure of merit used is the cost of electricity (COE) and the cost of syngas (COS), respectively. The latter is for clean syngas consisting only of H_2 and CO at a given ratio.

The data used for the cost model is summarized in Table 2.7. The model is based on the standard methodology used by NETL for the comparative assessment of power plant performance [68]. It was modified for syngas production applications, where necessary, with data from NETL's extensive study of industrial size gasification for syngas, substitute natural gas, and power production [69].

The availability of 80% used for IGCC corresponds to that assumed by NETL [11, 19] and agrees well with that reported for existing IGCC units [3, 49, 71]. The availability of the syngas production plant was estimated from that of IGCC, given the absence of operational data for an EFG-based syngas production plant. The value of 86% reported in Table 2.7 accounts for the fact that less outages will occur if there is no power island. It was discussed with experts [71] and was calculated from data for the Tampa Polk IGCC power station, whose power island is reported to cause unplanned outages about 21 days per year [49].

Table 2.7: Key data for cost model of plant [3, 11, 19, 68 74].

	IGCC	**Clean Syngas Production**
Cost basis	2011 U.S. Dollars	
Cost index	CEPCI	
Plant availability	80%	86%
Levelization factor	1.268	
Capital		
Reference bare erected costs	[11, 19, 69]	
Capacity scaling exponent	0.6	
EPC costs	9.4% of BEC	
Process contingency		
SoA equipment	0-20% of BEC	
PHICCOS	40-100% of BEC	
Project contingency	16% of BEC+EPC+PCC	
Owner's costs	23% of TPC	
Capital charge factor	0.1243	
Operation & Maintenance		
Fixed O&M costs	3.7% of TPC	2.6% of TPC
Variable O&M costs		
Slurry-fed	47 \$/kW$_{gross}$	0.45 \$/GJ syngas
Dry-fed	63 \$/kW$_{gross}$	0.60 \$/GJ syngas
Fuel and Utilities		
Bituminous coal	56.00 \$/tonne	
Lignite	17.33 \$/tonne	
Electricity	–	6.46 c/kWh
Steam (60 bar, 360°C)		
Bituminous coal	–	8.3 \$/1000 kg
Lignite	–	4.6 \$/1000 kg

Capital Costs

The total capital costs in the plant were estimated using the methodology depicted in Figure 2-12.

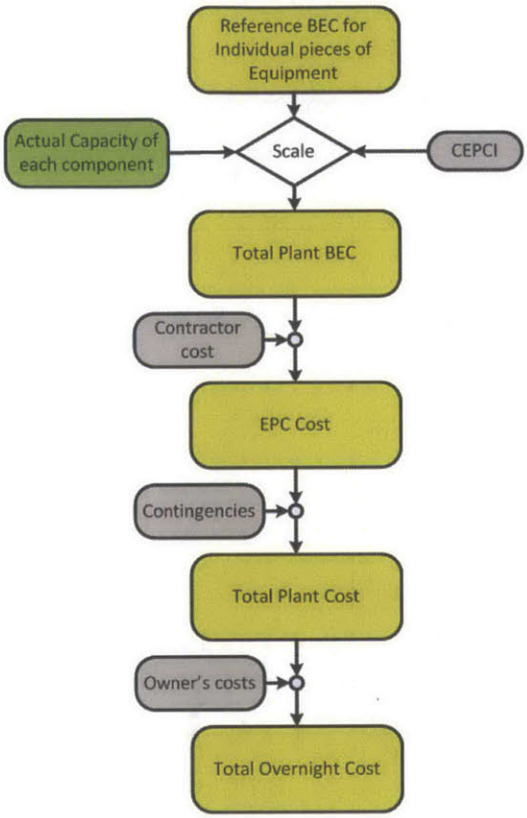

Figure 2-12: Methodology used for calculating the plant's Total Overnight Cost.

The total bare erected costs (BEC) are first calculated from reference BEC for the individual pieces of equipment in the plant. They originate from NETL's baseline estimates for an IGCC plant with the same feeding system and feedstock [11, 19]. The BEC includes process equipment, on-site facilities and infrastructure (e.g. shops, offices, labs, road, etc.), and the direct and indirect labor required for its construction and/or installation [11]. They are classified as a Class 4 Cost Estimate, according to the Association for the Advancement of Cost Engineering International (AACE). These feasibility stage estimates have an expected accuracy of -30% to +50% [11].

The reference BEC were converted to 2011 U.S. Dollars, where necessary, by using the Chemical Engineering Plant Cost Index (CEPCI) [72]. Furthermore, they were

scaled from their reference capacity to the capacity predicted by the simulations by using the *six-tenths factor rule* [73]:

$$\text{Cost of equipment } b = (\text{cost of equipment } a)\, X^{0.6}. \tag{2.8}$$

Here, a is the reference cost of any piece of equipment and b is the cost of a similar unit with X times the reference capacity.

In the syngas production plant, the balance of plant (BOP) equipment, cooling water system, accessory electric plant, instrumentation and control, improvements to sites, and buildings and structures are expected to be different than in an IGCC plant, given the absence of a power island. Hence, these costs were not taken from NETL's estimates for IGCC plant data but were estimated as a percentage of the total BEC. The percentages were taken from a similar syngas production plant in Case 1A of NETL's comprehensive study of syngas production technologies from fluidized-bed gasifiers [69].

All individual equipment costs within the PHICCOS feeding system are based on scaled data from Westinghouse's economic assessment of a commercial-scale LICADO unit [56], see Chapter 5. The costs of the coal-water slurry preparation unit within the PHICCOS feeding system constitute an exception: for consistency with CWS-fed cases, the capital costs of this unit were estimated through capacity-scaling of the costs reported by NETL for a CWS feeding system [19].

The Total Plant Cost (TPC) is calculated from the total plant BEC by adding the costs of services provided by the engineering, procurement, and construction (EPC) contractor, as well as process contingency (PCC) and project contingencies (PJC). The EPC costs and project contingencies are calculated from the percentages reported in Table 2.7, which presents also other economic assumptions used in this study.

A process contingency of up to 20% was used for all state-of-the-art (SOA) equipment, as itemized in NETL's estimates [11, 19]. For equipment in the PHICCOS feeding system, a process contingency of 40-100% was used, given the uncertainty associated with its costs. This corresponds to AACE's guideline for the least mature

Technology Status, i.e. a new concept with limited data [68].

The total overnight capital costs (TOC) are calculated by adding the plant owner's costs to the TPC. These are estimated using the Owner's Cost Factor in Table 2.7 and include royalties, start-up costs, working capital, inventory, land, and financing costs, among others. The TOC is expressed in base-year (2011) dollars and does not include escalation or interest during construction, which were not included in the estimates in this study. They represent approximately an additional 14%, but this varies depending on the finance structure of the plant.

Operation and Maintenance Costs

Operation and Maintenance (O&M) costs include operating labor, maintenance (material and labor), administrative and support labor, consumables, waste disposal, and co-product or by-product credit, among others. They have a fixed component and a component that varies with the amount of product produced in the plant.

Both the fixed and the variable O&M were estimated as a lump sum from data for a similar IGCC [11, 19] or syngas production [69] plant operating with a similar feedstock. O&M costs in a PHICCOS-fed plant were assumed to be the same as in one with CWS feed.

The O&M costs do not include the consumption of oxygen and nitrogen, since these gases produced internally in the ASU. Electricity and steam consumption are also not included. In the case of IGCC, these are produced in the plant so they are extracted directly from the generator and HRSG, respectively. The resulting plant output reduction is accounted for in the IGCC model.

In the syngas production plant, electricity and steam are not available. Electricity is purchased from the grid and steam is produced in a packaged boiler, whose capital costs were taken from the literature [73]. The fuel value of steam was used to calculate the operating cost of steam production, which is reported in Table 2.7 for each feedstock. A boiler efficiency of 90% was assumed [75].

Product Cost

The figures of merit used in this study is the product cost, which is the Cost of Electricity (COE) and Cost of Syngas (COS) in the IGCC and syngas production plants considered, respectively. This is the price that the plant owner must charge per generated unit of product (kW of electricity or m^3/h of clean, shifted syngas) in order to achieve a given internal rate of return on equity over the entire economic analysis period [11].

The product cost is the sum of capital costs, O&M costs, and fuel and utility costs. It is calculated from the plant performance and economics, as schematically illustrated in Figure 2-13.

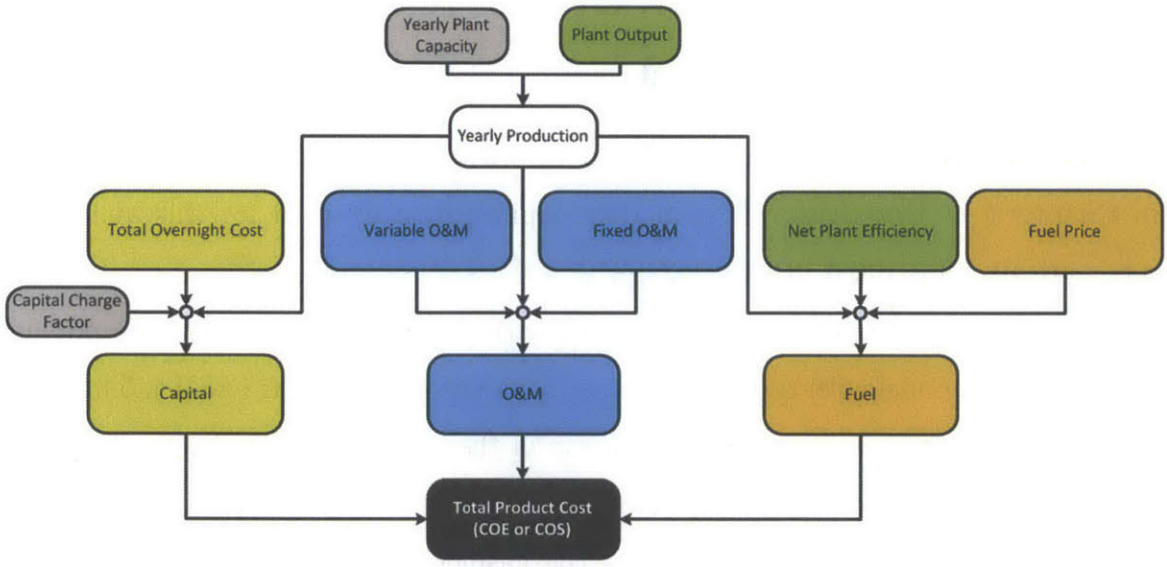

Figure 2-13: Methodology used for calculating the total product cost in an IGCC plant (COE) or in a syngas production plant (COS).

The TOC is annualized by using a capital charge factor, whose value depends on the global economic assumptions (taxes, depreciation, capital and financing terms, capital expenditure period, etc.) as well as on the finance structure of the plant. The capital charge factor used reported in Table 2.7 corresponds to that of an investor-owned plant with a high-risk profile and a capital expenditure period of 5 years [11].

2.4 Model Coupling Strategy

Each of the models described in the previous section has a different role: the ROM is necessary to study the gasification kinetics, the plant models give information about plant performance and equipment sizing, and the cost model puts everything together to calculate the overall plant economics. None of these models by itself is able to capture all the key aspects of the plant.

The calculation of the product cost in the IGCC and syngas production plants hence requires the exchange of information between the different models. This was automated by using an Excel interface, which allows the different tools to exchange inputs and outputs during the calculation.

2.4.1 Coupled Model for Overall Technoeconomic Assessment in IGCC Plant

The overall technoeconomics in an IGCC plant with coal-CO_2 slurry feed are discussed in Chapter 6 of this thesis. The model coupling strategy used for this analysis is schematically illustrated in Figure 2-14.

The IGCC plant model in A+ is coupled with the gasifier ROM in ACM and with the Excel cost model with the help of Aspen Simulation Workbook (ASW). The latter is an add-in for interfacing Excel with many of the tools offered by Aspen Tech.

The parent application, i.e. that from which the simulations are started, is ASW. When ASW is run from Excel, it runs the gasifier ROM in ACM and writes the syngas outlet conditions, oxygen demand, etc. to Excel. These results are then used by the plant model in A+, which is executed through a second ASW run. The results from the plant model are used by the economic model to compute the overall cost of electricity in the plant.

In the coupled model, the gasifier of the A+ model is only a black box. Its performance is not modeled but is imported from the ROM. This is different to the standalone IGCC model described in Section 2.3.1, in which the gasifier is modeled as an equilibrium reactor.

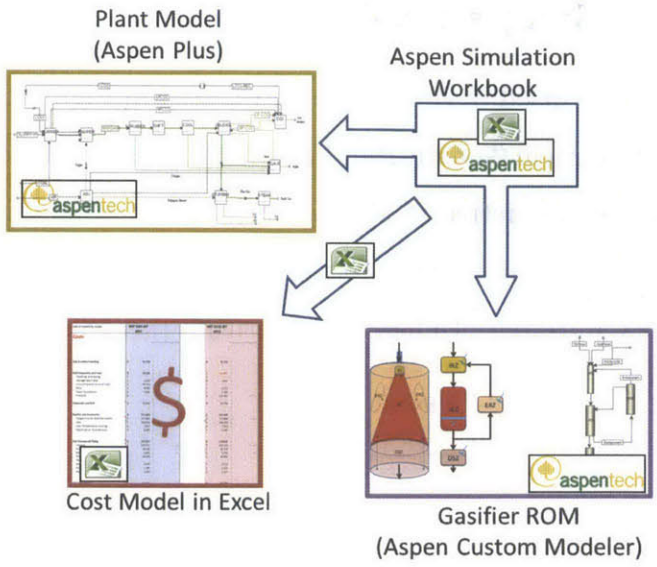

Figure 2-14: Model coupling strategy and tools for overall economic assessment in IGCC plant.

ASW only allows for one model to be active in Excel at a given time. Hence, deactivation of A+ followed by activation of ACM must be carried out in every coupled run. This is not problematic when only one run is necessary, as in this economic assessment. However, it would make the total simulation time unbearably long if a large number of runs were necessary, as for the optimization/uncertainty analysis below.

As an alternative to using ASW as an interface, A+ has a unit operation named User3 which is envisioned to run models in ACM from within A+. While this would have been a simpler and faster approach, it was not possible within the scope of this study as a result of incompatibilities between the ROM structure and the structure required to implement a User3 interface with ACM.

2.4.2 Coupled Model for Sensitivity, Optimization, and Uncertainty in Syngas Production Plant

The model coupling strategy used in this case is illustrated in Figure 2-15. As shown in the figure, the software Oracle Crystal Ball (CB) is the parent application. Crystal Ball is an Excel add-in for predictive modeling, forecasting, simulation, sensitivity, and optimization [76]. Its optimizer, *OptQuest*, incorporates metaheuristics and a form of adaptive memory into its optimization algorithm [77, 78].

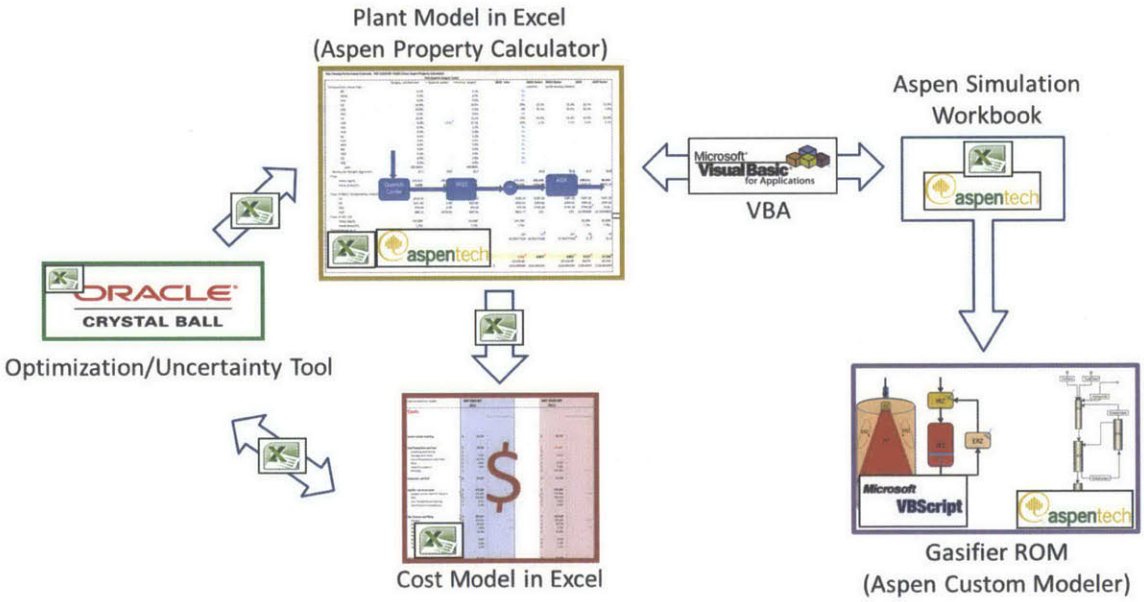

Figure 2-15: Model coupling strategy and tools for sensitivity, optimization, and uncertainty analyses in syngas production plant.

The simulations are started by running CB, which first adjusts the inputs to the plant and cost models as appropriate. If a probability distribution function has been defined for the model inputs, for example, it to conducts a random sampling of the corresponding variable.

Once CB is started, a subroutine in Visual Basic for Applications (VBA) [79] is automatically called, which runs ASW. The latter executes the ROM in ACM and, once it has converged, copies the results back to the plant model in Excel. These are used by the cost model for calculation of overall plant economics.

The random and extreme inputs involved in uncertainty/optimization are chal-

lenging for execution of the ROM, which is very sensitive to large changes in its input variables. Hence, a script was written in VB Script within ACM that changes the inputs slowly, helping convergence. It also provides information about a failed run so that it can be automatically excluded from the results.

2.5 Chapter Summary

The general methodology, tools, and assumptions used throughout this work for the comprehensive assessment of the PHICCOS feeding system were presented in this chapter.

A variety of models on different scales were developed and/or co-developed. These include two plant-level flowsheet models, a surrogate plant model, a component-level model of the gasifier with particle-scale phenomena and chemical kinetics, and a cost model. The models were described in this chapter, together with the strategy used to couple these. Multiscale model coupling allows for the assessment of plant technoeconomics under consideration of phenomena occurring at widely different scales.

The multiscale analysis methodology and tools described here constitute the pillars of this thesis. Beyond allowing for a quantitative assessment of the PHICCOS feeding system, these also illustrate the use of the multiscale approach, as applied to a particular problem.

Chapter 3

System-level Feasibility of Coal-CO_2 Slurry Feed in an IGCC Plant

While using liquid CO_2 instead of water in the feeding system is expected to improve the gasifier thermodynamics, it is the overall effect on the net plant efficiency that determines the real performance benefit of this concept. The energy required for re-capturing and re-compressing the CO_2 recirculated for slurry preparation must be quantified, calling for system-level analyses.

This chapter describes the system-level study conducted to evaluate the feasibility of coal-CO_2 slurry feed. The technical characteristics and trade-offs associated with this feeding system are assessed using steady-state process simulation. An IGCC plant with CCS is used as an example application. The net IGCC efficiency is the figure of merit considered for quantifying overall performance and comparing it with that of a state-of-the-art CWS-fed system.

3.1 Methodology and Cases Studied

The A+ system-level model described in Section 2.3.1 was used for the feasibility analysis. The IGCC plant considered has an as-received coal flow of 5,450 tonne/day

and corresponds closely to that studied by NETL in Cases 2 and 2a of the IGCC baseline studies [11, 19]. While the same flow was assumed for all coals here, in reality, however, either the reactor size or its throughput must be adjusted to satisfy the design requirements of downstream equipment within the plant. for an IGCC plant, for example, the gasifier is typically designed/operated to yield a specified gas turbine power output.

Conventional CWS feed and coal-CO_2 slurry feed were both modeled to allow for a fair comparison. In order to assess the impact of coal rank, bituminous coal, subbituminous coal, and Beulah-Zap lignite feedstocks were all considered. Furthermore, full-quench syngas cooling and combined radiant-quench cooling were both studied.

Finally, because the maximum achievable coal loading for CO_2 slurry is still uncertain, simulations were carried out for an upper, a nominal, and a lower loading. The nominal coal loading is 80%, see Section 2.2.2. An upper limit is 88% is used, which assumes that the loading reported by Peirson et al. [33] is achievable. The conservative case assumes that CO_2 slurry can carry only as much solids as H_2O slurry, i.e. it has a coal loading of 71%.

The following assumptions were made during the feasibility stage:

- Coal-CO_2 slurry can be prepared in the same way as CWS
- Conversion in the gasifier is nearly complete, i.e. it is not affected by the change from CWS to coal-CO_2 slurry

The validity of each these two two key assumptions is addressed in detail in Chapters 4 and 5, respectively.

3.2 Results and Discussion

Results obtained from the system simulations are presented and discussed in what follows. A unit feedstock energy basis has been used to normalize the results, where relevant. Results for radiant-quench and full-quench cooling are presented side-to-side only if they are different.

3.2.1 Oxygen Consumption

Figure 3-1 presents the specific oxygen consumption for all coals studied. Oxygen consumption is lowest for bituminous coal-CO_2 slurry, which is the case with the highest solids loading, see Table 2.2. The high loading is as a result of the low moisture in bituminous coal and of the use of CO_2 as slurrying medium.

The results agree well with the expectations: the higher the solids loading of the slurry entering the gasifier, the lower its water content and hence the lower the flow of oxygen required for providing heat to vaporize moisture through reactions (III-V). Accordingly, lignite coal-water slurry, which has the lowest solids loading, has the highest demand for oxygen of all cases studied.

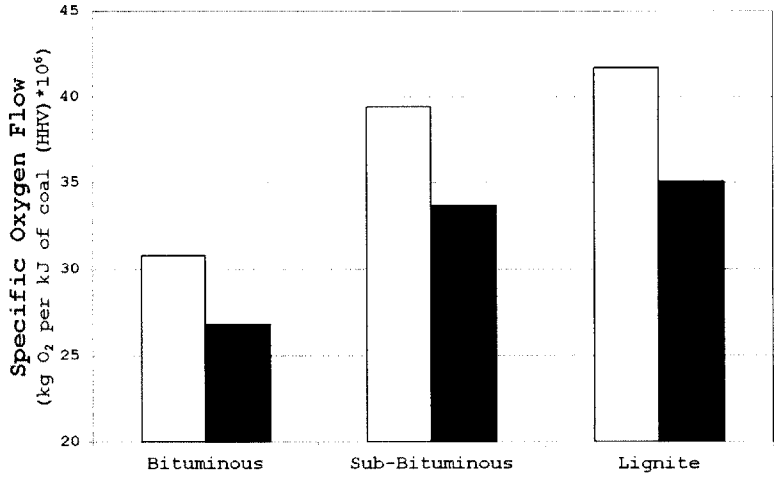

Figure 3-1: Specific oxygen consumption for a gasifier with coal-water slurry (□) and coal-CO_2 slurry (■) feed.

The effect of substituting water for liquid CO_2 is very significant: on average, a CO_2 slurry-fed gasifier consumes 15% less oxygen per unit feedstock HHV than a water slurry-fed one. This not only reduces the auxiliary power consumption of the air separation unit but most importantly its size, and thus capital cost. The 15% lower specific oxygen consumption observed for sub-bitumonus coal is in close agreement with the 13% reduction reported by Dooher et al. for a similar feedstock [46].

Notice that oxygen consumption does not decrease proportionally to the large re-

duction in the heat capacity and enthalpy of vaporization of CO_2, relative to H_2O, see Table 1.2. This can be attributed to the fact that the CO_2 gasification reaction (II), which plays an increasingly important role when CO_2 slurry feed is used, is about 30% more endothermic than the H_2O gasification reaction (I). This difference is significant since the gasification reactions dominate the energy requirement of the gasifier. While chemical equilibrium was assumed in this work, the actual contribution of the more endothermic CO_2 gasification reaction to the overall carbon conversion is determined by the heterogeneous reaction kinetics; this is addressed in Chapter 4.

3.2.2 Cold Gas Efficiency

The gasifier cold gas efficiency is presented in Figure 3-2 for all coals. This performance measure is directly linked to the oxygen consumption and similar trends are thus observed; oxygen is required for the combustion reactions which constitute the main source of cold gas efficiency loss.

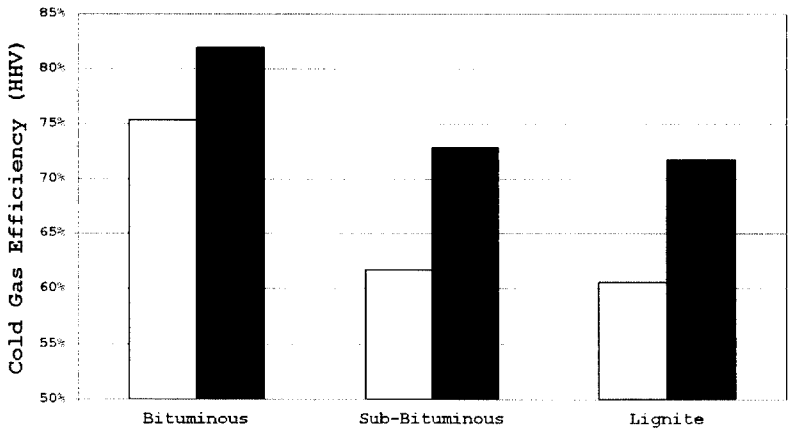

Figure 3-2: Cold gas efficiency of gasifier for coal-water slurry (□) and coal-CO_2 slurry (■) feed.

The cold gas efficiency of 82% observed for a gasifier operating with bituminous coal and CO_2 slurry feed is within the range of 78-83% typical for dry-fed systems gasifying a similar coal [3] and is far superior to the 75% resulting for conventional water-slurry feed. Overall, operation with CO_2 slurry leads to a significant increase in the cold gas efficiency, which ranges from an estimated 7%-points (%-pt.) for

bituminous coal to more than 11%-pt. for sub-bituminous coal and lignite-slurry.

The 11%-pt. increase observed for sub-bituminous coal is superior to the 7%-pt. reported by Dooher et al. for a similar feedstock. This deviation is likely to be the result of different assumptions regarding gasifier operation, such as conversion, temperature, or water-gas shift equilibrium, which are not reported in Dooher's original work [46].

Gasifier cold gas efficiency decreases steadily with the coal rank. Note, however, that gasification of lignite-CO_2 slurry results in a cold gas efficiency of 72%, which is almost as high as the 75% of bituminous coal-water slurry gasification. In other words, if water is substituted by CO_2 as slurrying medium, lignite coal can be gasified nearly as efficiently as bituminous coal in water slurry.

A higher cold gas efficiency signifies that more of the coal's energy content is retained in the synthesis gas. This is especially relevant for low-rank coal gasification, which typically requires large equipment and multiple process trains as a result of its low energy efficiency. The development of gasifiers with favorable economics for the gasification of low-rank coal has been identified as one of the key areas of future research for gasification-based plants [15, 80].

3.2.3 Gas Composition and Shift Steam Requirements

Figure 3-3 shows the H_2:CO ratio in the raw syngas leaving the gasifier cooler for all cases studied. For a given feedstock and slurrying medium, a gasifier with radiant-quench cooling produces raw syngas with a higher H_2:CO ratio than the corresponding full-quench option. This can be attributed to its slower cooling rate, which was modeled through a larger temperature approach to equilibrium, see Table 2.5, and allows for the water-gas shift reaction (VI) to proceed further before its rate freezes at lower temperatures.

The results in the figure show that the CO_2 gasification reaction (II) becomes increasingly important when the concentration of carbon dioxide in the feed increases: raw syngas produced in the CO_2 slurry-fed gasifier has a H_2:CO ratio which is as low as half that of its water slurry-fed counterpart. In general, the lower the total (slurrying

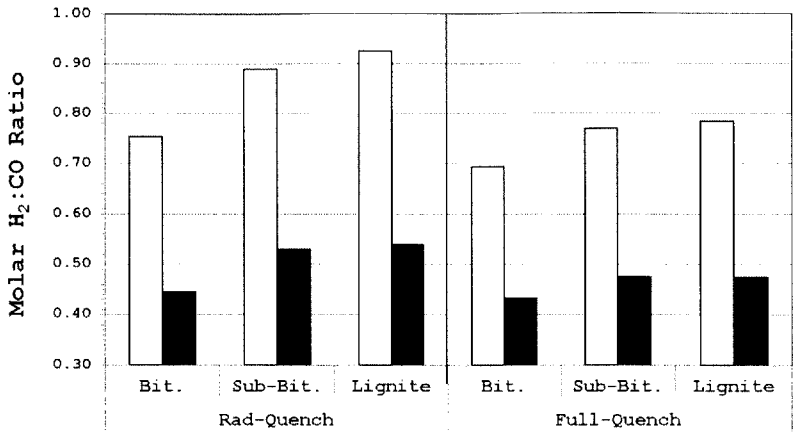

Figure 3-3: Molar ratio of hydrogen to carbon monoxide in raw syngas leaving the gasifier cooler for coal-water slurry (□) and coal-CO_2 slurry (■) feed.

medium plus coal moisture) amount of water in the feed, the lower the H_2:CO ratio of the syngas.

The high CO content of the syngas produced from CO_2 slurry-fed gasifiers leads to a higher shift steam requirement for the water-gas shift reactor. The specific flow of steam extracted from the steam turbine for this purpose is presented in Figure 3-4; this is important since it translates directly to a reduction in the steam turbine power output.

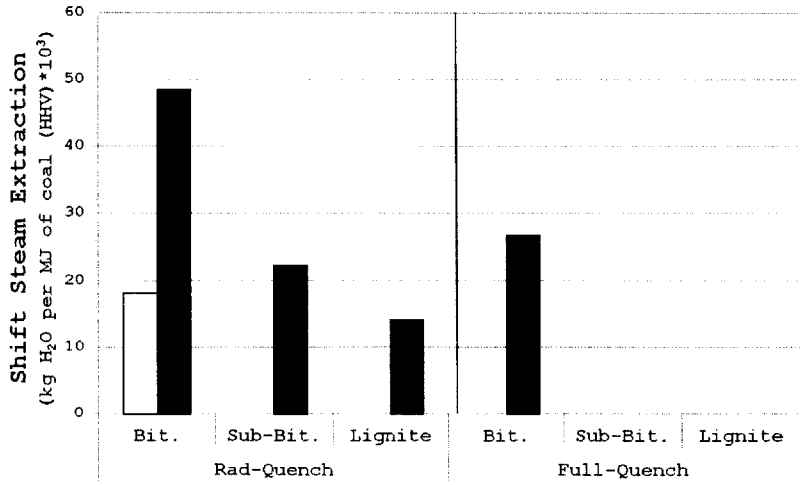

Figure 3-4: Specific shift steam requirement for plants with coal-water slurry (□) and coal-CO_2 slurry (■) feed. Missing data points indicate that enough H_2O is contained in the gas and shift steam extraction is not required.

For bituminous coal gasification and radiant-quench cooling, the syngas produced in a plant with CO_2 slurry feed requires more than twice the amount of shift steam than that of a plant with water slurry feed. This is the only water slurry-fed case for which steam extraction is necessary; excess water is present in the syngas for all other water slurry cases. Note that while radiant-cooling produces a gas with a higher H_2:CO ratio than full-quench cooling, its low moisture results in an overall higher shift steam extraction than for full-quench cooled cases.

Full-quench cooling can hence be implemented as a way to reduce the high shift steam requirement in plants with CO_2 slurry feed. This cost-effective cooling method introduces moisture while cooling the gas through direct contact with water. As depicted in Figure 3-4, the shift steam extraction in plants with CO_2 slurry is reduced by almost half for bituminous coal, and is made completely unnecessary for sub-bituminous coal and lignite if full-quench cooling is used.

Figure 3-5 compares the gas flow and composition history in a plant with water slurry with one based on CO_2 slurry for the exemplary case of lignite and rad-quench cooling; the material streams are presented for selected relevant locations throughout the plant. The results show that the composition difference between the syngas produced with either slurrying medium is evened out in the WGS reactor, where most of the CO is converted to CO_2 and H_2. From this point onward, there is no significant difference between the composition of the gas produced with either water slurry or CO_2 slurry. Noteworthy is the fact that for a given as-received coal flow, up to 20% higher flow of gas turbine fuel is produced if CO_2 slurry is used instead of H_2O slurry. This is a direct result of the higher cold gas efficiency in a CO_2 slurry-fed gasifier.

3.2.4 Auxiliary Power Consumption

The air separation unit, acid gas removal unit, and CO_2 compressor are the most important sources of auxiliary power consumption which are directly affected by the change of slurrying medium. The specific power consumption for each of these is presented in Figure 3-6 for each case.

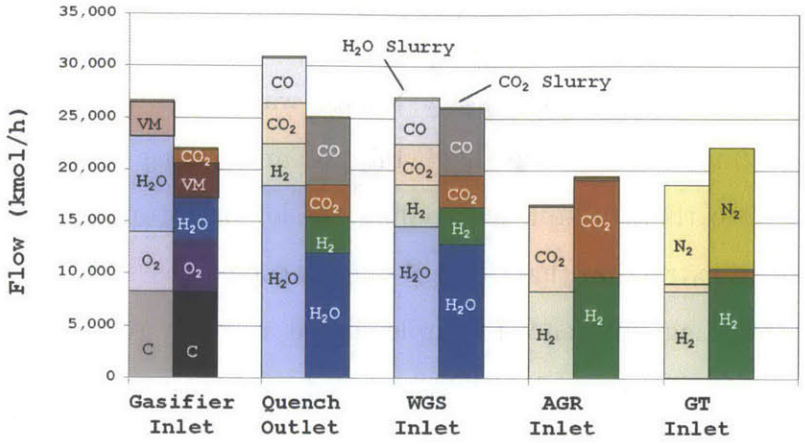

Figure 3-5: Evolution of material stream flow and composition for coal-water slurry (left-hand side bar) and coal-CO_2 slurry (right-hand side bar) feed. Results for a lignite-fed plant with rad-quench cooling are shown as an example. The volatile matter (VM) content of the feedstock is indicated at the gasifier inlet.

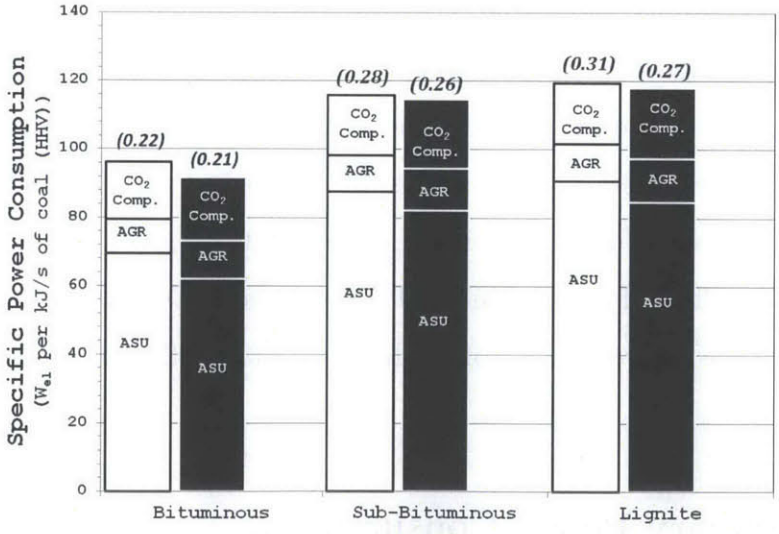

Figure 3-6: Specific power consumption of ASU, Selexol unit, and CO_2 compressor/pump for plants with coal-water slurry (□) and coal-CO_2 slurry (■) feed. The total power consumption of the three units per MW_{el} of gross plant output is presented in parenthesis.

The results show that the specific power consumption of the Selexol unit and CO_2 compressor is on average 15% higher for plants with CO_2 slurry feed; this results directly from the 10-15% CO_2 recirculation required for slurry preparation for the nominal 80% coal loading assumed here.

The specific ASU power reduction is, nevertheless, much larger and dominates the total auxiliary power consumption. An average 10% less power is consumed per unit feedstock energy input in the ASU of plants with CO_2 slurry feed as a result of the reduced oxygen requirement.

Overall, the total specific power consumption of the air separation unit, the acid gas removal unit, and the CO_2 compression chain is only modestly lower for a plant with CO_2 slurry feed; it consumes an average of 4% less power per unit feedstock HHV in these process units. This corresponds to a total auxiliary-to-gross power reduction of 7% in the case of sub-bituminous coal, as indicated in the figure, which agrees with the reduction reported by Dooher et al. for a similar coal. Note, however, that the absolute auxiliary-to-gross power is lower in the work by Dooher as a result of the integration between gas turbine and air separation unit [46].

3.2.5 Net IGCC Efficiency

The net power generation efficiency of the IGCC plant is presented in Figure 3-7 for all cases. The effect of the slurrying medium, coal rank, and syngas cooling method on the net system performance is shown. In addition, the uncertainty associated with the CO_2 slurry loading is indicated in the form of error bars. The relative efficiency improvement of a plant with CO_2 slurry is presented in parenthesis.

The results of this work show that the net power generation efficiency of plants with coal-CO_2 slurry feed is higher than that for plants with water slurry feed. Gasification of bituminous coal with radiant-quench cooling is the only exception, in which case the net plant efficiency is almost identical for both feeding systems. An up to 25% (5%-pt.) higher plant efficiency can be achieved for lignite, which benefits the most from the CO_2 slurry feeding system. The 10% (2.7%-point) higher IGCC efficiency predicted for sub-bituminous coal and rad-quench cooling agrees well with the

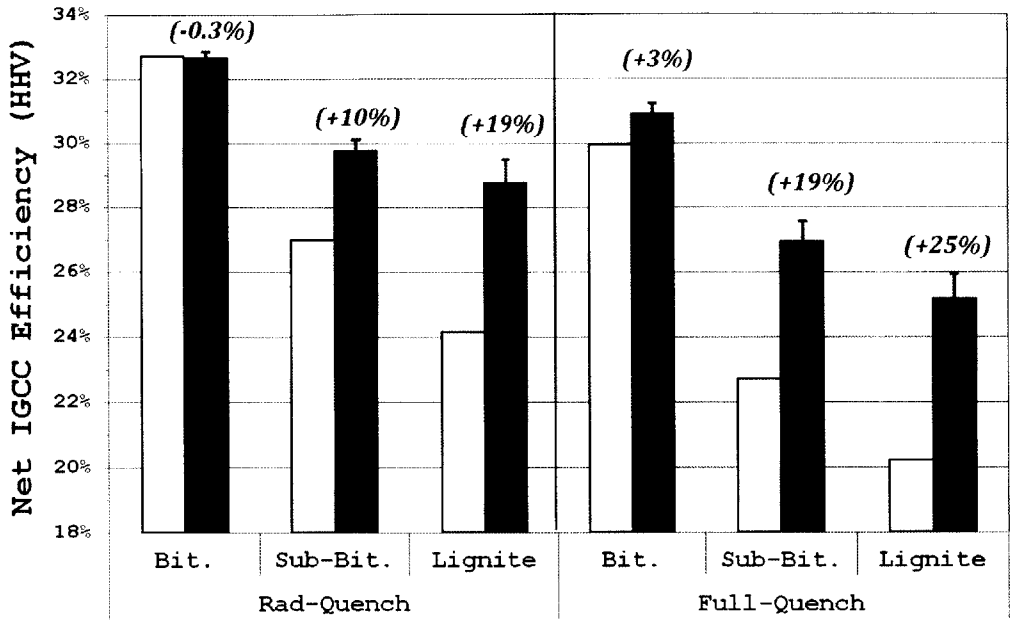

Figure 3-7: Net efficiency of IGCC plant with CCS and coal-water slurry (□) or coal-CO_2 slurry (■) feed. The relative plant efficiency increase resulting from a switch to CO_2 slurry feed is presented in parenthesis. Error bars indicate the uncertainty associated with the maximum achievable slurry loading.

9% (2.8%-point) increase predicted by Dooher et al. for a similar feedstock [46].

Effect of Coal Rank

The net system efficiency decreases with coal rank regardless of the slurrying medium used; the high moisture of low-rank coals -and thus low slurry loading- is responsible for this. What is noticeable is the fact that the plant efficiency drop resulting from switching to a lower rank coal is only about half as much if CO_2 is used for the slurry, instead of H_2O. For combined radiant-quench cooling, for example, a switch from bituminous coal feedstock to lignite leads to an net IGCC efficiency reduction of an estimated 26% (8.6%-pt.) for coal-water slurry, while only 12% (3.9%-pt.) plant efficiency is lost for coal-CO_2 slurry.

Effect of Syngas Cooling Method

Figure 3-7 shows that combined radiant-quench cooling results in an estimated 2-4%-point higher plant efficiency than full-quench cooling. This is expected since steam

produced in the radiant cooler contributes to the power production in the steam turbine while there is no steam generated in a full-quench cooled gasifier. While radiant cooling always results in a higher plant efficiency than full-quench cooling, this may not be the most economically attractive option for cases where the shift steam requirement of the WGS reactor is high, i.e. for syngas with a low H_2:CO ratio like that produced in a gasifier with CO_2 slurry feed.

For such cases, a significant fraction of the steam produced in the radiant cooler must then be extracted from the turbine and mixed with the syngas to provide enough moisture for the water-gas shift reaction; the decision to invest in a radiant cooler is questionable in the first place. Alternatively, a full-quench cooler can be installed; it supplies most of the moisture required in the WGS reactor through evaporative cooling and is a more cost-effective option.

The relative plant efficiency benefit of a plant with CO_2 slurry feed can be more than doubled if full-quench cooling is used, as the numbers in parenthesis in Figure 3-7 indicate. This is particularly true for high-rank coal, which produces a relatively dry syngas as a result of its low moisture content. In other words, the relative IGCC efficiency reduction resulting from full-quench cooling is up to 40% lower if the feed system uses liquid carbon dioxide rather than water.

Effect of Slurry Loading

The calculated net IGCC efficiency observed in Figure 3-7 changes by a maximum of 1%-point as a result of the slurry loading uncertainty, which had not been considered in public studies. The plant efficiency increase predicted for systems with CO_2 slurry feed is outside the uncertainty range associated with the maximum achievable slurry loading for all cases. The only exception is for gasification of bituminous coal and radiant-quench cooling, in which case the net IGCC efficiency difference between both feeding concepts is within the loading uncertainty range.

3.3 Chapter Summary

The feasibility of coal-CO_2 slurry was studied by quantifying the performance of an IGCC plant with CCS and coal-CO_2 slurry feed and comparing it with that of a state-of-the-art CWS-fed plant. The impact of coal rank, slurry loading, and syngas cooling method were considered.

The analysis was conducted with a system-level model of the plant, which assumes full carbon conversion in the gasifier and does not consider the challenges of preparing coal-CO_2 slurry. The results show that the specific oxygen consumption in the plant is reduced by an average of 15% if CO_2 slurry is used, instead of CWS. The gasifier cold gas efficiency improves by an estimated 7-11%-pt.. However, the gasifier produces syngas with a significantly lower H_2:CO ratio. Thus, the shift steam requirement is more than twice that of a plant with CWS feed, penalizing the steam turbine.

Shift steam extraction for the WGS reactor can be avoided in most cases if full-quench syngas cooling is used instead of combined radiant-quench cooling. This cooling method is also a significant source of capital cost savings and leads to a higher relative performance increase for plants with CO_2 slurry feed.

The reduction in specific ASU power is accompanied by an increase in the power requirement of the AGR and CO_2 compressor. Hence, there is a very modest 4% reduction in the total specific parasitic power consumption of these units.

Overall, the net plant efficiency is up to 25% (5%-pt.) higher when the feeding system uses CO_2 slurry instead of CWS. With a single exception, the observed improvement is outside the uncertainty range of the CO_2 slurry loading. Low-rank coal and full-quench cooled gasifiers benefit the most.

Chapter 4

Heterogeneous Gasification Kinetics of Coal-CO_2 Slurry

The previous chapter demonstrated the system-level advantages of gasification-based plants equipped with CO_2 capture and CO_2 slurry feed, under the assumption that carbon conversion remains unchanged. However, the validity of this assumption must be verified, since gasification in carbon dioxide has been observed to be slower than in steam.

This chapter studies the impact of using CO_2 slurry feed on the heterogeneous gasification kinetics and ultimately on carbon conversion and oxygen consumption in a single-stage, slurry-fed EFG operating with bituminous coal.

A Langmuir-Hinshelwood kinetic rate expression taken from the literature, which can reproduce experimental observations reliably under the conditions of interest, is combined with a reactivity adjustment parameter and used to model the gasification kinetics in the gasifier ROM. The results are compared with those from a reactor with conventional CWS feed.

4.1 Gasification in H_2O and CO_2

As shown in Section 3.2.3, coal-CO_2 slurry gasification produces syngas with a significantly higher CO:H_2 ratio than CWS gasification, a trend that has been verified

experimentally through laboratory-scale experiments [46]. This has be attributed to the increasingly dominant role of CO_2 gasification, relative to steam gasification reactions [18].

The effect of higher CO_2 concentrations in the feed on the heterogeneous gasification kinetics and carbon conversion in gasifiers with coal-CO_2 slurry feed has, nevertheless, not been addressed to date. Carbon conversion is one of the key performance measures of a gasifier; incomplete conversion is undesired as it increases the operating costs related to feedstock consumption and ash disposal, as well as capital costs through the need for larger equipment when operating at lower thermal efficiencies.

4.1.1 Mechanism

Several mechanisms have been proposed for the reaction of char with steam and CO_2. It is believed that the principal steps are the dissociative adsorption of the gasification agent on an active site on the char surface, followed by associative desorption of the surface complex [81–83]. For CO_2 gasification, the reduced mechanism is:

$$C_f + CO_2 \underset{j_{VII}}{\overset{i_{VII}}{\rightleftharpoons}} C(O) + CO \tag{VII}$$

$$C(O) \xrightarrow{i_{VIII}} CO, \tag{VIII}$$

where C_f represents a free site on the char surface, C(O) a chemisorbed atom on a free site, and i and j are the forward and backward rate constants, respectively. Similarly, the main steps in the reaction of char with steam are:

$$C_f + H_2O \underset{j_{IX}}{\overset{i_{IX}}{\rightleftharpoons}} C(O) + H_2 \tag{IX}$$

$$C(O) \xrightarrow{i_X} CO \tag{X}$$

In these oxygen-exchange mechanisms, the well-known retarding effect by the products CO and H_2 is accounted for via reverse reactions (VII) and (IX), respectively. Other, more complex, mechanisms which consider additional steps as well as inhibition through different routes such as direct adsorption of the products onto active sites have also been proposed [84 87].

The rate of char gasification in pure CO_2 has been measured to be slower than that in pure H_2O but within the same order of magnitude. A selection of experimental observations comparing CO_2 and H_2O gasification rates under conditions at which the chemical reaction alone controls the rate of reaction is presented in Table 4.1.

Table 4.1: Relative rates of CO_2 and H_2O gasification in the kinetic control regime

Feedstock	Partial Pressure	Temperature	Rate		Source
			CO_2	H_2O	
Purified carbon	4-40 bar	800-870 °C	1	3-6	[85, 88]
Bituminous coal char	< 60 bar	900 °C	1	3-4	[65]
Brown coal char	< 1 bar	800 °C	1	2	[89]
Bituminous coal char	1-30 bar	850-900 °C	1	2-4	[90]

4.1.2 Competition for Active Reaction Sites

Extensive work has been performed characterizing the gasification kinetics in the CO_2/CO and H_2O/H_2 systems in which the products CO and H_2 have been shown to retard the CO_2 and H_2O gasification reactions, respectively (e.g. [65, 84, 91–94]). However, the kinetics in a mixed $CO_2/H_2O/CO/H_2$ environment typical of commercial gasifiers have not been characterized extensively, in particular at high pressures. Of particular interest here is whether the presence of CO_2 slows down the overall gasification rate in a mixed CO_2/H_2O environment, relative to a system containing only steam; this is especially relevant for gasifiers with CO_2 slurry feed. The underlying question is whether the gasification agents CO_2 and H_2O compete for the same active sites on the char surface or whether they react on separate sites, a topic for which much disagreement still remains.

At atmospheric pressure conditions, this question was addressed independently by

Blick [95], Everson et al. [96], and Huang et al. [92] for chars from coals of different ranks. All three groups concluded that the surface mechanism which accounts for the reaction of C-CO_2 and C-H_2O on separate active sites is best at explaining the experimentally observed rates in a mixture of $CO_2/H_2O/CO/H_2$. The overall gasification rate under kinetic control conditions, r, could be successfully predicted by adding the individual rates:

$$r = \frac{k_{CO_2} P_{CO_2}}{1 + \kappa_{CO_2} P_{CO_2} + \kappa_{CO} P_{CO}} + \frac{k_{H_2O} P_{H_2O}}{1 + \kappa_{H_2O} P_{H_2O} + \kappa_{H_2} P_{H_2}}, \tag{4.1}$$

where P is the partial pressure of each gas component in the mixture.

The rate parameters k and κ in eq. (4.1) have an Arrhenius-type temperature dependence and are determined empirically. Their functional relationship to the elementary reaction rates i_{VII}-i_X and j_{VII}-j_{IX} depends on the reaction mechanism assumed and hence differs between authors. Nevertheless, different mechanism often lead to the same form for the kinetic rate expression. In general, the parameters k_{CO_2} and k_{H_2O} correspond to elementary reaction rates or multiples thereof, whereas κ_{CO_2}, κ_{CO}, κ_{H_2O}, and κ_{H_2} are elementary reaction rate ratios.

In contrast to the observations at atmospheric pressure conditions, Roberts and Harris [93] showed that in a pressurized system containing a mix of CO_2 and H_2O, the slower CO_2 gasification reaction inhibits the H_2O gasification reaction by occupying active sites on the char surface, effectively slowing down the overall char gasification rate through competition for active sites. Gasification in a mixed gasifying agent environment with 50 vol.% CO_2 was shown to be up to two times slower than in pure H_2O under identical conditions. Measurements were carried out for three different bituminous coal chars at partial pressures of up to 10 bar.

Similary, Muehlen et al. [65, 97] combined all the reaction steps proposed by Blackwood et al. for CO_2 and H_2O gasification at high pressure [85, 88] and assumed single surface coverage to derive a rate expression of the combined form:

$$r = \frac{k_{CO_2} P_{CO_2} + k_{H_2O} P_{H_2O}}{1 + \kappa_{CO_2} P_{CO_2} + \kappa_{CO} P_{CO} + \kappa_{H_2O} P_{H_2O} + \kappa_{H_2} P_{H_2}}, \tag{4.2}$$

which succeeded in predicting the reaction rate of a German bituminous coal char in a semitechnical-scale fluidized bed reactor operating at 40 bar in an environment with mixed gasifying agents and products. The rate constants were determined for the binary systems CO_2/CO and H_2O/H_2 at pressures of up to 70 bar. Note that squared and hydrogasification terms contained in Muehlen's original work have been neglected in equation (4.2) since they have been shown to be 3-5 orders of magnitude smaller at the high temperatures characteristic of an EFG [98, 99].

The work conducted by Muehlen et al. is of especial significance. It is still, to date, to the best of our knowledge, the only research group who has published a Langmuir-Hinshelwood (LH) kinetic expression for char gasification at high pressure derived from their own experiments, accounting for the presence of mixed gasifying agent and products, and validated with data from a semitechnical plant.

More recently, Liu [100] determined LH rate constants for the CO_2/CO and H_2O/H_2 systems from published high pressure experiments for different chars. Liu found that the rate expression (4.2) is significantly better than equation (4.1) at predicting the rates measured by Goyal et al. [101] at high pressure in a mixed $CO_2/H_2O/CO/H_2$ environment. In later work, Liu and Niksa [98] conducted an extensive survey of the literature for pressurized coal gasification and used mean rate constants as a basis for the development of the Carbon Burnout Kinetics Model for Gasification (CBK/G). This commercial kinetics package models the gasification rate in a mixed gas environment using an equation of the same form as equation (4.2) and thus assumes competition between CO_2 and H_2O for active sites.

The observations above indicate that there is no general agreement regarding the role of the competition for active sites between CO_2 and H_2O in char gasification kinetics. Data at ambient pressure tends to support the independent active site assumption, whereas the competing active site mechanism has been shown by multiple authors to apply at high pressures, where surface saturation is high.

Most recently, an alternative surface mechanism was proposed by Umemoto et al. [102], who found that both the competing and the independent active site mechanisms fail to explain experimental observations for three bituminous coal chars in a mixed

$CO_2/H_2O/CO/H_2$ environment under atmospheric pressure conditions; the former underpredicts the gasification rate while the latter overpredicts it. According to the proposed mechanism, which proved to be successful at predicting the measured rates, active sites on the char surface are neither independent nor competing but rather shared by CO_2 and H_2O. An analogous study at pressurized conditions has not been published.

4.2 Methodology

The gasifier ROM described in Section 2.3.3 was used to quantify carbon conversion in a reactor with bituminous coal-CO_2 slurry feed and compare it with that of one based on conventional CWS. For CO_2 slurry, two cases were considered: one where the gasifier operates at the reference temperature and one where it operates at the reference conversion.

The slurry coal loading was assumed to be a nominal 71% for both slurries, to allow an easier comparison of the kinetics. In reality, the maximum loading in CO_2 is expected to be higher than that of water slurry [33, 34, 45].

4.2.1 Intrinsic Heterogeneous Kinetics at High Pressure

The kinetic submodel in the ROM was modified to include an LH expression, which is valid under the high partial-pressure conditions relevant to this work. LH kinetics are derived from multistep adsorption-desorption reaction mechanisms and thus have a more mechanistic basis than power-law kinetic expressions of the form

$$r = k_{\mathrm{CO_2}} P_{\mathrm{CO_2}}^{n_{\mathrm{CO_2}}} + k_{\mathrm{H_2O}} P_{\mathrm{H_2O}}^{n_{\mathrm{H_2O}}}, \tag{4.3}$$

which are strictly empirical. In equation 4.3, k is the reaction rate constant, which has an Arrhenius-type temperature dependence, P is the partial pressure of the gas, and n is the pressure order, which is uncertain at pressures beyond the validity range of the kinetic expression. The intrinsic gasification rate r, in inverse time units, is the

rate under conditions at which the kinetics alone control the gasification reactions, i.e. typically at temperatures below about 1000°C.

LH kinetics are especially attractive for high pressure applications since they are able to reproduce the asymptotic rate behavior caused by surface saturation under those conditions, as well as to account for the inhibiting effect of the reaction products [94].

The LH kinetic expression used in this work is of the form:

$$r = \frac{k_{CO_2} P_{CO_2} + k_{H_2O} P_{H_2O}}{1 + \kappa_{CO_2} P_{CO_2} + \kappa_{CO} P_{CO} + \kappa_{H_2O} P_{H_2O} + \kappa_{H_2} P_{H_2}}, \tag{4.4}$$

The underlying assumption behind the combined form of eq. (4.4) is that the competing active site mechanism is valid, as indicated by the high pressure observations by Muehlen [65], Roberts and Harris [93], Liu [100], and Liu and Niksa [98].

Gasification rates have been observed to differ from coal char to coal char under otherwise identical conditions. Such differences arise predominantly from the specific char reactivity and morphology resulting from the parent coal characteristics. For a given gasification environment, the gasification rate has been observed to be highest for coals with low carbon content; for low-rank coal, the amount and type of mineral matter in the parent coal is also a key factor. Heating rate differences, though not considered in this work, also have a significant effect on the char reactivity [103–105].

The relative reactivity factor, ψ, is the parameter used in this work to account for such reactivity differences when predicting the gasification rate in the ROM. This feedstock-specific adjustment parameter, first introduced by Johnson [104], allows the calculation of the gasification rate from eq. (4.4) for chars other than the reference char for which the kinetic rate parameters were determined:

$$r^* = \psi \cdot r. \tag{4.5}$$

Here, r is the reference gasification rate predicted with eq. (4.4) for the reference char and r^* is the reactivity-adjusted gasification rate for a different char. The rate

parameters reported by Muehlen et al. for a reference, german bituminous coal char were selected for calculation of the reference gasification rate in equations (4.4) and (4.5) [65, 97]. The parameters are summarized in Table 4.2 and resulted in the lowest root mean square (RMS) deviation when compared with 124 gasification rate measurements at high pressure taken from the literature [101, 106–111].

Table 4.2: Kinetic rate parameters by Muehlen [65] for use in eq. (4.4): $k, \kappa = Aexp^{\frac{-E}{RT}}$

	A		E	
k_{CO_2}	$2.71 \cdot 10^4$	$bar^{-1}\ min^{-1}$	153.1	kJ/mol
k_{H_2O}	$2.96 \cdot 10^5$	$bar^{-1}\ min^{-1}$	154.0	kJ/mol
κ_{CO_2}	$2.06 \cdot 10^{-2}$	bar^{-1}	-23.0	kJ/mol
κ_{CO}	$3.82 \cdot 10^{-2}$	bar^{-1}	-48.1	kJ/mol
κ_{H_2O}	$1.11 \cdot 10^1$	bar^{-1}	29.5	kJ/mol
κ_{H_2}	$1.53 \cdot 10^{-9}$	bar^{-1}	-209.2	kJ/mol

Figure 4-1 is a parity plot comparing the reactivity-adjusted gasification rate predicted here for a given set of conditions with the corresponding experimental data points. The narrow confidence interval range indicates that the gasification rate prediction can reproduce the experimental data with reasonable accuracy despite the wide range of feedstocks and conditions and the over four orders of magnitude spread of the rate data. No systematic deviations are observed.

A single value of ψ was calculated for each char according to:

$$\psi \equiv \frac{\sum_{z=1}^{Z} \frac{r\ (T_z, P_{H_2O,z}, P_{CO_2,z}, P_{CO,z}, P_{H_2,z})}{r_{exp}\ (T_z, P_{H_2O,z}, P_{CO_2,z}, P_{CO,z}, P_{H_2,z})}}{Z}. \tag{4.6}$$

Here, $r_{exp}(T_z, P_z)$ is the z^{th} experimentally measured gasification rate for a given char at a temperature and reactant partial pressure of T_z and P_z, respectively, and $r(T_z, P_z)$ is the rate predicted by eq. (4.4) for the reference char under the same set of conditions. The variable Z is the number of experimental measurements available for each char, which is 8 on average for the dataset considered here [101, 106–111]. Note that ψ is a relative factor, as its name says, and its value is hence specific to the pair of chars used in eq. (4.5).

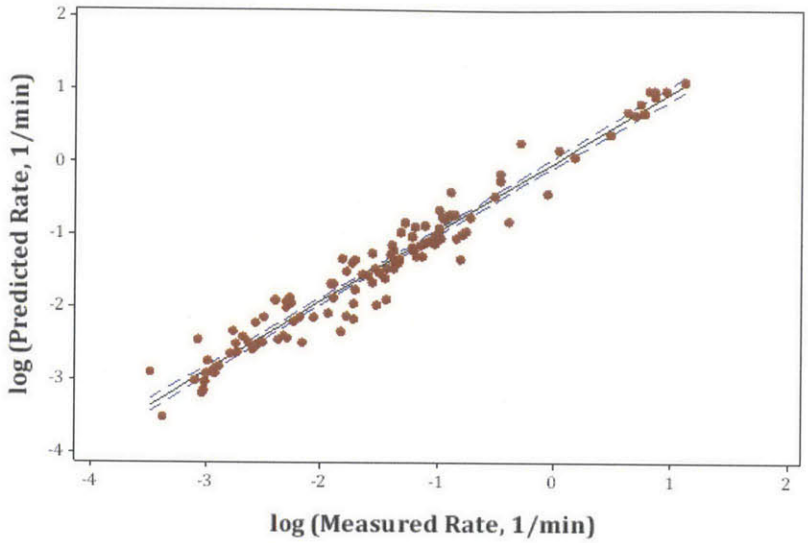

Figure 4-1: Parity plot comparing gasification rate prediction with experimental measurements from the literature [101, 106–111]; dashed lines indicate the 95% confidence interval. The RMS deviation is 0.23 min^{-1}.

The resulting relative reactivity factors are presented in Figure 4-2 as a function of the parent coal's dry ash-free carbon content (C_{daf}). The magnitude of ψ extends over three orders of magnitude, which agrees well with the range reported elsewhere [103, 112]. The trend of increasing reactivity with decreasing carbon content is correctly represented, though with a wide spread of the data, in particular for low-rank coal. The latter is likely due to the reactor-specific contribution to ψ, which cannot be accounted for by the C_{daf} only, as well as to additional factors such as mineral matter content. Simple char properties alone have been observed to be an unsuitable indicator for char reactivity [103].

4.2.2 High Temperature Heterogeneous Kinetics

The effectiveness factor approach was used in the ROM in order to account for the transition from the kinetically-limited regime into the pore diffusion-limited regime at high temperatures. In this approach, the observed gasification rate, r_{obs}, which is dominated by both chemical kinetics and mass transport limitations, is estimated from the reactivity-adjusted intrinsic rate r^* and the effectiveness factor η, which is

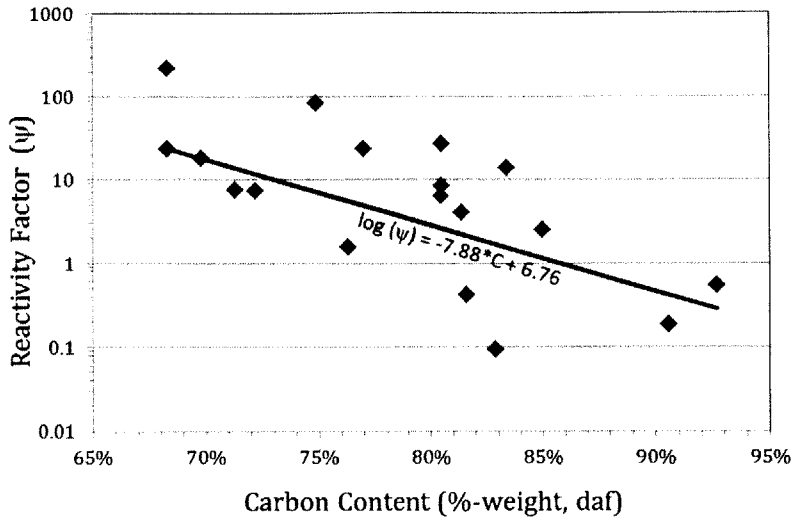

Figure 4-2: Relative reactivity factor as a function of dry, ash-free carbon content of parent coal

defined as

$$\eta \equiv \frac{r_{\text{obs}}}{r^*}. \tag{4.7}$$

The effectiveness factor is widely used to account for intra-particle diffusion effects on kinetics in catalytic pellets and solid fuels. It is, per definition, less than 1 when internal mass transport limitations exist. In spherical coordinates, η can be predicted by [113 115]:

$$\eta = \frac{1}{\phi}\left(\frac{1}{tanh(3\phi)} - \frac{1}{3\phi}\right) \tag{4.8}$$

where (ϕ) is the Thiele Modulus:

$$\phi = \frac{L\nu_0 r^*(P_{i,s})}{\sqrt{2}}\left[\int_0^{P_{i,s}} D_e \nu_0 r^*(P_i) dP\right]^{-1/2} \tag{4.9}$$

The Thiele Modulus is a measure of the ratio of the surface reaction rate to the rate of diffusion through the pores of the char particle. In equation 4.9, P_i is the local partial pressure of the reacting gas in the particle and $P_{i,s}$ the partial pressure at the particle surface. L is the characteristic length of the particle, which is $R/3$ for a sphere, where R is its radius. ν_0 is the stoichiometric factor of the reactant per mole of carbon consumed and D_e is the effective diffusivity, which combines the effects of

molecular and Knudsen diffusion and depends strongly on the particle morphology. In the ROM, the calculation of D_e is based on an assumed char particle porosity of 0.25 in combination with an average pore radius estimated from the random pore model [61].

While calculation of the effectiveness factor is straightforward in the case of power-law kinetics, this is not the case for LH kinetics, since no analytical solution exists for ϕ. Approximate values were estimated following the methodology by Hong et al. [115], which requires manipulation of eq. (4.4) by conducting a mass balance inside the char particle and solving a system of differential equations [116].

Calculation of the observed reaction rate under pore diffusion-limited conditions according to eq. (4.7) requires extrapolation of r to high temperatures, an approach that has been used successfully in the past for combustion applications [117, 118]. Nevertheless, this is one of the factors which contributes most to the uncertainty of the present kinetic analysis. The experimental measurements of high pressure, high temperature gasification kinetics is the topic of current research [117].

4.2.3 Cases Studied

Bituminous coal is studied here due to the availability of conversion data for this feedstock, which is required for the development of the kinetic model. This is the most conservative case, however, since CO_2 slurry feed is particularly attractive for low-rank coal.

The reactor resembles the 900 ft^3 gasifier used in the Cool Water IGCC Demonstration Project, see Table 2.3. The Illinois 6 coal in Table 2.1 was used for the analysis. It is very similar to the Illinois 6 used in the Cool Water gasifier.

The CWS-fed Cool Water gasifier has a reported single-pass carbon conversion of 96.5% [52]. This value was used as a reference for the direct estimation of ψ for this reactor-coal combination. The availability of a conversion datum allowed for validation of the more general correlation in Figure 4-2, which can be used for the estimation of ψ when no reference conversion is available, as in the case of lignite.

The direct estimation of the relative reactivity factor was carried out by running

the ROM with different values of ψ until the estimated conversion was in agreement with the reported conversion. A value of ψ = 8.3 was calculated in this way for bituminous coal. It is within the range expected for its C_{daf} in Figure 4-2.

The reactivity factor estimated for bituminous coal and used throughout this work is reported in Table 4.3. The value for lignite is also shown and was estimated using the correlation in Figure 4-2, given the lack of reference conversion data for this feedstock in a commercial-scale EFG like the one considered here. The gasification kinetics of lignite are not discussed here in detail but are considered in the overall technoeconomic analysis in Chapter 6.

Table 4.3: Relative reactivity factor (ψ) of bituminous coal and lignite used in this study

	Bituminous	**Lignite**
ψ	8.3	9.8

The ROM was first used to simulate the base case operation of a CWS-fed gasifier. Next, the performance of a CO_2 slurry-fed reactor of the same size and operating with the same feedstock as for the base case was studied. For comparison purposes and because the gasifier is the component of interest in this study, the coal throughput was left unchanged, i.e. the residence time of the water slurry and CO_2 slurry-fed gasifiers is assumed to be essentially equal.

The oxygen flow rate to the CO_2 slurry-fed reactor was initially varied to achieve the reference gasifier outlet temperature. This corresponds to the cases labeled `CO2_T`. Because it is expected that the gasifier refractory can tolerate variation of the reactor temperature within a certain range, an additional case was considered. For the latter, the gasifier outlet temperature - and hence oxygen flow rate - was varied to achieve the reference conversion, rather than the reference temperature.

The overall process economics determine whether it is worthwhile to aim at a high conversion at the cost of a higher oxygen consumption or not. The economic attractiveness of operation at higher temperatures is studied in Chapters 6 and 7 for IGCC and syngas production applications, respectively.

4.3 Results and Discussion

The main results obtained from simulations with the ROM are presented in this section. Profiles are plotted as a function of the gasifier length, which is taken here to be the distance from the injection point at the top of the reactor, see Figure 2-9.

Because node spacing cannot be optimized during ROM runs with the simulation tool used, the ROM contains finer node spacing at the beginning of each zone, where the steepest gradients are expected [61]. This leads to the uneven distribution of data points observable in the gasifier profiles presented. All profiles begin at the outlet of the IRZ zone, i.e. following the devolatilization and mixing of the inlet streams with the recirculating gasification products. Dotted lines in the profile charts presented indicate zone transitions.

4.3.1 Gas Phase Composition

The mole fraction of the main gas phase components estimated from the simulations is presented in Figure 4-3 along the length of the gasifier for the H_2O slurry and CO_2 slurry cases with the same outlet temperature. The depletion of oxygen in the figure marks the beginning of the gasification reactions.

The CO_2 content at the beginning of the gasification process is calculated to be only marginally higher in a reactor with CO_2 slurry feed. There are two reasons for this; first, the mass flow of CO_2 replacing H_2O in the slurry represents a smaller contribution on a mole basis due to the high molecular weight of CO_2. Only about 60% of the liquid inlet to the gasifier is CO_2, on a mole basis, while the remaining 40% is coal moisture. Second, CO_2 produced in the initial, heating section of a CO_2 slurry-fed gasifier is calculated to be 30% lower than in a reactor with water slurry feed. CO_2 heats up and vaporizes more readily than water so less oxidation of volatiles and char is required to heat up the feed to a specified temperature.

The largest difference in the gas phase composition predicted for a gasifier with CO_2 slurry is its H_2O and CO content. The fraction of H_2O to which the char is exposed during gasification decreases by almost half when the feed is CO_2 slurry, as

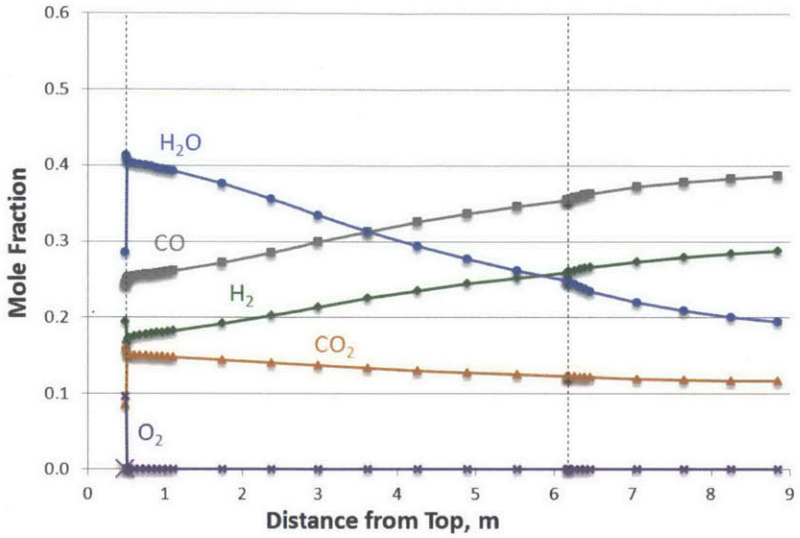

(a) Coal-water slurry feed

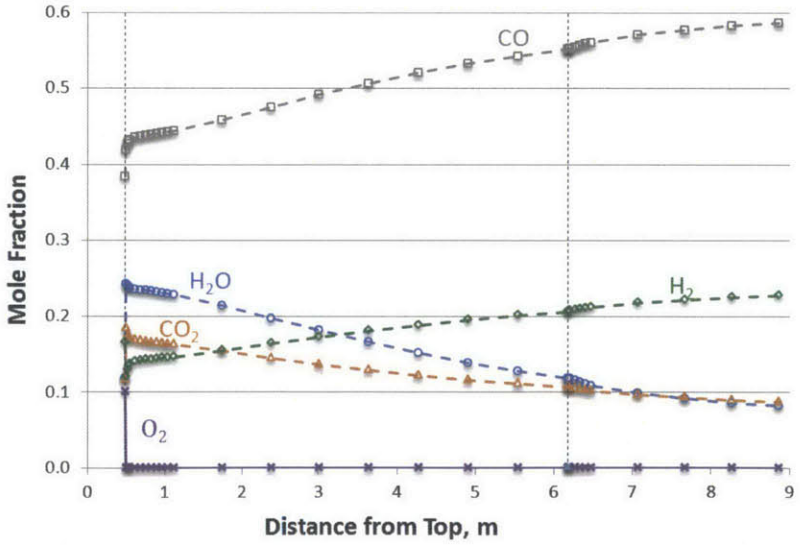

(b) Coal-CO_2 slurry feed

Figure 4-3: Gas composition profile along gasifier for H_2O slurry feed and CO_2 slurry feed. The reactor operates with bituminous coal and at the reference outlet temperature.

the figure shows. Less water in the feed and less oxidation of the hydrogen-containing volatiles are the main causes for this, analogous to the discussion above for CO_2.

The almost two times higher concentration of CO calculated in a CO_2 slurry-fed gasifier indicates that the CO_2 gasification reaction, eq. (VII)-(VIII), plays a more important role in the overall carbon conversion process when CO_2 is used in the feeding system. For the case of water slurry, on the other hand, conversion is strongly dominated by the steam gasification reaction, eq. (IX)-(X), as a result of the very high ratio of H_2O to CO_2. This ratio is estimated to decrease by a factor of two when the feeding system is based on CO_2, thus increasing the contribution of the CO_2 gasification reaction.

4.3.2 Temperature Profile

The heat of reaction for CO_2 gasification is about 30% higher than that of steam gasification. Overall, gasification in a reactor with CO_2 slurry is thus more endothermic than in a reactor with water slurry. This can be seen in Figure 4-4, where the temperature profile inside the gasifier is shown. For the reference outlet temperature of 1,443 °C, an almost 100K higher peak temperature is required in the gasifier with CO_2 slurry to provide enough heat for the endothermic gasification reactions.

4.3.3 Gasification Rate

The higher contribution of the CO_2 gasification reaction to the overall carbon conversion in a reactor with CO_2 slurry feed raises questions related to how this reaction affects the process outcome. Of particular interest is whether the trend of the slower kinetics of CO_2 gasification observed at low temperatures (see Table 4.1) applies at higher temperatures and the degree to which a higher CO concentration inhibits the gasification reactions.

The intrinsic and observed gasification rate profiles obtained from the ROM simulations are plotted in Figure 4-5. The results show that for both water slurry and CO_2 slurry, internal mass transport limitations play an important role in the early

gasifier stages, where the temperature is highest and the kinetics fastest: the observed reaction rate is up to 2 times lower than the intrinsic rate. The role of internal mass transport limitations diminishes along the reactor as the intrinsic reaction rate drops with the temperature and with product accumulation; the process becomes fully kinetically controlled by the time the syngas leaves the gasifier.

The observed reaction rate predicted for a system with CO_2 slurry feed is 20-60% lower than one with water slurry feed. This is true both in the pore diffusion-limited regime near the gasifier inlet, where the intrinsic rates are nearly equal, and in the kinetically limited region near the outlet. The results thus indicate that CO_2 slurry has a detrimental effect on both the intrinsic kinetics and the mass transport processes taking place inside the char particle.

Intrinsic Gasification Kinetics in Pure CO_2 and H_2O

A comparison between the intrinsic reaction rate of Illinois 6 char in pure H_2O and pure CO_2, as predicted by the Langmuir-Hinshelwood kinetic expression used in this study, is presented in Figure 4-6. The normal probability density functions (PDF) shown were constructed from the RMS deviation between prediction and experiments in Figure 4-1.

The results in the figure show that the predicted gasification rate (mean of PDF) is about 4 times slower for CO_2 than for H_2O at low temperatures. This result agrees well with experimental observations under similar conditions, see Table 4.1.

For the conditions inside the entrained flow gasifier considered, however, the situation is somewhat different. The intrinsic gasification rate in pure CO_2 is predicted to be the same or higher than in pure H_2O in the range 1,400-2,000 °C. This can be attributed to the slightly higher temperature dependence of the CO_2 gasification rate constant in the rate expression used, a fact that is supported by multiple experimental observations (e.g. [89]).

For practical purposes and in view of the large areas of overlap in Figure 4-6, the intrinsic rates of CO_2 and H_2O gasification can be considered to be nearly equal at entrained flow gasifier conditions. Observations of slower intrinsic reaction kinetics

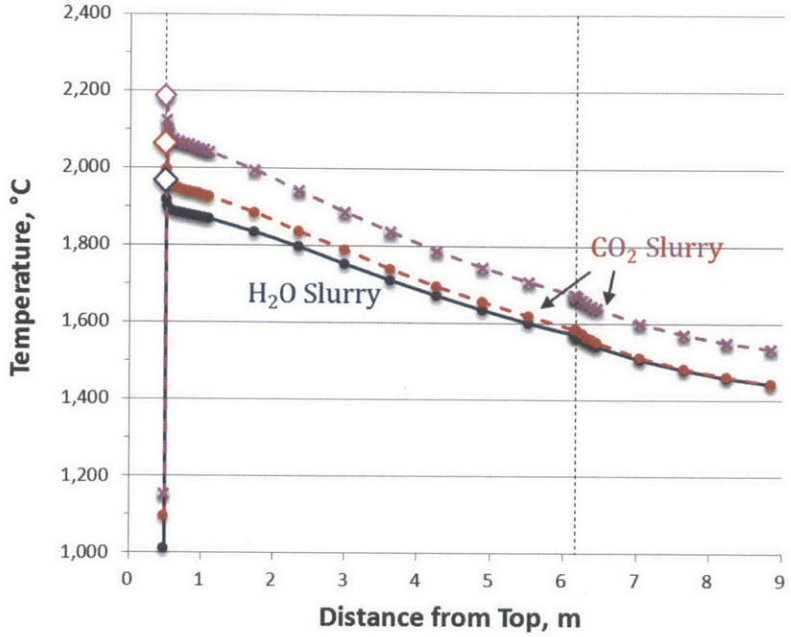

Figure 4-4: Temperature profile in gasifier operating at the reference outlet temperature (•) and H_2O slurry (—) or CO_2 slurry (---) feed. A case in which the CO_2 slurry-fed reactor operates at the base carbon conversion (higher outlet temperature) is also shown (×). The peak reactor temperature is indicated in each case (◇).

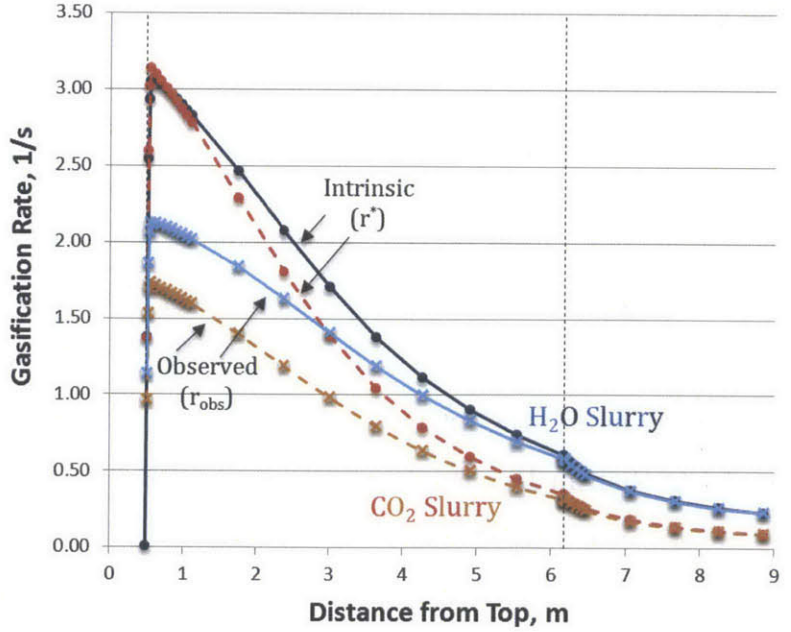

Figure 4-5: Intrinsic (•) and observed (×) reaction rate for a gasifier with water slurry (—) and one with CO_2 slurry feed at the reference outlet temperature (---)

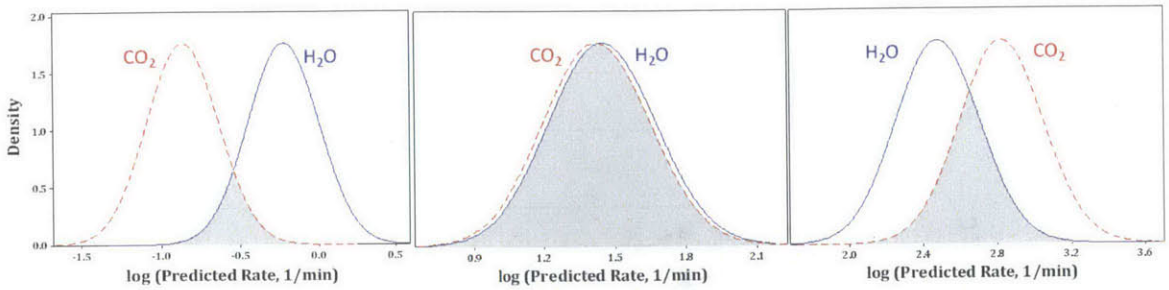

Figure 4-6: Probability density function of intrinsic gasification rate in pure H_2O (—) and pure CO_2 (---) at 30 bar and 900 °C (left), 1,400 °C (middle), and 2,000 °C (right) as predicted by eq. (4.5)

for CO_2 gasification at low temperatures can therefore not be extended to high temperature conditions in order to explain the slower intrinsic rates in Figure 4-5 for gasification of coal-CO_2 slurry.

CO Inhibition

Given that the partial pressure of CO is estimated to be almost two times higher in gasifiers with CO_2 slurry feed, CO inhibition of the gasification reactions is considered to be a potential cause for the slower intrinsic gasification kinetics observed for this feeding system.

While both CO and H_2 are known to inhibit the intrinsic gasification reaction (e.g. [84, 85, 88, 91]), CO has been reported to have a stronger effect than H_2 [119, 120]. This trend is correctly reproduced by the kinetic expression used in this study, as shown in Figure 4-7, where the predicted inhibitory effect of CO and H_2 are compared at different temperatures for a fixed partial pressure of the gasifying agents.

As illustrated in the figure, the intrinsic reaction rate is inhibited more strongly in the presence of CO than in H_2. Product inhibition is predicted to decrease with increasing temperature, as expected [121]. For the temperatures above 1,400 °C relevant to entrained flow gasifiers, H_2 inhibition is negligible compared to CO inhibition. Inside the gasifier, inhibition by CO is augmented by the higher concentration of this gas, relative to H_2. This is particularly true for gasifiers with CO_2 slurry feed, for which the ratio of CO to H_2 is twice as high as in gasifiers with water slurry feed.

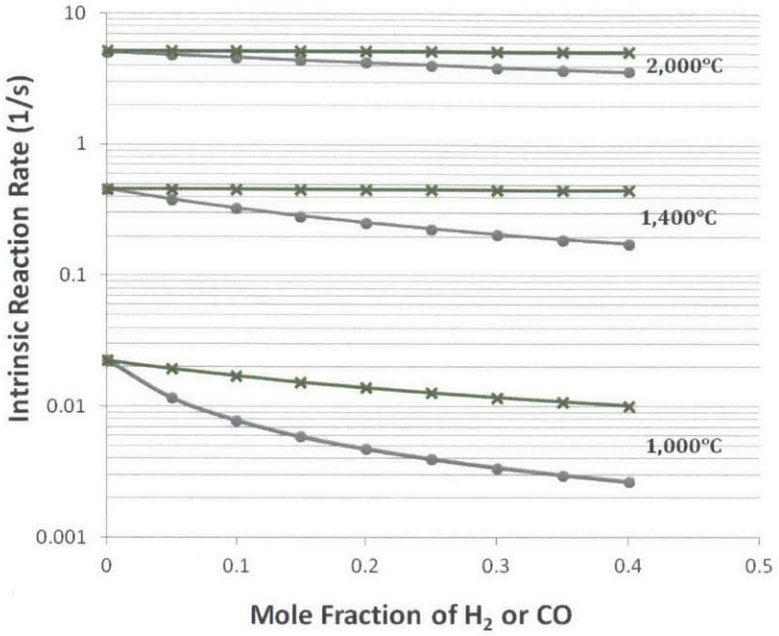

Figure 4-7: Inhibiton of intrinsic gasification rate by CO (•) and H_2 (×) at different temperatures and a total pressure of 30 bar as calculated with eq. (4.5). The mole fraction of H_2O and CO_2 in the mixture is assumed to be 0.2.

Pore Diffusion Limitations

The increased concentration of CO_2 and CO relative to H_2O and H_2 in a gasifier with CO_2 slurry feed proved to also affect the degree of internal mass transport limitations. Near the gasifier inlet, where this effect is most significant, Figure 4-5 shows that the ratio of intrinsic to observed reaction rate, i.e. the effectiveness factor, is expected to be about 20% lower in a reactor with CO_2 slurry feed despite the fact that the intrinsic reaction rate is almost the same. This result can be attributed to the compositional change of the gas phase in gasifiers with CO_2 slurry feed, in combination with the fact that CO_2 and CO have a lower diffusivity than H_2O and H_2.

4.3.4 Carbon Conversion

The slower gasification rate in a reactor with CO_2 slurry feed results in a reduction of the carbon conversion achieved for a given outlet temperature. The results in Figure 4-8 show that when the gasifier outlet temperature is maintained at its base

value of 1,443 °C, carbon conversion drops from 96.5% for water slurry to 89.8% for CO_2 slurry.

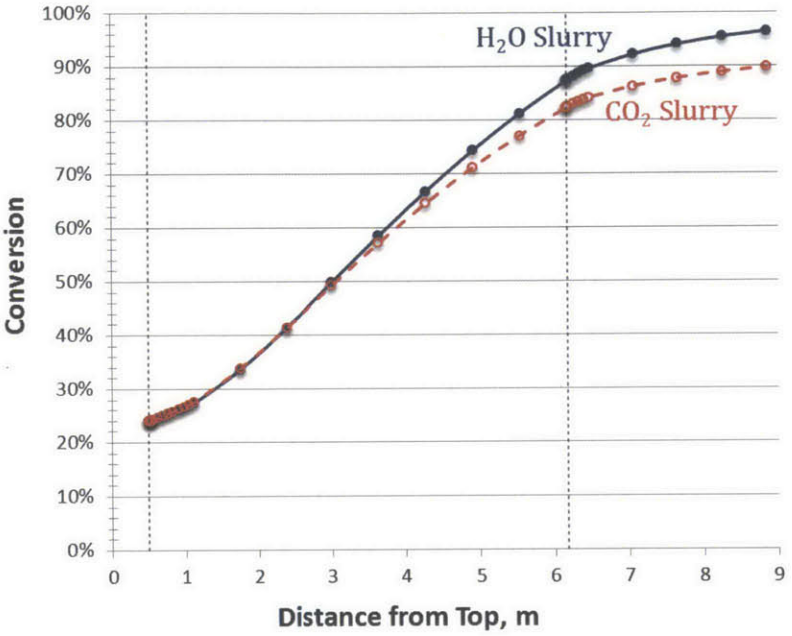

Figure 4-8: Carbon conversion in a gasifier with H_2O or CO_2 slurry feed and operating at the reference outlet temperature.

To quantify how significant the estimated conversion reduction is, the gasifier throughput was adjusted in the model to achieve the base case conversion of 96.5%. The simulation results show that a 45% throughput reduction would be necessary to outweigh the slow kinetics in a reactor with CO_2 slurry.

Because the reaction rate near the gasifier outlet proved to be limited by the intrinsic gasification kinetics, the conversion in a CO_2 slurry-fed gasifier can be increased by raising its operating temperature. The results of this study showed that a 90K higher outlet temperature is necessary in order to achieve the same conversion as with a water slurry fed reactor. As shown in Figure 4-4, this increase leads to a 220K higher peak gasifier temperature near the inlet, relative to a reactor with water slurry feed, and could thus compromise the integrity and lifetime of the refractory and burner.

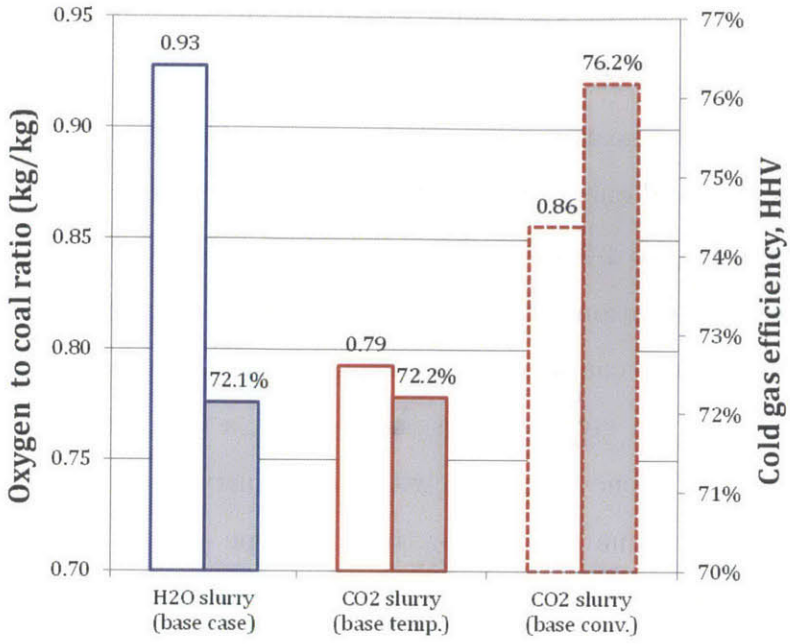

Figure 4-9: Ratio of oxygen to dry coal (□, left axis) and cold gas efficiency (■, right axis) for a gasifier with water slurry feed and one with CO_2 slurry feed operating at the reference temperature or at the reference conversion.

4.3.5 Oxygen Consumption and Cold Gas Efficiency

Previous work for a similar feedstock and slurry loading as those used here reported oxygen savings of an estimated 10% for a gasifier with CO_2 slurry feed; the gasifier outlet temperature and carbon conversion were assumed to remain unchanged, relative to a gasifier based on water slurry [18]. However, this study shows that previous assumptions are not realistic since carbon conversion will decrease significantly in a gasifier with CO_2 slurry feed if the gasifier outlet temperature is kept constant.

Results in Figure 4-9 show that once the conversion reduction is accounted for, the estimated oxygen consumption in a system based on CO_2 slurry is 15% lower than in a system with water slurry feed for the base case outlet temperature of 1,443 °C. However, if the base case conversion of 96.5% is to be maintained in a gasifier with CO_2 slurry feed, the net oxygen savings account for 8%, relative to a case with water slurry feed, as a result of the required 90K increase in the outlet temperature.

The gasifier cold gas efficiency is also presented in Figure 4-9. In contrast to the

carbon conversion in Figure 4-8, which quantifies the percentage of carbon that is converted to gas, irrespective of whether the product is CO_2 or CO, the cold gas efficiency considers the heating value of the syngas. It is defined as the fraction of the feedstock's chemical energy that is retained in the cooled gaseous product.

The results in Figure 4-9 show that, once the carbon conversion reduction introduced by slower gasification kinetics is accounted for, the cold gas efficiency in a gasifier with bituminous coal-CO_2 slurry feed is almost identical to that of one with water slurry feed. For a given conversion, however, a CO_2 slurry-fed gasifier has a 6% higher cold gas efficiency than one with water slurry feed. This advantage is less than the previously estimated 10% for this coal type [18] as a result of the higher gasification temperature required to maintain the carbon conversion unchanged.

4.4 Chapter Summary

The heterogeneous gasification kinetics were modeled for a gasifier with bituminous coal-CO_2 slurry feed in order to assess the impact of this alternative feeding system on carbon conversion, oxygen consumption, and cold gas efficiency inside the reactor. A Langmuir-Hinshelwood intrinsic rate expression from the literature, which was developed at high pressure and validated in an environment of $H_2O/CO_2/CO/H_2$, was selected based on its ability to reproduce a wide range of experimental observations at high pressures. This expression assumes that there is competition between CO_2 and H_2O for active sites on the char surface. A reactivity adjustment parameter was introduced to account for the rank-dependency of the feedstock reactivity. Moreover, an effectiveness factor approach was used to account for internal mass transport limitations at high temperatures.

The results from the gasifier ROM show that a gasifier with CO_2 slurry feed produces up to two times more CO than one with water slurry feed as a result of the higher CO_2:H_2O ratio in the feed and hence higher contribution of the CO_2 gasification reaction to the overall conversion process. The observed gasification rate is up to 60% lower: the CO_2 slurry feed penalizes the intrinsic reaction rate, through

CO inhibition, and reduces pore diffussive transport, through the lower diffusivities of CO and CO_2 relative to H_2O and H_2.

A gasifier operating with bituminous coal-CO_2 slurry is predicted to consume 15% less oxygen than one with water slurry feed and the same outlet temperature. As a result of the slower gasification rate, however, a 7%-point lower carbon conversion and an unchanged cold gas efficiency are expected.

In order to achieve the same conversion as in a water slurry fed gasifier, the gasifier outlet temperature must be raised by 90K. This increases the oxygen consumption, relative to previous estimates which assumed unchanged conversion and unchanged reactor outlet temperature. In reality, oxygen consumption savings of only 8% are estimated if the temperature increase required to maintain conversion at its base value is accounted for. Additionally, the peak reactor temperature increases by 220K, which could compromise component integrity. The economics of the process will determine whether it is preferable to operate a CO_2 slurry-fed gasifier with lower conversion and higher oxygen savings or viceversa. This tradeoff is addressed in Chapters 6 and 7.

Chapter 5

The PHICCOS Feeding System

The preparation of coal-CO_2 slurry is challenging and proposed methods require the use of lock-hoppers and cryogenic cooling, which may undermine the use of coal-CO_2 slurry feed.

This chapter introduces the Phase Inversion-based Coal-CO_2 Slurry (PHICCOS) feeding system, a novel method which operates at ambient temperature and without the use of lock hoppers. Furthermore, this system achieves very high feed pressures while reducing the moisture and ash content of the feedstock, which makes it especially attractive for low-rank and high-ash coal.

The physics of phase inversion are discussed here and the main experimental findings from the LICADO process are summarized, on which the PHICCOS design is partly based. The characteristics of the PHICCOS feeding system are then presented, together with an estimate of its capital costs and of the submodel used to include it in existing models.

5.1 The Challenge of Preparing Coal-CO_2 Slurry

The underlying assumption in early studies evaluating the merits of a plant with coal-CO_2 slurry feed is that the slurry can be prepared in a mixing vessel at ambient pressure, in a similar way than coal-water slurry can [18, 46].

However, the triple point pressure of CO_2 is about 5 bar. As the phase diagram

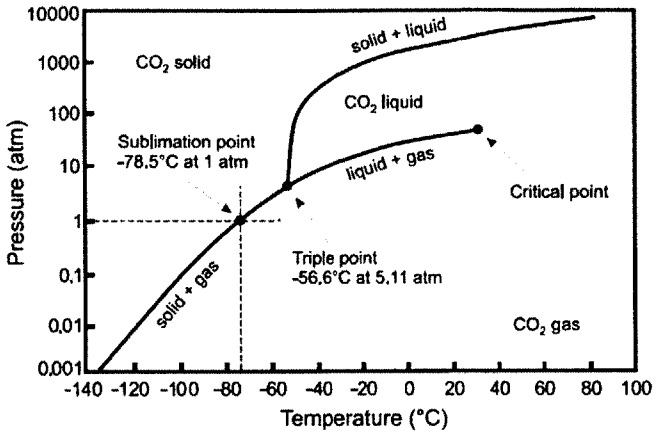

Figure 5-1: Phase diagram of carbon dioxide [122].

in Figure 5-1 shows, coal must be pressurized from ambient conditions to at least this pressure before it can be mixed with CO_2 in its liquid state. This requires a lock hopper and potentially also cryogenic cooling.

A semi-continuous method for the preparation of coal-CO_2 slurry was successfully tested by Arthur D. Little in the 1980's at both lab and pilot scales [33]. In this method, coal is initially charged to a pressure vessel at atmospheric conditions and gaseous CO_2 is then injected until the vessel reaches saturation pressure. This is followed by the injection of liquid CO_2, which brings the mixture to final pressure. A mixer is activated once the desired liquid level is reached and the homogeneous slurry mixture is fed to the slurry pump.

The semi-continuous process described above resembles a lock hopper similar to that used in dry-fed gasifiers. Various methods following this principle, often in combination with cryogenic cooling, have been proposed [47, 123, 124]. The high costs of cryogenic cooling, together with the need for lock hoppers, may defeat the purpose of the slurry concept in the first place.

5.2 Phase Inversion of Coal-Water Slurry

The key to the PHICCOS feeding system design is in the preparation of coal-CO_2 slurry *via* coal-water slurry. This is possible thanks to the preferential wetting of the

hydrophobic coal surface by CO_2 and the preferential wetting of its mineral impurities by water [59, 125]. This physical phenomenon is known as phase inversion and is schematically illustrated in Figure 5-2.

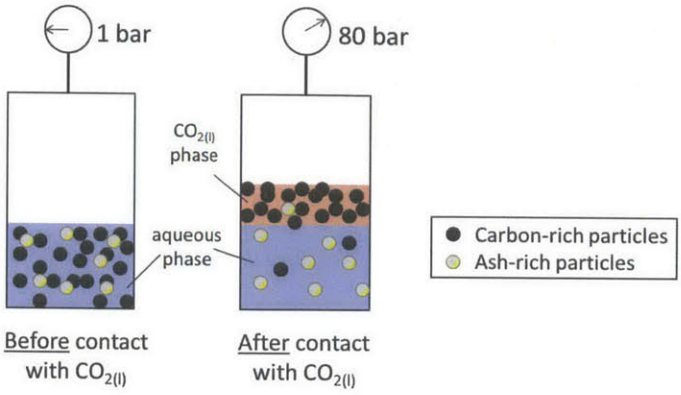

Figure 5-2: Schematic of phase inversion of coal with liquid CO_2. Adapted from [126].

Due to the heterogeneous nature of coal, pulverized coal particles are almost entirely carbonaceous, or entirely ash [127]. When thoroughly mixed with coal-water slurry, a hydrophobic liquid like CO_2 hence displaces water from the surface of coal through adsorption onto its carbonaceous particles. A coal-rich CO_2 phase can be separated from a mineral-rich aqueous phase. Also referred to as *selective agglomeration* or *hydrophobic displacement*, this long-known phenomenon has been traditionally studied for the purpose of coal deashing and dewatering.

Several processes based on selective agglomeration have been proposed and developed, with the Otisca T process being the most representative example [128]. The high cost associated with the recovery of the non-aqueous medium, also known as agglomerant, has been the biggest hurdle to their commercialization. Many agglomerants such as fuel oil, n-pentane, n-heptane, and liquid carbon dioxide have been studied [128–134].

5.2.1 Mechanism of Phase Inversion

Most of the knowledge about phase inversion is from the field of coal beneficiation using oil as an agglomerant. Experience with this process has shown that, in the presence of enough agglomerant and sufficient mechanical agitation, drops of agglomerant

dispersed in CWS collide with hydrophobic coal particles, which become enveloped in or attached to them. This displaces the aqueous phase from the coal but does not affect the hydrophilic mineral particles [129, 135].

The mechanism of the stage that follows collision of individual coal particles with the individual agglomerant drops is not yet very well understood. The macroscopic phenomenology is that, after about 1-5 minutes of high shear-rate stirring, agglomerates of clean coal are observed [135], which consist of groups of coal particles covered in agglomerant and bridged by water droplets, as schematically illustrated in Figure 5-3.

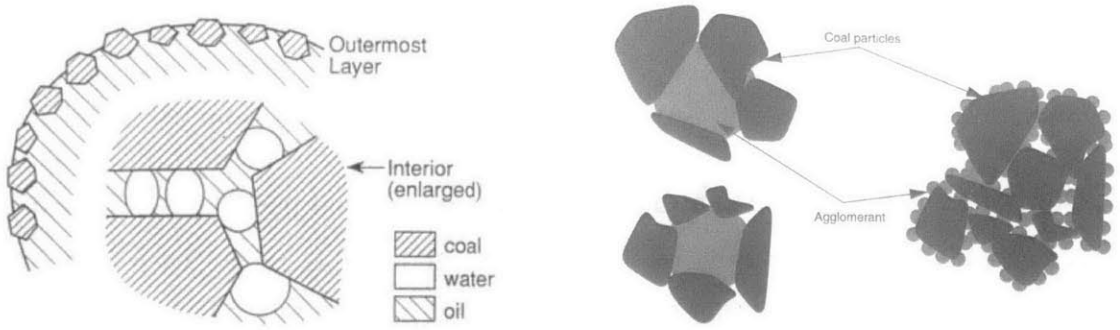

Figure 5-3: Liquid bridges in a coal-CO_2 agglomerate [129, 135]

The maceral and mineral matter in coal are thus effectively segregated: Carbon-rich particles get coated with agglomerant, collide with each other and are held together by capillary forces [129]. Hence the most commonly used name *selective agglomeration.* The agglomerates are surrounded -and bridged- by the mineral-containing aqueous phase.

The agglomerates must be removed from the slurry to separate them from the unagglomerated material in the water. For agglomerates which are loose, fluffy, and less dense than water, the most effective way is to allow them to float to the surface and skim them off [129]. This is shown in Figure 5-4, where the dense, mineral-rich aqueous aqueous phase is being separated from the lighter, coal-rich phase.

The exact physics behind the process of phase inversion are complex and the mechanism is not well understood yet. It is a surface property-driven process, which is governed by the interactions among the interfacial, shearing, and body forces present

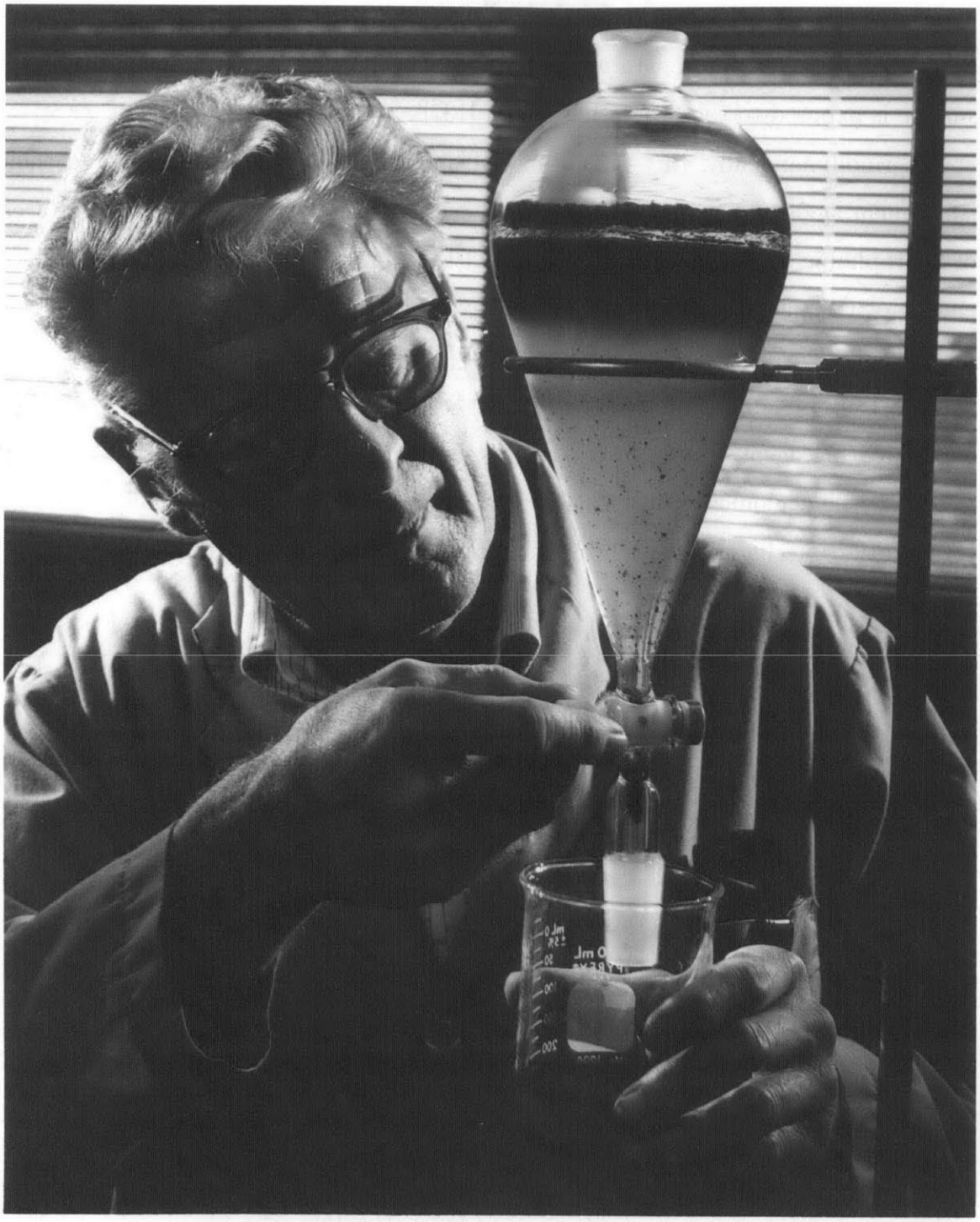

Figure 5-4: Henry F. Mesta, using a separatory funnel, is deashing coal through the method of selective agglomeration, NETL Coal Preparatory Laboratory, Circa 1970s - 1980s (Reproduced with permission from NETL [136]).

in the coal particle-agglomerant-water system. The shearing and body forces are determined by the physical properties of the coal particles as well as by the hydrodynamic conditions in the separation process, which control the way in which the coal surface is exposed to the processing media [137].

Thermodynamically, the wetting of coal particles by the agglomerant and their subsequent agglomeration reduces the total energy of the system by reducing the area of hydrophobic surface that is in contact with water. At the same time, the surface energy of the interface between the solid particles and the agglomerating liquid is minimized.

The best possible performance will be achieved when the energy of the solid-agglomerating agent interface approaches zero. This thermodynamic limit is determined by the agglomerant and coal characteristics but can also be modified through the addition of chemicals, such as surfactants, which can alter the surface energy [129].

5.2.2 Characterization of Phase Inversion Performance

From a macroscopic perspective, the phase inversion process performance is determined by the characteristics of the coal product. The latter is coal leaving the phase inversion process with the agglomerant, i.e. the dark phase at the top of the funnel in Figure 5-4. It is also known as the *clean coal* coal due to its low ash content. In particular, the ash and moisture content of the coal product and the enthalpy recovery of the process are of interest.

The enthalpy recovery is a measure of process yield. It is the fraction of the feedstock's chemical energy that is recovered in the coal product:

$$\text{Enthalpy Recovery} = \frac{(\dot{m}_{\text{product}})\,(HHV_{\text{product}})}{(\dot{m}_{\text{feed}})\,(HHV_{\text{feed}})}. \tag{5.1}$$

Most of the work conducted on the phase inversion of coal has been within the context of coal beneficiation, thus targeting product with a low ash content at an acceptable enthalpy recovery. In contrast, very high enthalpy recoveries are essential

to the economics of the PHICCOS feeding system, whose main purpose is not coal beneficiation but the pressurization and subsequent recovery of coal. Enthalpy recovery is hence the most important performance characteristic of PHICCOS. Any ash and moisture content reduction is considered to be an added benefit.

Experimental data for phase inversion using CO_2 as an agglomerant is very limited. Furthermore, there is no experience under conditions of high enthalpy recoveries. This work uses available experimental data from the literature as an indication of the PHICCOS process performance and operational trends. However, experimental work under high enthalpy recovery conditions is required for a more accurate estimate of the technoeconomics of the PHICCOS process, as well as for its further development.

5.3 Experimental Observation of Phase Inversion of Coal with CO_2

Experimental observations and cost estimates of phase inversion of CWS with CO_2 have been documented by the University of Pittsburgh and Westinghouse as part the Liquid Carbon Dioxide (LICADO) project, funded by the U.S. Department of Energy (DOE) in the 1980's [56, 126, 137–141].

The project was devoted to studying this phenomenon as a way to significantly reduce the mineral matter content of bituminous coal. Its main objective was to design and test the major unit operations of the process in an integrated, continuous real time basis in order to establish technical feasibility through generation of firm engineering data [56].

The feasibility of using phase inversion with liquid CO_2 for coal beneficiation was first tested in a batch research unit (BRU) with a volume of 3 L; a 6 L research development unit (RDU) operating in semi-continuous mode followed. A fully automated continuous research unit (CRU) with a capacity of 10 lb/h of upgraded coal was then built and successfully operated with the purpose of gathering data for the design of a 1 ton/day pilot unit. A detailed engineering design of the individual pilot plant com-

ponents was finalized by Westinghouse based on these results. A budgetary estimate of the capital and operating costs of a commercial-scale unit producing 200 ton/day of beneficiated coal [56] was also conducted.

Oil prices fell and interest in coal beneficiation ended, and with it the LICADO development, before the process operating conditions could be optimized. The pilot-scale plant was never built. Nevertheless, the results from the LICADO project are well documented [56, 126, 137–141] and were leveraged in this work for the design of the PHICCOS process and as an indication of its performance, economics, and sensitivity to specific design and operating variables.

5.3.1 Main Findings of the LICADO Project

Experiments were conducted on eight different bituminous coals ranging from very hydrophobic to very hydrophilic. A very low product coal ash content of 2-5% (dry basis) was achieved consistently, even for coal with a high as-received ash content of 27%.

The performance of phase inversion of coal with CO_2 was found to closely match the coal's washability data. The later refers to the results from coal flotation, which is also used for beneficiation of coal and it is a gravity-settling process. It depends on particle density and relies on a very different mechanism [56].

Some of the coal was entrained in the aqueous stream after phase inversion, resulting in enthalpy recovery losses. Typical enthalpy recovery values were in the range of 80-95%. A tradeoff between ash rejection and enthalpy recovery was identified, as can be observed in Figure 5-5, where selected washability data and LICADO results are presented. Very high enthalpy recoveries of 95% are achievable for cases with low ash removal [56, 59].

A low moisture content of 5-15% was measured consistently in the LICADO product for all coals studied. While the moisture content of the as-received coal is not specified in the original report and moisture results are not reported in detail, the low moisture content of the product was identified as one of the main advantages of this method [56]. In fact, the removal of surface and inherent moisture from coal through

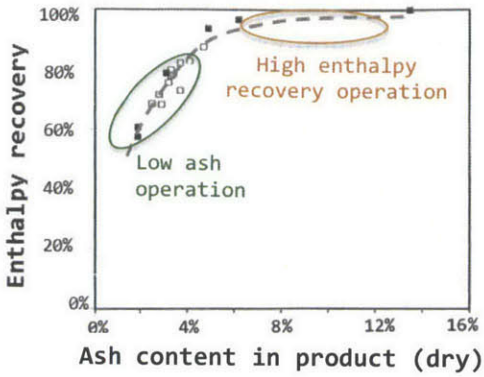

Figure 5-5: Tradeoff between ash removal and enthalpy recovery resulting from phase inversion of coal with liquid CO_2. The results are for Upper Freeport Coal, with an initial ash content of 13.5%, and originate from the LICADO project [56].

phase inversion with a hydrophobic liquid has been studied as an energy-efficient alternative to thermal drying. Several agglomerating agents have been studied or proposed for this purpose, including propane, butane, pentane, ethane, and liquid CO_2 [131, 132, 134, 142].

5.3.2 Influence of Main Operating Parameters

Some of the most important variables which affect the performance of the phase inversion process include the characteristics of the coal, the type and amount of agglomerant used, the mixing intensity, the temperature of the slurry, conditioning agents, and the percent of solids in the slurry [129].

Some of these were studied within the scope of the LICADO experiments. CWS was first saturated with CO_2 and then more CO_2 was introduced from the bottom of the phase inversion vessel with the aid of a micron-size fritted disc distributer providing uniform dispersion of liquid CO_2 bubbles in the water phase. Different coals were tested and the influence of mixing speed, residence time, particle size and CO_2 flow were studied.

Observations from some of these parametric studies will summarized in what follows. These were very useful for understanding trends and defining guidelines for the design of the PHICCOS feeding system. Note, however, that the parametric

studies were not conducted under optimized process conditions, so only the trends, but not the absolute performance numbers shown here, are representative.

For more details on the influence of operating and design variables on the phase inversion performance, the reader is referred to the original contributions from the LICADO process [56, 126, 137–141] and to extensive literature on the selective agglomeration of coal with oil and other agglomerants [128–134, 143].

Coal Hydrophobicity

The coal surface wettability is one of the most important variables in a surface force-driven process like phase inversion.

The contact angle of water on pelletized coal was measured during the LICADO experiments both at ambient pressure, prior to phase inversion, and at high pressure in the presence of CO_2. Very hydrophobic coals as well as very hydrophilic coals were studied.

The hydrophobicity of all coals was observed to increase in the presence of CO_2. These observations agree well with experimental evidence from the literature: hydrophobicity is known to vary with pH [129] and acids, like the carbonic acid formed when CO_2 is in contact with water, have been shown to be effective for the pretreatment of low-rank coal prior to coal beneficiation [144–147].

The contact angle of water with one of the coals studied was measured to be zero, i.e. it is fully hydrophilic. Its enthalpy recovery was observed to be lower than for the more hydrophobic coals. However, it increased steadily upon addition of parts per million of 1-Octanol, reaching the same range as the more hydrophobic coals tested. This chemical acts as a co-agglomerating agent and facilitates the attachment of droplets of liquid CO_2 to the coal particles [56].

The latter observation is important, since the phase inversion behavior of low-rank coal, like lignite, was not studied in the LICADO project, and is of interest in the present work. The evidence above suggests, however, that the natural hydrophilicity of lignite does not represent a barrier for the implementation of phase inversion to this feedstock. Selective agglomeration of low-rank coals has been indeed achieved in

the past [129, 147, 148].

Mixing Speed

The kinetics of phase inversion strongly depend on the mixing speed. High shear rates in the aqueous phase provide a better contact of the hydrophobic coal surface with CO_2 and increase the number of interparticle collisions [56, 129].

High shear rates in the CO_2 phase improve the ash separation behavior: the agglomerates are frequently broken, worked, and re-formed. This gives opportunities for mineral particles within the bridging water droplets to be released [129].

Both the water phase and of the CO_2 phase were mixed in the LICADO experiments and the effect of varying the impeller speed was studied. The effect of impeller speed on the ash and moisture content of the product and on the enthalpy recovery is presented in Figure 5-6.

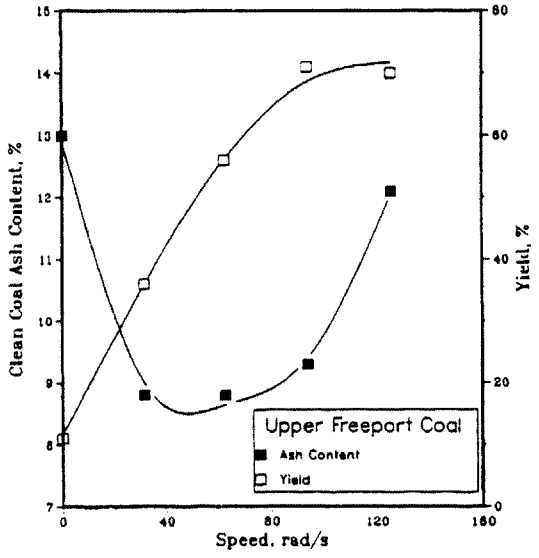

Figure 5-6: Effect of mixing speed on phase inversion performance from BRU [56]. Conditions are not optimized for high enthalpy recoverqy.

The results in the figure show that a maximum impeller speed exists, above which ash gets entrained in the CO_2 phase, increasing the ash content of the product. There is a direct correspondence between the product moisture content and its ash content: moisture is also entrained at high mixing speeds.

The optimum mixing speed is coal-dependent and is a tradeoff between enthalpy recovery and ash and moisture content of the product. It also depends on whether the process is targeting ash separation or high enthalpy recoveries.

Coal Particle Size

Processes which require pulverized coal feedstock have clear synergies with phase inversion-based feed since the latter requires enough grinding to release the mineral matter of the coal [135]. Laboratory experiments have shown that coal can be agglomerated when the particle size is as large as 200 μm in diameter [135].

Particle sizes in the range of about 20-90μm were studied in the LICADO experiments. The results showed that there is a sharp decrease in the enthalpy recovery for particles larger than about 70μm.

Fine grinding enhances the enthalpy recovery but a substantial portion of the finely ground mineral matter is entrapped in the clean coal agglomerates. This can be avoided by conducting the process in two stages, whereby the agglomerates from the first stage are reformed in the second stage [56].

Grinding energy increases rapidly for sizes much smaller than 100μm. A coal particle size of 200 mesh (74 μm) was found to be a good compromise between beneficiation efficiency and grinding energy [56].

Residence Time

The LICADO experiments showed that a total residence time of about 5-10 minutes provides a good product yield and quality for coal beneficiation applications. It is dominated by the time required for phase separation, though the mixing time is of utmost importance.

First, CWS and CO_2 are mixed through high-shear rate stirring in order to ensure intimate contact of the coal surface with CO_2. The residence time in the mixer is of the order of a few minutes and is coal-dependent. Hydrophobic coals require less mixing time than hydrophilic ones.

Next, the CO_2 and aqueous phases are separated from the top and bottom of a

settling vessel, respectively. Low-shear rate stirring of the settling vessel helps to avoid the settling of coal agglomerates into the water phase. Furthermore, it promotes the breaking-up of agglomerates and subsequent release of entrapped mineral material. The commercial plant design by Westinghouse has a phase separation residence time of 5 minutes [56].

CWS Loading

The CWS loading is known to affect the agglomeration performance, but its effect is small compared to other factors. The loading must be high enough for the coal to be able to contact and combine with CO_2 in a reasonable time, but not too high that the impurities become mechanically entrapped in the agglomerates [129].

In the LICADO experiments, the effect of CWS loading was not found to be conclusive. Only very low solid loadings of 3-17% were considered. Higher loadings were not tested due to equipment capacity limitations.

A solids loading of 20% was selected by Westinghouse for the commercial LICADO unit design [56]. This agrees with the 15-20% practical limit reported elsewhere [143].

Flow of CO_2

The effect of increasing the flow of CO_2 is not conclusive from the LICADO experiments, as it seems to depend on the design of the phase inversion equipment.

In general, the role of CO_2 is twofold: first, and most importantly, it is required in the mixer in order to wet the coal particles for phase inversion to occur.

Second, CO_2 bubbles attach to agglomerates, helping them float to the surface of the phase separation vessel. The hydrodynamics of agglomerate flotation have been studied before for agglomeration with oil [127].

The LICADO experiments showed that, for a given flow of CO_2 in the separator, increasing the flow of CO_2 in the mixer does not have a significant impact. The latter is true, provided that there is enough CO_2 for wetting of the coal particle surface.

On the other hand, the flow of CO_2 introduced into the phase separator for floating the agglomerates to the top of the vessel was observed to exert a significant influence

on the enthalpy recovery.

Using large flows of CO_2 is expensive, so the commercial-scale LICADO plant was designed by Westinghouse with CO_2 injection only in the mixing vessel and at ratio of CO_2:CWS ratio of 0.5 only (by weight). This design is based on the experimental results from the CRU and RDU, which showed that the flow of CO_2 can be reduced through the proper design and operation of the separator vessel.

It is hence concluded that while increasing the flow of CO_2 is likely to increase recovery, this can also be achieved through an adequate design of the phase separation column. The latter was identified as one of the key elements in the design and development of the LICADO process. For high enthalpy recovery operation, it is preferable to enhance the mixing of CWS and CO_2 than to increase the flow of CO_2.

From the point of view of beneficiation, an optimum agglomerant flow has been reported [143, 149] due to excessive entrainment of ash in large agglomerates.

5.3.3 Recommendations for High Enthalpy Recovery Operation

Experience from the LICADO experiments and from selective agglomeration with oil shows that very high enthalpy recoveries can be achieved by promoting intimate contact between the coal surface and the CO_2 phase, i.e. through long mixing times and shear rates, small particle and droplet size, etc. The addition of small quantities of reagents may be necessary and/or helpful for aged or low-rank coal with low hydrophobicity.

The hydrodynamics of agglomerate flotation in the phase separation equipment are a also key determinant of enthalpy recovery. The design of this piece of equipment must be optimized and is essential to process performance.

Further experimental work in the high enthalpy recovery regime is required in order to quantify the influence of operating variables in more detail.

All the measures increasing enthalpy recovery tend to increase the ash content of the product. For coals with very high ash contents, it may be desirable to reevaluate

the operating conditions and sacrifice the enthalpy recovery in order to reduce the feedstock's ash content. Ultimately, the conditions must be optimized to yield the best overall plant economics.

5.4 The PHICCOS Process

The PHICCOS feeding system is based on phase inversion of CWS with liquid CO_2 and is depicted in Figure 5-7. Its main operating conditions and design variables are summarized in Table 5.1 and are based on the experimental observations and trends discussed in Section 5.3

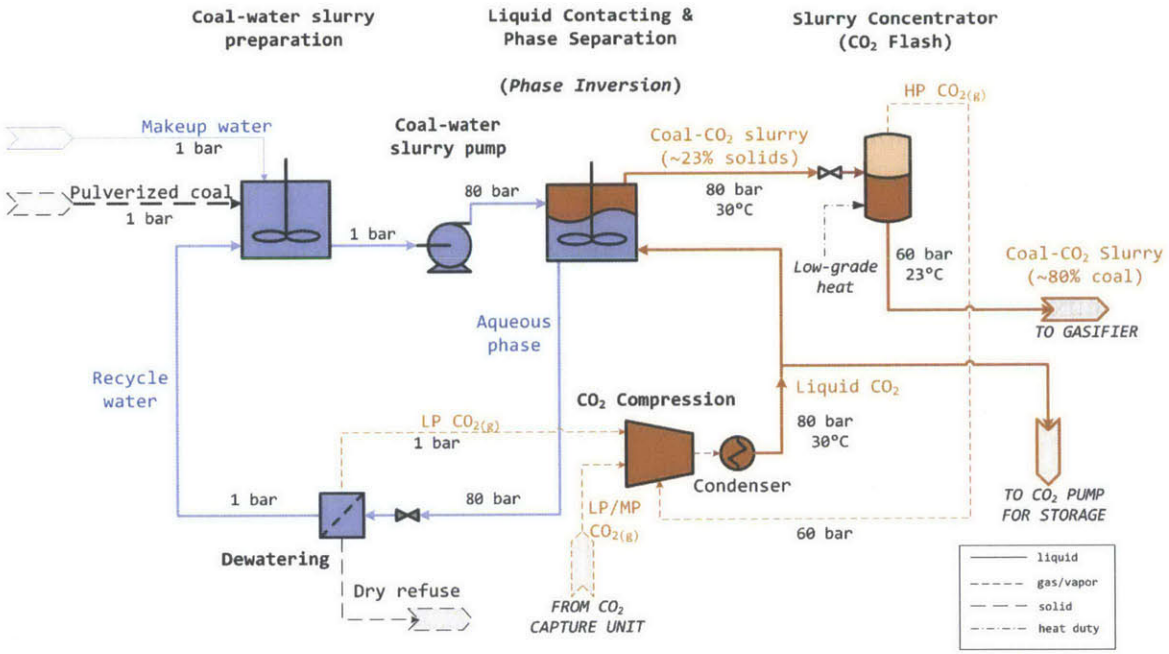

Figure 5-7: Process flow diagram of the PHICCOS preparation and feeding system [125].

5.4.1 Process Description

CWS is first prepared in a conventional slurry preparation unit at ambient conditions. It is pumped to the same pressure as that of the liquid CO_2 stream available for slurry preparation, which is 80 bar if the CO_2 has been condensed at 30°C.

The CWS is thoroughly mixed with liquid carbon dioxide, forming a water-rich

Table 5.1: Key operating and design variables for PHICCOS process [56, 59]

CWS loading	20%-wt. ar coal
Flow of CO_2	CO_2:CWS = 0.5 (wt.)
Phase inversion	
Pressure	80 bar
Temperature	30 °C
Residence time	5 min.
CO_2 flash	
Pressure	60 bar
Temperature	23 °C
Heat duty	< 0.12 kJ/kg CO_2
Overall performance	
Enthalpy recovery	95%
Coal product ash	10%-wt. (dry)
Coal product moisture	10%-wt.

and a CO_2-rich phase. Exposure of the coal surface to CO_2 leads to phase inversion; the low-ash, hydrophobic coal particles thus accumulate in the lighter CO_2 phase whereas high-ash, hydrophilic particles and moisture remain in the denser, aqueous phase. The two phases can be continuously removed from the top and bottom of the mixing/settling vessel, respectively. The ash and moisture content reduction experienced by the feedstock during the phase inversion process is what is here referred to as the *beneficiating*, or upgrading, effect of PHICCOS.

The aqueous ash-rich refuse leaving the liquid contacting vessel is brought to ambient pressure and dewatered before separating and disposing of the high-ash solid stream. The carbon content of the latter depends on the fraction of organic coal particles lost to the aqueous phase upon phase inversion, i.e. by the enthalpy recovery of the process.

After separating its solids content, the refuse water is recirculated back to the CWS mixing vessel. Low-pressure (LP) CO_2 desorbed from the refuse during decompression is recompressed in the plant's CO_2 compressor.

The CO_2 slurry separated from the top of the mixing vessel has a low coal loading of about 20-25 weight-% (wt.-%) [56]. It is hence concentrated before being fed to the gasifier: its CO_2 content is reduced to achieve a coal loading of 80 wt.-%, which is the maximum loading for a slurry of coal in CO_2 [18]. This is accomplished by

evaporating excess CO_2 in a flash stage through a combination of pressure reduction and low-grade heat addition. The medium-pressure (MP) CO_2 released in the flash stage is recompressed and the concentrated, pressurized coal-CO_2 slurry is fed to the gasifier.

5.4.2 PHICCOS vs. LICADO

The liquid contacting and separating unit of the PHICCOS process uses the same physical phenomenon as the LICADO process. However, the overall process design and target application are different. Unlike the LICADO process, for example:

- CWS is prepared at ambient pressure
- Operating temperatures are kept at a minimum of 30°C to allow for use of process cooling water. As a consequence, the liquid contacting is carried out at pressure of 80 bar
- The coal-CO_2 slurry product is concentrated and the slurry is used as gasifier feedstock

The preparation of CWS at ambient pressure in PHICCOS is perhaps the most important difference. The LICADO process was designed to maintain CO_2 in its liquid phase in order to minimize CO_2 recompression costs. This, nonetheless, comes at the expense of high-pressure equipment, such as a pressurized auger filter for clean coal separation and lock hoppers for CWS preparation. These have been identified as the main reason for the high costs associated with LICADO [129].

5.4.3 Capital Costs

Figure 5-8 presents the bare erected capital costs estimated for the PHICCOS feeding system. The corresponding costs of a CWS and a dry feeding system with the same coal throughout are also shown for comparison.

The figure shows that for a given as-received coal flow, the capital costs of the PHICCOS process are about 60% higher than that of coal-water slurry feed, but still

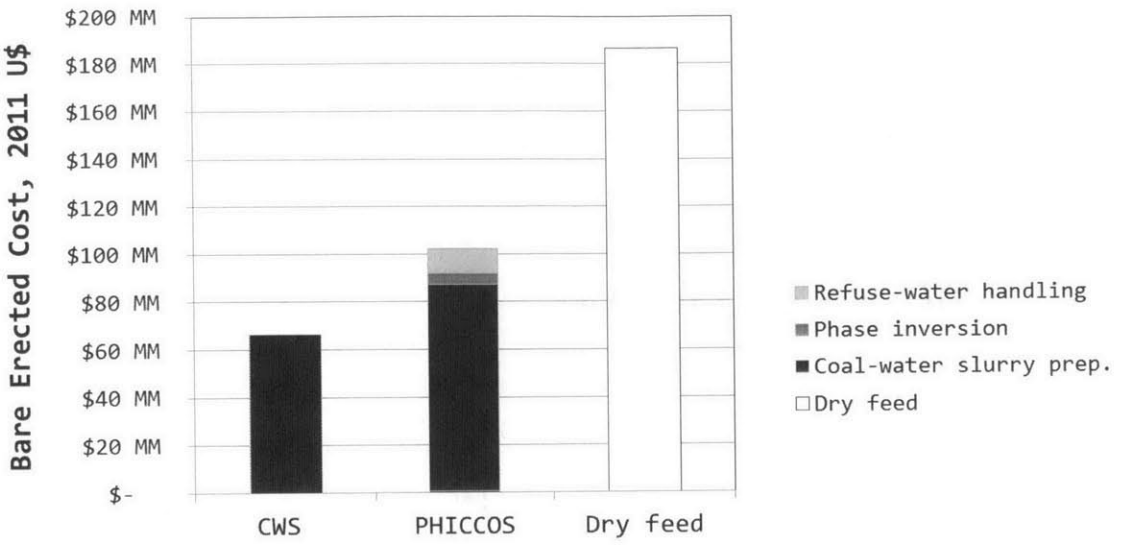

Figure 5-8: Capital cost of PHICCOS feeding system and comparison with alternative technologies [11, 19]. All costs are for 200 tonne/h as-received coal and include coal handling, preparation and feeding. Process contingency is not included.

only about half of that of a dry feeding system. The additional costs of PHICCOS, relative to CWS, come primarily from the larger coal-water slurry preparation equipment but also from the refuse water handling. The former is estimated to be about five times larger than for conventional CWS systems given the low CWS loading of 20% in the PHICCOS process.

The pressurized H_2O-CO_2 contacting equipment, where phase inversion occurs, is predicted to have a modest contribution to the capital costs of PHICCOS. It is estimated that 4 vessels, of about 60 m^3 each, are required to provide the total residence time required in the mixing/separating process. While each tank hence has approximately the same volume as the reaction (i.e. syngas cooler excluded) section of a the largest GE gasifier in the market, it is relatively standard equipment operating at ambient temperature. Despite the large size, its capital costs are expected to be low compared to other, more complex process units.

5.4.4 Comparison with Other Technologies

Table 5.2 presents a qualitative comparison of the feedstock flexibility, pressure flexibility, power consumption, and capital costs of PHICCOS with commercial feeding

systems and other technologies under development. Feedstock flexibility is constantly ranked as one of the top customer requirements in the gasification industry [150]. The ability to gasify low-rank coal has largely driven the increasing market share of dry-fed gasifiers such as Shell's, which, in the absence of better technologies, is projected to dominate the market in the future [6].

Table 5.2: Qualitative comparison of commercial feeding systems (*) and technologies under development. The criteria are rated as insufficient (-), acceptable (o), exceptional (+), or unknown (?).

	CWS FEED	**DRY FEED**		**CCO2S FEED**	
	Slurry pump*	Lock hoppers *	Dry Pump	EPRI [151]	PHICCOS
Feedstock flexibility	-	o	o	o	+
Pressure flexibility	+	-	+	+	+
Power consumption	+	+	+	?	-
Capital cost	+	-	?	?	o

Due to its upgrading effect and thus better feedstock flexibility, the PHICCOS feeding system offers more advantages than a dry feeding system. It is the only technology that inherently reduces the ash and moisture content of the feedstock and it can achieve very high pressures with less capital requirement than commercial dry feeding systems based on lock hoppers [59].

The power consumption of PHICCOS is higher than that of pump-based systems as well as of lock hopper-based dry feeding systems, which typically use spare nitrogen from the air separation unit. Plants with CO_2 slurry must recapture and recompress the CO_2 used for feeding coal to the gasifier, increasing power consumption [18]. Furthemore, the PHICCOS process requires recompression of low-pressure (LP) and medium-pressure (MP) CO_2 released from the aqueous phase at 1 bar and from the slurry concentrator at 60 bar, respectively, see Figure 5-7.

5.5 PHICCOS Submodel

A submodel of the PHICCOS feeding system was included in the plant-level models presented in Chapter 2. A screenshot of the submodel is presented in Figure 5-9.

The A+ submodel considers the fluid and solid phases separately. The water

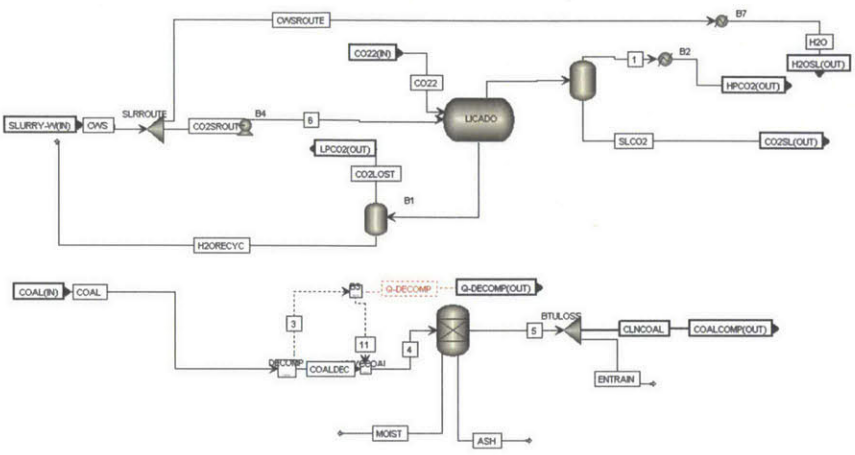

Figure 5-9: Submodel of PHICCOS preparation and feeding system in Aspen Plus.

slurry-CO_2 slurry liquid-liquid equilibrium is modeled as the binary H_2O-CO_2. Minor components in the recirculated CO_2 stream are not considered [59].

The Predictive Redlich-Kwong-Soave (PSRK) property method was used for modeling the liquid-liquid phase equilibrium in the water-CO_2 contacting vessel, which is represented by a DECANTER model in A+. The PSRK method was found to accurately reproduce the solubility of liquid CO_2 in H_2O, which is has been measured to be 6 wt.-% at 80 bar and 30°C [152] and is thus significant.

The coal stream was modeled separately as a non-conventional component in A+. A fraction of the ash content, moisture, and organic matter in the as-received coal are separated upstream of the gasifier to account for the performance of the PHICCOS feeding system, which is characterized by the ash and moisture content in the coal product (i.e. gasifier feed) as well as by the coal enthalpy recovery. The latter is defined as the fraction of the as-received coal enthalpy that is recovered in the CO_2 phase of the phase inversion process.

The data used for modeling the PHICCOS feeding system is that in Table 5.1 and is based on the experience obtained through the LICADO project for beneficiation of bituminous coal [56]. The PHICCOS system is designed to operate in a high enthalpy recovery mode, i.e. the low ash content of the feedstock delivered to the gasifier is a benefit but not its main performance target.

5.6 Chapter Summary

The challenge of preparing a slurry of coal in liquid CO_2 was addressed in this chapter. The Phase Inversion-based Coal-CO_2 Slurry (PHICCOS) feeding system was presented, which is proposed in this work as an alternative to CO_2 slurry preparation methods involving lock hoppers and cryogenic cooling.

The PHICCOS feeding system takes advantage of a phenomenon known as phase inversion. The latter is associated with the preferential wetting of hydrophobic coal surfaces by CO_2 and the preferential wetting of its mineral impurities by water.

The mechanism of phase inversion was discussed and experimental observations from the field of coal beneficiation were presented. These were used as a basis for this work.

Finally, this chapter presents an estimate of the capital costs of PHICCOS and describes the submodel used to include it into the plant-level models described in Chapter 2.

Chapter 6

Technoeconomics of an IGCC Plant with PHICCOS Feed

The system-level analysis presented in Chapter 3 showed that the thermal benefits of CO_2 are significant. However, the component-level and particle-level study presented in Chapter 4 revealed kinetic limitations associated with gasification in an environment with a high content of CO_2. Furthermore, preparation of coal-CO_2 slurry has proved to be significantly more challenging than that of CWS. The PHICCOS preparation and feeding system was introduced in Chapter 5 but its capital costs and performance have not been accounted for so far.

This chapter presents a comprehensive technoeconomic assessment of the proposed PHICCOS feeding system under under consideration of all aspects above: thermodynamics, kinetics, and slurry preparation. An IGCC plant with carbon capture is used as an example application and the cost of electricity is used as the figure of merit to compare PHICCOS with commercial feeding systems for high and low-rank coal. Furthermore, the plant economics are used to determine whether it is preferable to operate a PHICCOS-fed gasifier at the reference outlet temperature (and with a reduced conversion) or at the reference carbon conversion (and with a higher temperature).

6.1 Methodology and Cases Studied

An IGCC plant with 90% CO_2 capture and with conventional CWS feed or PHICCOS feed was considered for the analysis. A nominal coal slurry loading of 71% and 80% was used, respectively, see Table 2.2.

The plant operates with two 1,800 ft^3 gasifiers, each of which resembles the GE gasifier at the Tampa IGCC Polk power station, see Table 2.3. Full-quench syngas cooling is assumed and both bituminous coal and North Dakota lignite were considered in order to account for a wide range of coal ranks.

Figure 6-1 presents a schematic of the IGCC plant operating with either feeding system. The modeling approach is also indicated in Figure 6-1 and is described in detail in Section 2.4.1: the detailed reduced order model of the gasifier is coupled with the system-level model of an IGCC plant, which includes a submodel for the PHICCOS feeding system, see section 5.5.

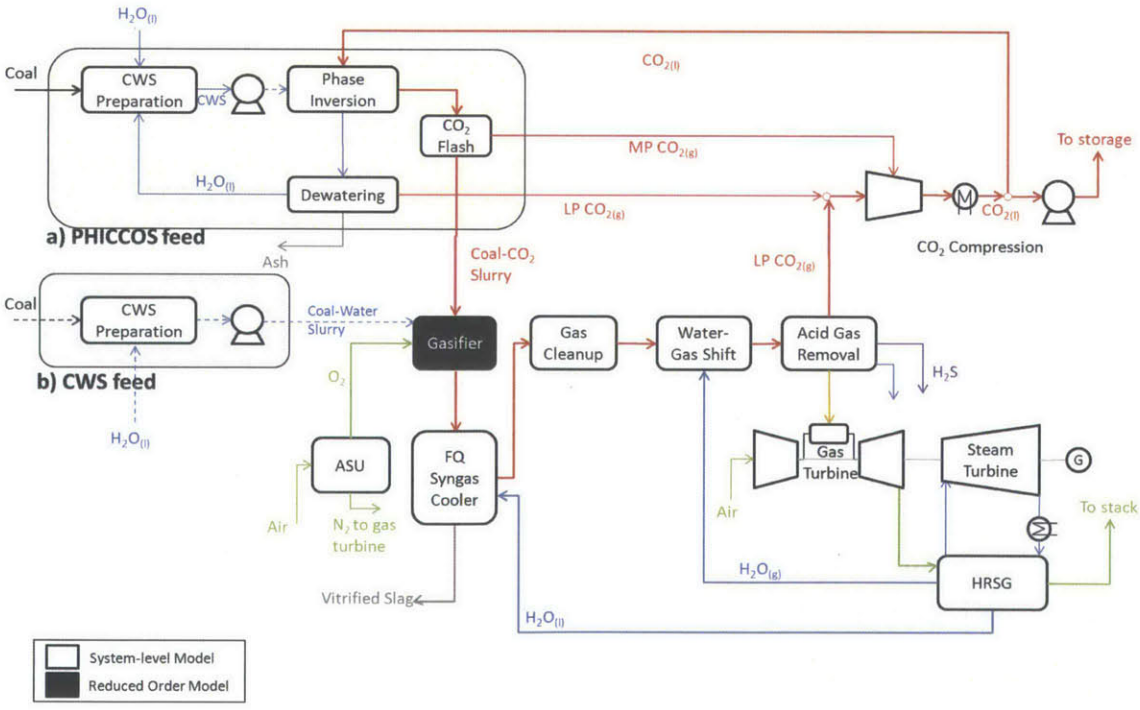

Figure 6-1: Schematic of IGCC plant with a) PHICCOS feed and b) conventional CWS feed. The scope of the multiscale modeling tools used is also indicated.

6.2 Results and Discussion

The gasifier and IGCC plant performance are presented here for all cases studied. For all slurry-fed cases, the data corresponds to the result of simulations with the multiscale models described. For dry-fed systems, performance numbers from the literature are presented for comparison purposes only and should hence be interpreted with caution.

6.2.1 Carbon Conversion in Gasifier

The kinetic performance of the gasifier can be quantified by the degree of carbon conversion. High carbon conversions are desirable in order to minimize fuel consumption and capital costs.

Figure 6-2 presents the carbon conversion and outlet temperature in the gasifier, as calculated from the ROM for all slurry-fed cases, and taken from the literature for dry-fed ones. The results show that for a given gasifier outlet temperature, substituting coal-water slurry by PHICCOS feed is detrimental to carbon conversion for both bituminous coal and lignite. This can be attributed to the gasification kinetics alone since coal losses introduced by the PHICCOS feeding system are not included in the gasifier carbon conversion but rather in the system-level results. The observed conversion reduction was discussed in detail in Chapter 4 for a smaller reactor operating at a somewhat lower temperature.

For bituminous coal, a gasifier operating with PHICCOS feed has a 9%-pt. lower conversion than one with the same outlet temperature and fed with CWS. As shown in the figure, the gasifier outlet temperature would have to be raised by 112 K in order to achieve the same conversion as with CWS feed. These results are in good agreement with the estimates for this coal type in the Cool Water reactor, see Chapter 4.

For lignite, a 13%-pt. conversion reduction is predicted. An even higher temperature increase than for bituminous coal is thus required in order achieve the reference conversion: the reactor outlet temperature must be raised by 167 K. The higher conversion reduction of lignite can be attributed to the larger moisture content reduction

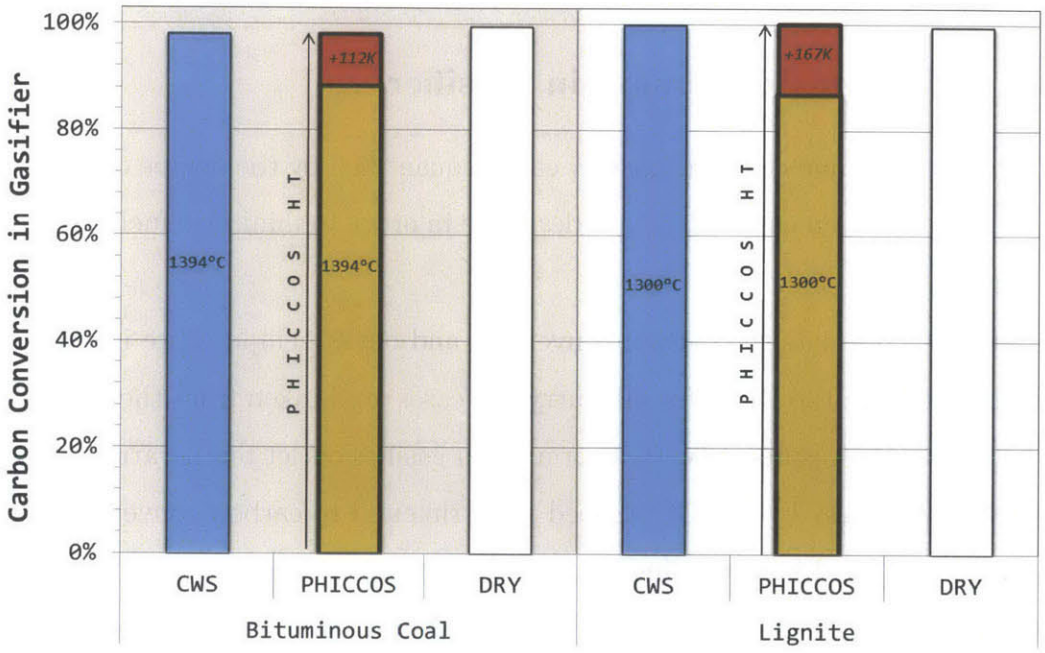

Figure 6-2: Carbon conversion in gasifier fed with bituminous coal (left) or lignite (right). The gasifier outlet temperature is indicated in each case. A reactor with CWS feed (■) is compared with one with PHICCOS feed and the same outlet temperature (PHICCOS, ■). The conversion and temperature increase required in a PHICCOS-fed system in order to achieve the same conversion as a CWS-fed reactor are also shown (PHICCOS HT, ■). Coal losses in the feeding system are not included. Conversion data for a dry-fed gasifier from the literature [11, 19] is displayed for comparison (□).

that it experiences during phase inversion, which translates into a lower steam partial pressure in the gasifier.

Results in Figure 6-2 show that increasing the gasifier temperature is an effective measure for raising carbon conversion. Nonetheless, higher temperatures come at the expense of more oxygen consumption. Alternatively, conversion could be improved by increasing the residence time in the reactor. This can be achieved by either reducing the coal throughput or by increasing the gasifier size. Previous work suggests that this option is not economically feasible: the gasification rate is so slow near the reactor outlet that the throughput would have to be halved -or the reactor volume doubled- to make up for the lost conversion in a reactor with coal-CO_2 slurry feed [66].

6.2.2 Oxygen Consumption

The presence of ash and excess water in the feedstock are detrimental for the gasifier thermal performance: they increase the amount of heat needed to maintain high-temperature operation, which in an autothermal gasifier is supplied through feedstock oxidation. Oxygen consumption is hence a good measure of gasifier thermal performance.

A high oxygen consumption is undesirable since it increases the capital and operating costs associated with the ASU, which are very significant. Furthermore, feedstock oxidation produces gas with little to no heating value, increasing feedstock consumption and equipment size.

Figure 6-3 presents the specific gasifier oxygen demand obtained from the ROM for all slurry-fed cases studied. Literature values are shown for dry-fed cases. For a given gasifier outlet temperature, the oxygen savings in a PHICCOS-fed gasifier, relative to one with CWS feed, are significant: 23% for bituminous coal and 41% for lignite.

Because carbon conversion is also lower, a higher gasifier temperature is required to achieve the same conversion as in a CWS-fed reactor. Once the additional oxygen required to raise the gasifier temperature is accounted for, the results show that the overall oxygen savings for PHICCOS are reduced, but are still a significant 14% for

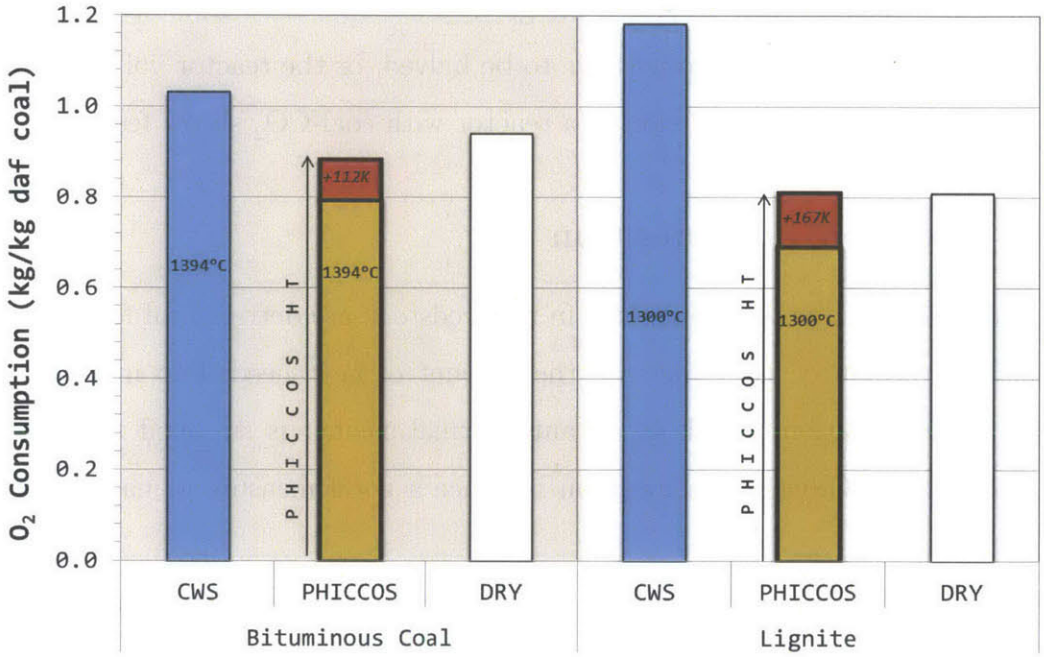

Figure 6-3: Specific O_2 consumption for bituminous coal (left) and lignite (right) gasification. The gasifier outlet temperature is indicated in each case. A reactor with CWS feed (■) is compared with one with PHICCOS feed and the same outlet temperature (PHICCOS, ■) or the same conversion and a higher outlet temperature (PHICCOS HT, ■). Data for a dry-fed gasifier from the literature [11, 19] is shown for comparison (□).

bituminous coal and 31% for lignite. The real value of increasing conversion at the price of a higher oxygen consumption is a matter of economics and is addressed in Section 6.2.5 and in Chapter 7.

The lower oxygen consumption in a PHICCOS-fed gasifier is a result of the lower specific heat capacity and enthalpy of vaporization of CO_2, with respect to water, and of the higher achievable solids loading in a slurry of CO_2 [18, 46]. Furthermore, the feedstock moisture and ash content reduction resulting from the beneficiation effect of PHICCOS reduces the thermal load of the gasifier even more than that previously anticipated [18, 66]. This is especially true for lignite given its higher ash and moisture content.

For a CWS-fed gasifier, it is not surprising that operation with lignite leads to a higher specific oxygen consumption than operation with bituminous coal: due to its high moisture content, a lignite-water slurry has a lower solids loading than a bituminous coal-water slurry and this imposes a higher thermal load on the gasifier.

For a PHICCOS-fed reactor, however, the results in Figure 6-3 show that the oxygen consumption is about 10% lower for lignite than it is for bituminous coal. This is counter-intuitive and can be attributed to the higher reactivity of lignite: the gasifier feedstock is expected to have a similar ash and moisture content for both coals if the PHICCOS process is used, see Table 5.1, but the gasification temperature is lower for the more reactive lignite.

For a given conversion, the results show that a PHICCOS-fed gasifier has a similar specific oxygen consumption as a dry-fed gasifier. The thermal advantage of a low-ash feedstock in the PHICCOS system is offset by the additional oxygen required to raise the gasifier temperature -and hence conversion-. Note that the feedstock moisture content is about the same in both cases due to the presence of phase inversion and thermal drying in PHICCOS and dry feeding systems, respectively.

6.2.3 Gasifier Cold Gas Efficiency

The gasifier CGE estimates from the ROM, for all slurry-fed cases, are presented in Figure 6-4, together with literature values for a dry-fed gasifier. Unlike previous

analyses studying individual aspects in isolation, these results account for both the thermal and the kinetic effects of CO_2 on the gasifier performance, as well as for the feedstock composition (ash and moisture) changes introduced by the PHICCOS slurry preparation process. The coal losses in the latter are not included here but rather in the overall plant results: the CGE calculation uses gasifier feedstock, rather than as-received coal, as a basis.

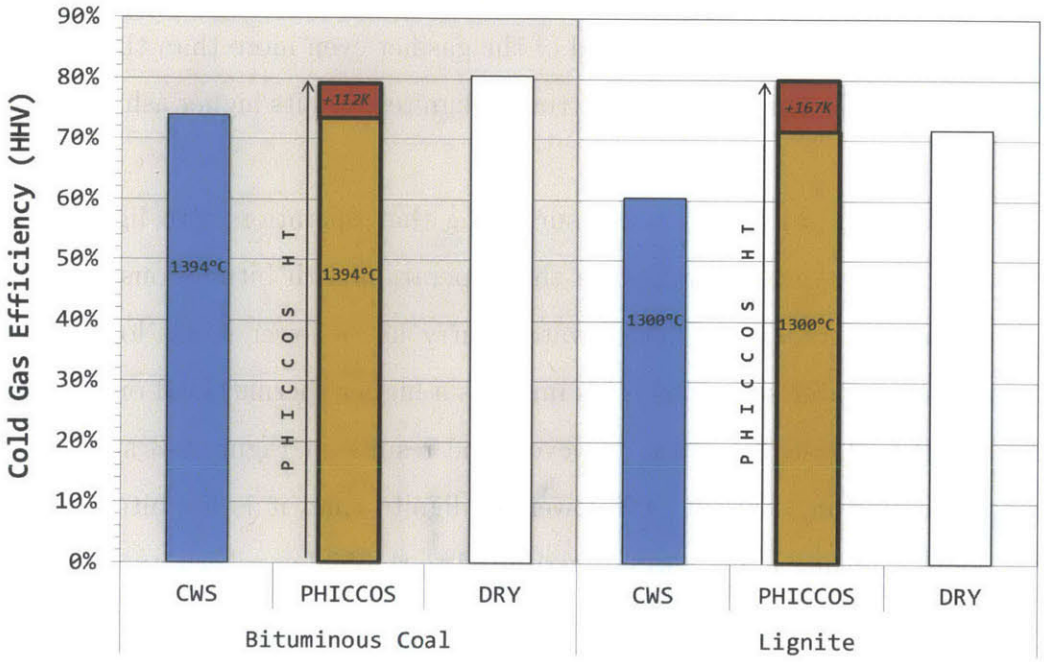

Figure 6-4: Gasifier cold gas efficiency for bituminous coal (left) and lignite (right). The gasifier outlet temperature is also indicated in each case. A reactor with CWS feed (■) is compared with one with PHICCOS feed and the same outlet temperature (PHICCOS, ■) or the same conversion and a higher outlet temperature (PHICCOS HT, ■). Coal losses in the feeding system are not included. Data for dry-fed gasifier from the literature [11, 19] is shown for comparison (□).

The results in the figure show that once all the above is accounted for, the CGE of bituminous coal gasification with PHICCOS feed is equal to that of a reactor with CWS feed operating with the same outlet temperature. The modest thermal advantages of CO_2 for this low-moisture feedstock are offset by its kinetic limitations. However, if the gasification temperature is raised to increase carbon conversion, the CGE of a PHICCOS-fed gasifier is 6%-pt. higher than that of a gasifier with bituminous CWS feed and hence as high as that of a dry-fed reactor.

For lignite, which yields a very low gasification performance in CWS due to its high moisture content, the thermal benefits of PHICCOS exceed the kinetic limitations of CO_2: the CGE is 8%-pt. higher for a PHICCOS-fed reactor than for one with CWS feed operating with the same outlet temperature. It is equally high as the CGE of a dry-fed gasifier. Furthermore, if the temperature of the PHICCOS-fed reactor is raised to achieve full conversion, the CGE advantage of lignite gasification increases to a significant 16%-pt. relative to CWS, and 8%-pt. relative to a dry-fed gasifier.

6.2.4 IGCC Plant Performance

The IGCC plant performance obtained for all slurry-fed cases by coupling the system-level model with the gasifier ROM is summarized in Table 6.1. The plant efficiency of the corresponding dry-fed cases, obtained from the literature, is also included for comparison.

Table 6.1: IGCC plant performance summary. Values for CWS and PHICCOS were obtained from the simulations. Literature values are reported for a plant with dry feed for comparison [11, 19].

	Bituminous				Lignite			
	CWS	**PHICCOS**		*DRY*	**CWS**	**PHICCOS**		*DRY*
			HT				**HT**	
$\dot{m}_{coal}$, tonne/d	5,444	5,731	5,731	–	9,180	9,663	9,663	–
P_{gross}, MW	680	701	700	–	585	632	712	–
P_{net}, MW	492	516	505	–	348	433	489	–
η_{net} **(HHV)**	**28.9%**	**28.8%**	**28.1%**	*31.2%*	**20.4%**	**24.1%**	**27.2%**	*31.9%*

The plant is designed for a fixed thermal input to the gasifier. A larger as-received coal flow ($\dot{m}_{ar\ coal}$) is thus required in systems operating with the low-heating value lignite. Likewise, PHICCOS-fed cases require a larger coal input to the system due to the losses associated with phase inversion.

The net plant efficiency (η_{net}) presented in Table 6.1 shows that an IGCC plant operating with bituminous coal, carbon capture, and PHICCOS feed can achieve at most the same efficiency as a similar plant with CWS feed. For lignite, however, a plant based on the PHICCOS feeding system can achieve an almost 7%-pt. higher efficiency.

Operation of the gasifier at a higher temperature only increases plant performance in the case of lignite. For bituminous coal, the additional ASU power required to raise the temperature more than offsets the benefits of a higher carbon conversion.

This can be observed in Figure 6-5, where the specific auxiliary power consumption in the IGCC plant is presented for all slurry-fed cases. The results show that for every unit gross plant output (P_{gross}), the ASU in a plant with PHICCOS feed consumes about 15% less power than in a CWS-fed plant, for bituminous coal, and up to 40% less in the case of lignite. This is significant, especially considering that the ASU is responsible for at least half of the parasitic power consumption in the plant.

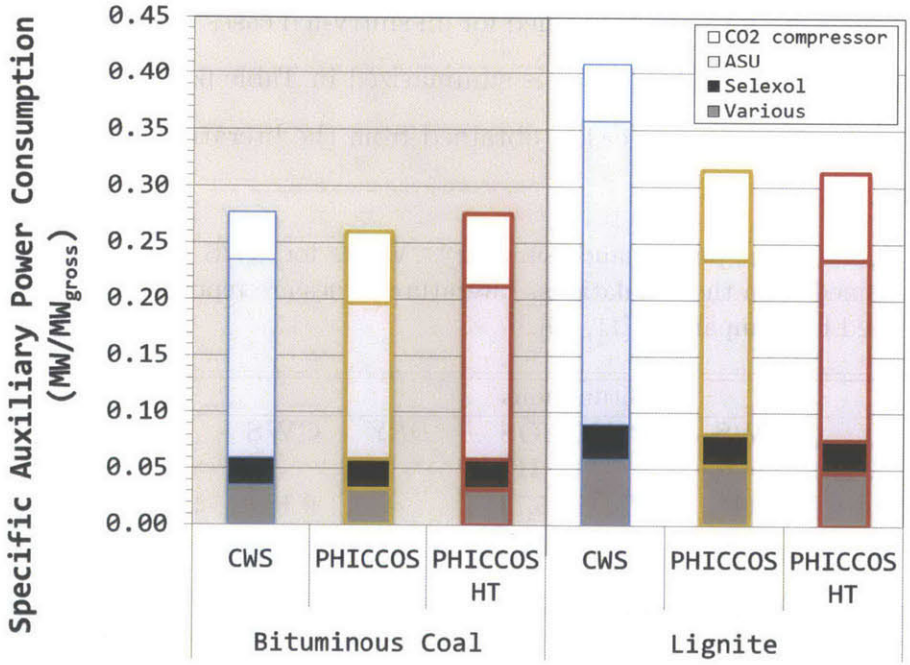

Figure 6-5: Auxiliary power consumption in IGCC plant as a fraction of gross power output for bituminous coal (left) and lignite (right) feedstock. A plant with CWS feed is compared with one based on PHICCOS feed with the same gasifier outlet temperature and lower conversion (PHICCOS) and at a higher gasifier temperature and unchanged conversion (PHICCOS HT).

Nonetheless, the flow of CO_2 that must be compressed in a PHICCOS-fed plant is more than three times that of the flow of CO_2 captured, as the schematic in Figure 6-6 shows. The CO_2 compressor, which is the second largest single consumer of electric power, hence consumes about 50% more power in a PHICCOS-fed system for every MW of gross power produced.

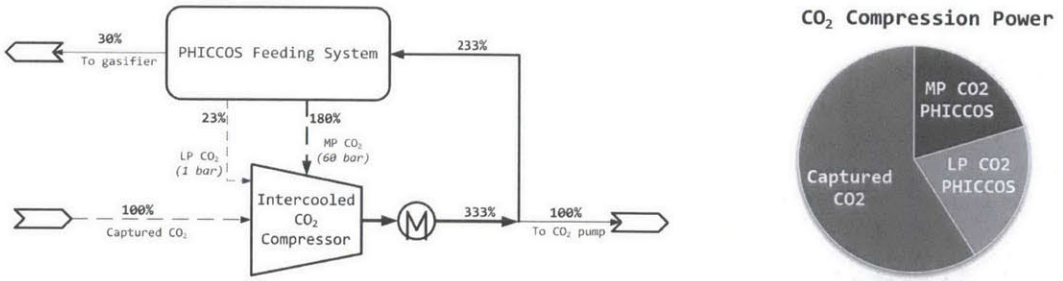

Figure 6-6: Relative flows of CO_2 to the compressor in a PHICCOS-fed system (left) and their contribution to the total power consumption in the CO_2 compressor (right).

The large flow of CO_2 required for operation of the phase inversion process was taken from the LICADO project experience [56], see Table 5.1. An estimated 70% of the CO_2 compressor outlet flow must be recirculated for the PHICCOS feeding system.

The majority of the recirculated flow does not enter the gasifier with the feedstock but is flashed out at low or medium pressure during slurry preparation. As shown in Figure 6-6, recompression of these streams almost doubles the CO_2 compression power, relative to what is required to compress the captured CO_2 alone.

Overall, the CO_2 recompression requirements are large enough to almost completely offset the benefits of a low ASU power consumption in the case of bituminous coal feed, as Figure 6-5 shows. For lignite, on the other hand, the very large ASU power savings dominate and, despite the high CO_2 recompression power, the total specific auxiliary power consumption is 25% lower than in a system with CWS feed.

Different options for reducing the CO_2 recompression power in a PHICCOS-fed plant were examined. For example, the release of some or all the LP and MP CO_2 from PHICCOS to the atmosphere was considered. In its most extreme case, this approach limits the CO_2 recompression stream to the minimum required for CO_2 slurry preparation, resulting in zero net carbon capture in the plant.

The results showed, however, that while the net plant efficiency can be increased by up to 1%-pt. and the CO_2 compressor costs cut by half, the overall plant economics (i.e. LCOE) are only improved by a few percent through this measure. This can be

attributed to the small contribution of the CO_2 compressor costs to the total plant capital, which is the key determinant of IGCC plant economics.

6.2.5 Plant Economics

The capital cost of the PHICCOS feeding system were presented in Section 5.4.3. For a given as-received coal flow, the absolute bare erected cost for PHICCOS is about 60% higher than that of CWS feed, but still only about half that of a dry feeding system.

Figure 6-7 presents the specific (i.e. dollars per kilowatt of net power output) bare erected equipment cost of the entire plant for all cases modeled as well as for a dry-fed system based on a Shell gasifier. The specific equipment costs are dominated by the costs of the power cycle, air separation unit, gasifier, AGR (Selexol) unit, and feeding system.

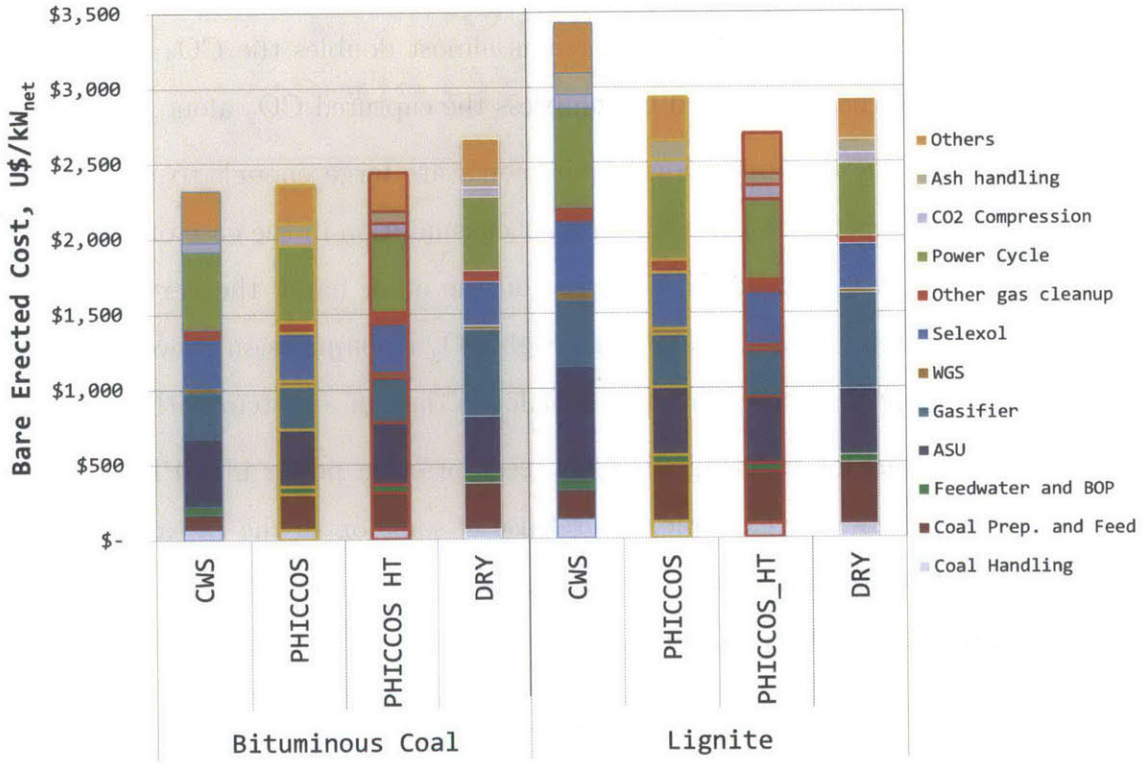

Figure 6-7: Bare erected equipment cost per unit net IGCC power output. "Others" includes accessory electric plant, instrumentation & control, improvements to site, and buildings & structures. Process contingency is included.

For bituminous coal, Figure 6-7 shows that the total specific equipment costs in the slurry-fed systems studied are 10-15% lower than for a dry-fed IGCC. The latter has a more expensive feeding system, as expected. Furthermore, the dry-fed Shell gasifier is more costly than the full-quench GE reactor used for the slurry-fed systems, which is the simplest and hence cheapest gasifier in the market.

The specific BEC in a plant with bituminous coal and PHICCOS feed are almost the same as that of a plant with CWS feed, which is the cheapest commercial technology for this feedstock. The lower costs of a smaller air separation unit in a plant with PHICCOS feed are offset by its more expensive feeding system, relative to CWS.

For lignite, CWS feed is prohibitively expensive due to its low efficiency, which results in large, expensive equipment. In this case, the equipment in a plant with PHICCOS feed is more than 20% cheaper than in a plant with CWS feed and almost 10% cheaper than for a dry-fed plant, which is the cheapest commercial technology. The relative advantage of a PHICCOS-fed plant can in this case be attributed mainly to the cheaper gasifier, since the feeding system and air separation unit have about the same costs per unit net power output.

Finally, the levelized cost of electricity for all cases is presented in Figure 6-8, where the net efficiency and total owner's costs of the plant are also shown. For a plant with PHICCOS feed, only the case resulting in the lowest LCOE is shown for each feedstock.

The LCOE is used as the figure of merit, as it combines the efficiency, capital costs, and operational costs into a single number. Note that the same cost model was used to calculate the LCOE for all cases. While the absolute costs must be treated with caution, as they are associated with a large degree of uncertainty, the relative costs between the technologies studied are a good indication of the relative merits of each.

For bituminous coal, the calculated LCOE is similar for all feeding systems. An IGCC plant with PHICCOS feed produces electricity at almost the same cost as one with CWS, which is the cheapest commercial technology for this feedstock. Dry feed results in an estimated 5-10% higher LCOE than slurry-fed systems.

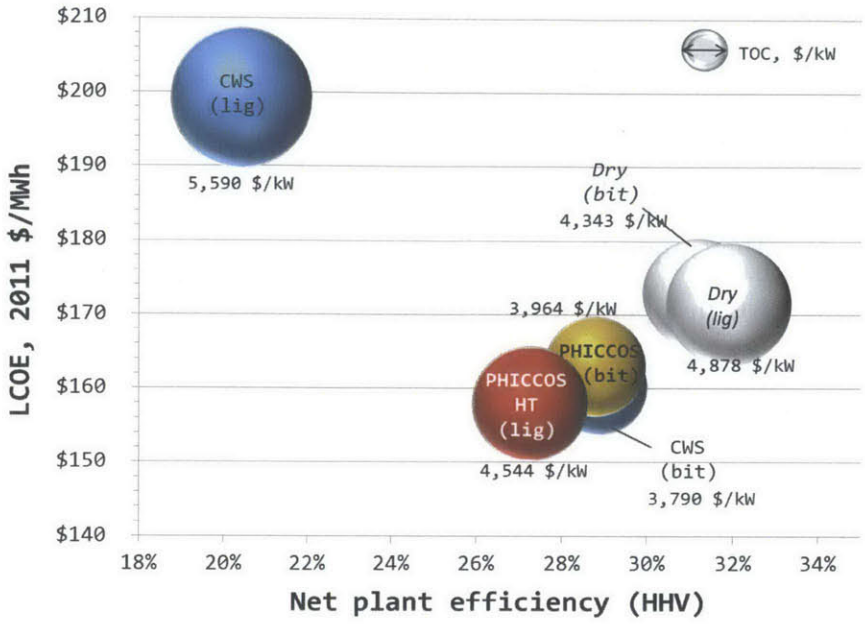

Figure 6-8: Results summary: Levelized cost of electricity, net plant efficiency, and total overnight costs for an IGCC plant with 90% carbon capture operating on bituminous coal (bit) and lignite (lig). The PHICCOS feeding system (PHICCOS/PHICCOS HT) is compared with competing commercial technologies.

For lignite, a plant with PHICCOS feed leads to an 8% lower LCOE than a dry-fed plant, which is the cheapest commercial technology for this feedstock.

Increasing the gasifier temperature as a means to achieve full conversion in a plant with PHICCOS feed proved to be attractive only for lignite. A 10% reduction of the LCOE was calculated as a result in this case. For bituminous coal, the temperature increase would have led to a 5% increase of the LCOE. Optimization of the gasifier temperature is conducted in Chapter 7.

6.3 Chapter Summary

The overall technoeconomics of the PHICCOS feeding system were studied in this chapter through multiscale analysis, which couples system-level and component-level modeling and simulation. An IGCC plant with carbon capture was used as an example application and both bituminous coal and lignite feedstocks were considered. The modeling approach used here integrates thermodynamic, kinetic, and slurry prepara-

tion aspects of a PHICCOS-fed plant. These had only been considered individually in previous chapters.

A PHICCOS-fed reactor has a significantly lower carbon conversion than one with CWS feed. While conversion can be increased by raising the gasifier temperature, this comes at the cost of a higher oxygen consumption. The analysis showed that increasing the gasifier temperature to achieve the same conversion as in a CWS-fed reactor is attractive only in the case of lignite.

For bituminous coal, PHICCOS feed results in a cost of electricity that is comparable to that of CWS feed, which is the cheapest commercial technology for this feedstock. For lignite, PHICCOS offers more attractive economics than a dry-fed system, which is the competing technology.

The economics of a plant with PHICCOS feed are consistently attractive regardless of the coal rank. This results from a combination of a good process efficiency, an intermediate-cost feeding system, a smaller ASU, and a less expensive full-quench, refractory-lined gasifier.

Chapter 7

Optimization of Operating Conditions in a Syngas Production Plant with PHICCOS Feed

The previous chapter showed that the low carbon conversion in a gasifier with CO_2 slurry negatively affects plant economics. Conversion can be increased by raising the reactor temperature, and with it the gasification rate, but at the price of a higher O_2 consumption.

Alternatively, or in addition to this, conversion can be improved by addressing the actual source of the slow gasification kinetics: the high fraction of CO_2 in the gasification agent. This fraction can be reduced by either injecting less CO_2 or more H_2O into the reactor, both of which can be practically implemented in a PHICCOS-fed system.

This chapter examines CO_2 slurry skimming, or flashing, in combination with steam injection and with a gasifier temperature increase, as ways to raise conversion in a PHICCOS-fed gasifier. The coupled multiscale model described in Section 2.4.2 is used to examine the thermal and kinetic tradeoffs of CO_2 and H_2O injection. These are optimized, together with the reactor temperature, in order to achieve the best possible plant economics.

The focus turns from IGCC as an example application to a more general syngas

production plant. The product is clean syngas with a H_2:CO ratio of 2.0 after water-gas shift, as appropriate for the production of synthetic liquid fuels. The figure of merit considered for the optimization is the cost of syngas production.

7.1 Gasification Thermodynamics and Kinetics

The thermal and kinetic components of the gasifier cold gas efficiency were discussed in Section 1.1.2. The potential for better thermal performance in a reactor with coal-CO_2 slurry feed has been the main motivation for conducting research in this field [18].

Nonetheless, the presence of CO_2 in a CO_2 slurry-fed gasifier was shown in Chapters 4 and 6 to be detrimental to the gasification kinetics and to lead a reduction of carbon conversion of about 10%-points, relative to a reactor with CWS feed with the same residence time and operating at the same temperature [54, 66].

7.1.1 Role of CO_2 and H_2O in the Feed

In view of the thermal advantages of CO_2 as slurrying medium and of the kinetic advantages of H_2O as a gasification agent it is desirable to combine these two in order to optimize gasifier performance and economics.

This is schematically illustrated in Figure 7-1, which shows qualitative trends based on preliminary calculations. For a given gasifier temperature and total flow of gasification agent (CO_2+H_2O), extreme cases of gasification only with H_2O and only with CO_2 are shown, as well as intermediate cases in which both H_2O and CO_2 are injected.

The figure shows that a gasifier with CO_2 as the sole gasification agent has low O_2 consumption but also low carbon conversion. On the other hand, a reactor with only H_2O converts more of the coal's carbon content to gas but at the cost of a higher oxygen demand. Overall, the gasifier performance can be optimized by introducing both H_2O and CO_2 with the feed to achieve the best tradeoff between oxygen consumption and conversion, i.e. a maximum gasifier cold gas efficiency.

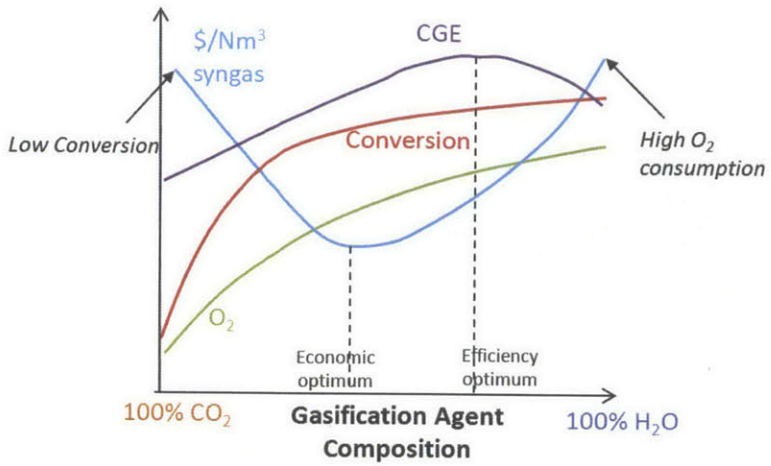

Figure 7-1: Qualitative performance and cost trends as a function of the gasification agent composition, for a given gasifier temperature.

The efficiency optimum may or may not coincide with the economic optimum. Given the high cost of producing pure O_2, the latter is likely to lie to the left of the performance optimum, as the figure shows, where the CGE is lower but so is the oxygen consumption.

PHICCOS Feed with CO_2 Skimming and Steam Injection

The combination of CO_2 and H_2O in the gasifier feed can be achieved regardless of the reactor and feeding system characteristics. Nonetheless, CO_2 slurry-fed reactors are an especially appealing platform: CO_2 is inherently contained in the feed and its flow to the gasifier can be adjusted through CO_2 skimming, or flashing. As illustrated in Figure 7-2, this can be combined with steam injection to achieve the optimum conditions in Figure 7-1.

Steam injection is common practice in dry-fed gasifiers like Shell's, which operate with a steam to dry coal ratio of about 0.11, by weight [19]. CWS-fed reactors, on the other hand, do not have the possibility of optimizing the gasification agent flow, since the amount of H_2O in the slurry is dictated by the slurry rheology. Evaporating excess water from the slurry prior to its injection would be prohibitively expensive, given the thermophysical properties of water.

The idea behind CO_2 skimming is to evaporate, or flash, some of the CO_2 in the

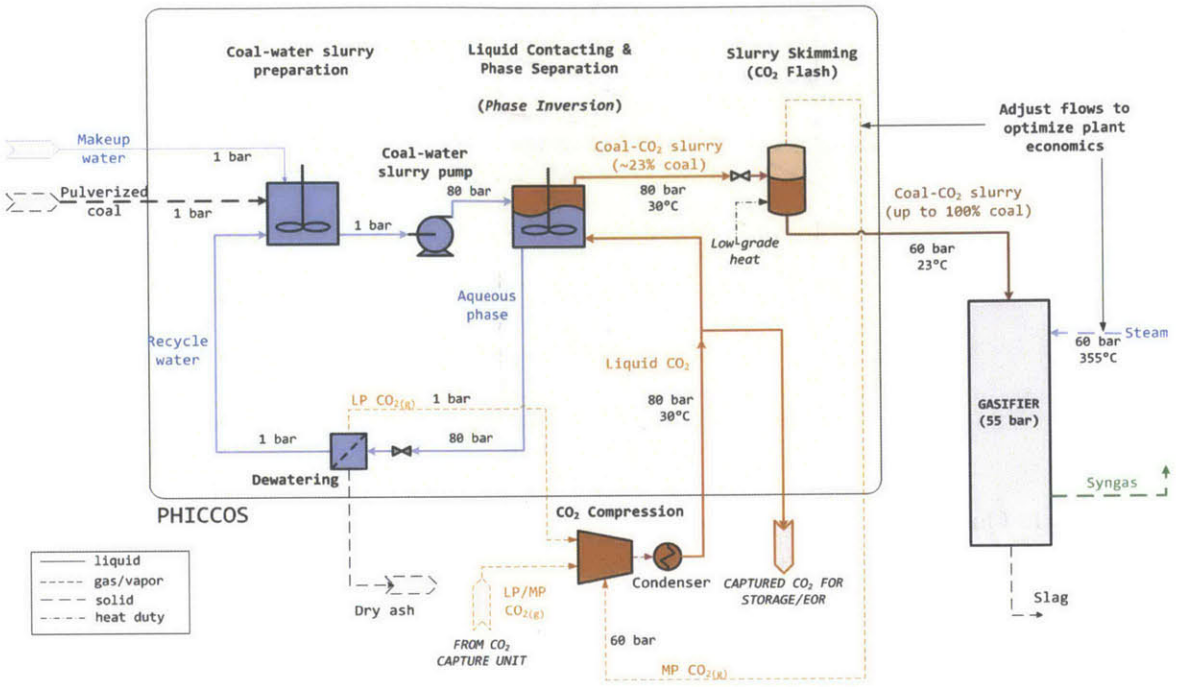

Figure 7-2: PHICCOS-fed gasifier with CO_2 slurry skimming and steam injection.

slurry before it enters the reactor in order to avoid the kinetic limitations imposed by this gas. CO_2 skimming can be achieved relatively easily in a PHICCOS-fed system due to the proximity of pressurized CO_2 to its saturation line.

This is illustrated in Figure 7-3 for a gasifier operating at 55 bar, like the one considered in this work. Slurry skimming is attained by reducing the pressure of the dilute coal-CO_2 slurry from 80 bar to 60 bar in a flash unit, where it enters the liquid-vapor two-phase region. Due to its proximity to the critical point, where the saturated liquid and saturated vapor line meet, the amount of heat required to evaporate CO_2 in the flash unit is low at close to 100-200 kJ/kg CO_2.

Furthermore, low-grade heat is sufficient, since the saturation temperature of CO_2 at 60 bar is only 23°C. In practice, the low-grade heat addition in Figure 7-3 is carried out in a separate heat exchanger. Warm water at a temperature of about 30-50°C can be used as a heat source and coal loadings as high as 100% coal, i.e. dry feed conditions, can be achieved.

For very high coal loadings of about 80% and above, the slurry becomes very viscous and can no longer be handled as a liquid. For such cases, a heated screw

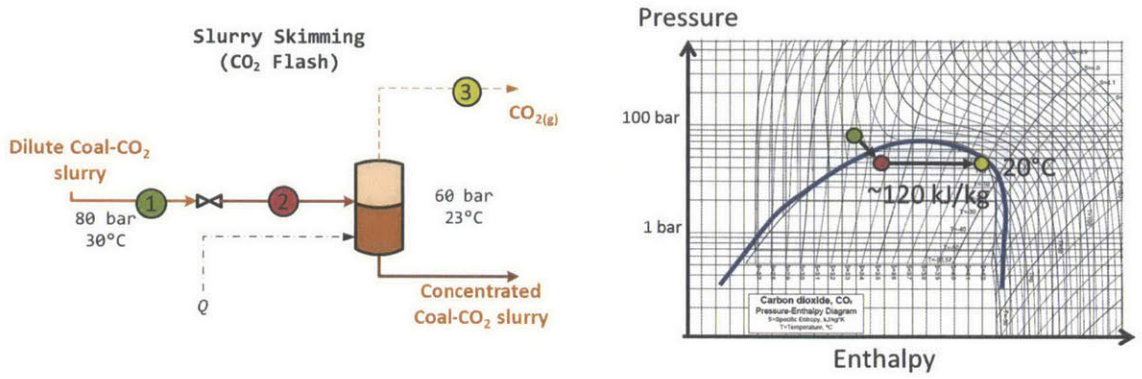

Figure 7-3: Representation of CO_2 slurry skimming (left) in pressure-enthalpy diagram of CO_2 (right).

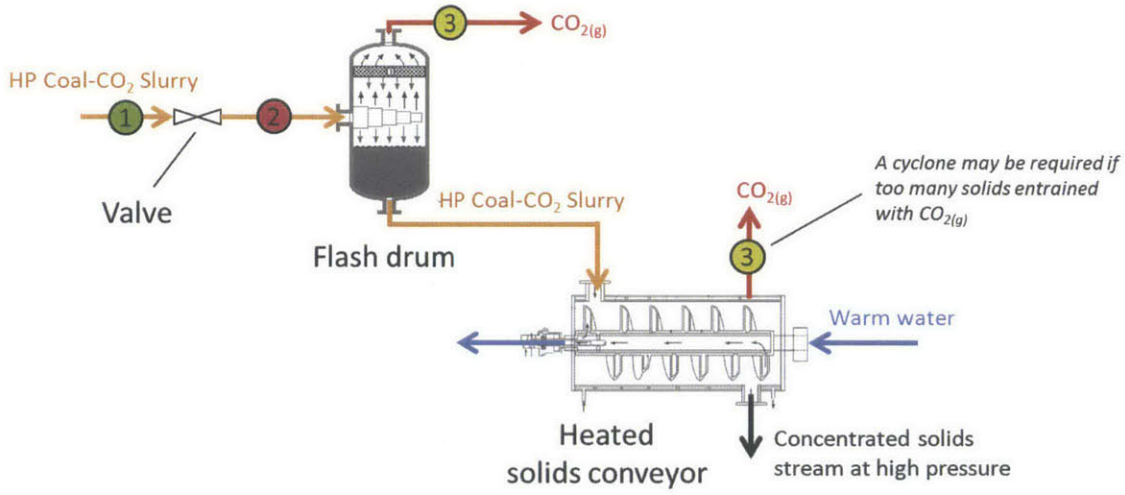

Figure 7-4: Slurry skimming equipment for loadings of more than 80%, for which a conveyor is required [153].

conveyor such as that shown in Figure 7-4 is necessary for skimming and transporting the pressurized, dense solids into the gasifier [153]. Other than its mild internal heating, the conveyor resembles that used in lock-hopper based dry feeding systems to transport the pressurized solids from the hopper to the gasifier.

7.1.2 Role of Gasifier Temperature

Increasing the gasifier temperature is an effective way to speed up the gasification kinetics, given the exponential dependence of the intrinsic reaction rate constants on this variable [66]. It can be implemented as a way to increase conversion in a PHICCOS-fed gasifier either as an alternative to, or in addition to, CO_2 skimming and steam injection.

For a gasifier with coal-CO_2 slurry feed, a slurry loading of 80%, and no steam injection, for example, full conversion can be achieved if the gasifier outlet temperature is raised by about 100K, relative to operation with CWS feed [54, 66]. However, oxygen consumption increases by 10-20% [54, 66] so the attractiveness of this measure is a matter of overall plant economics.

For a constant composition of the gasifying agent, increasing the gasifier temperature has a similar qualitative effect on the plant technoeconomics as increasing the fraction of H_2O entering the gasifier, see Figure 7-1. An optimum gasifier temperature hence exists, which represents the best tradeoff between low conversions at low temperatures and a high oxygen consumption at high temperatures.

7.2 Methodology and Cases Studied

The technoeconomics of a PHICCOS-fed syngas production plant with slurry skimming and steam injection to the gasifier were studied. Bituminous coal and North Dakota lignite were considered. Due to the upgrading effect of the PHICCOS feeding system, the moisture and ash content of the feedstock delivered to the gasifier is expected to be 10% each, for both coals, see Chapter 5. The main difference between the two coals is in their fixed carbon and oxygen content, as well as in their reactivity,

which ultimately leads to different gasification temperatures.

The plant considered contains two full-quench gasifiers, each of which resembles a commercial-scale 1,800 ft^3 full-quench GE gasifier, see Table 2.3. Unlike a GE gasifier, however, the reactor is steam-injected and is not fed with CWS but with coal-CO_2 slurry via the PHICCOS feeding system. Furthermore, the gasifier can be operated in dry feed mode if the entire CO_2 content of the slurry is skimmed before injection.

First, the influence of the CO_2 skimming and steam injection are studied at the reference gasifier temperature, see Table 2.3. The effect of temperature on plant performance and economics is subsequently considered. The CO_2 slurry loading, steam/coal ratio, and gasifier temperature are then jointly optimized in order to achieve the most favorable plant economics. The figure of merit used is the cost of producing one unit of clean syngas. The syngas consists of H_2 and CO at a molar ratio of 2:1, after water gas shift and CO_2 separation, and has a final pressure of 52 bar.

The results are compared with competing commercial feeding systems, i.e. with a CWS-fed plant based on a full-quench GE-type gasifier and with a dry-fed plant based on a Shell gasifier and with downstream syngas compression.

The coupled multiscale model presented in Section 2.4.2 was used for the analysis. The scope of the system studied is presented in Figure 7-5, where the tools used are also indicated. Except for the gasifier, all process units are modeled as 0-D components using the surrogate syngas production plant model presented in section 2.3.4. For the gasifier, the detailed, 1-D reduced order model with presented in Section 2.3.3 is used. It is capable of predicting carbon conversion through the high-pressure chemical kinetics submodel described in Chapter 4.

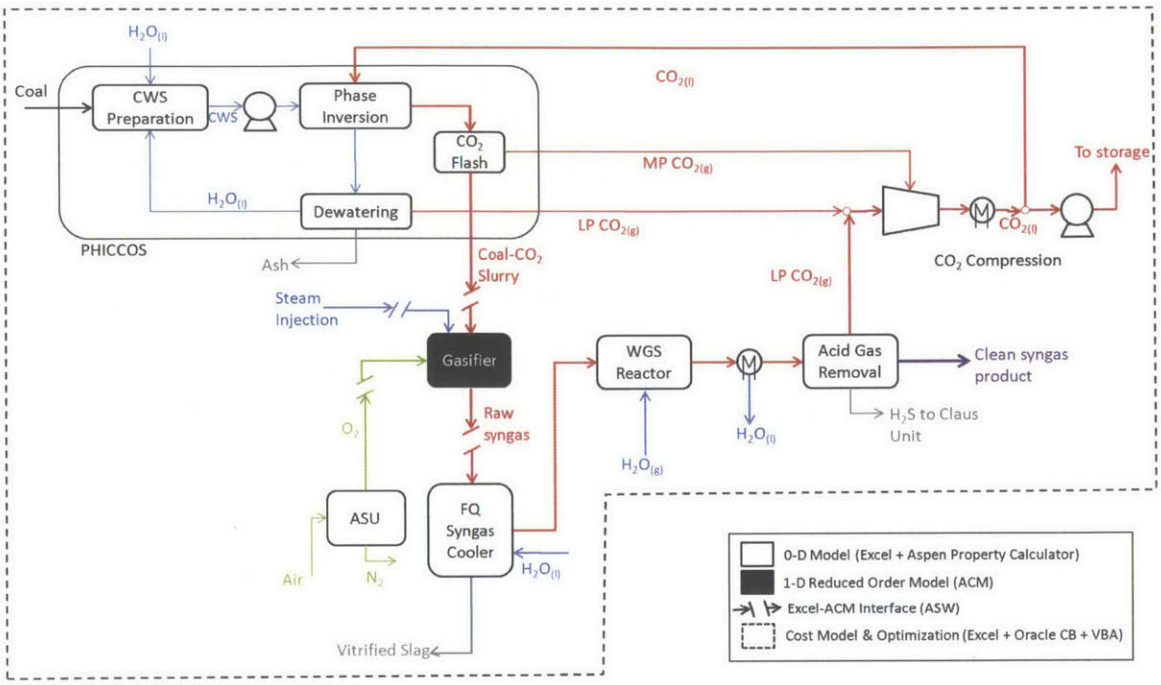

Figure 7-5: Scope of syngas production plant considered and summary of tools used for the analysis. Coal preparation and handling, ash handling, and Claus unit were not modeled but are included in the cost model.

7.3 Results and Discussion

7.3.1 Influence of CO_2 and H_2O in Feed

The influence of CO_2 and H_2O in the gasifier feed was quantified by conducting a sensitivity analysis varying the CO_2 slurry loading, through skimming, and the steam injected to the gasifier. The gasifier outlet temperature was kept constant during this analysis and corresponds to the reference gasifier temperature, for each feedstock, see Table 2.3.

The specific oxygen consumption and carbon conversion in the gasifier are presented in Figure 7-6 as a function of the coal-CO_2 slurry loading and steam injection ratio. The asymptotic behavior of the conversion surface in the figure reflects the Langmuir-Hinshelwood kinetics underlying the gasifier model. These account for the effect of product inhibition at high conversions [66].

The results in the figure show that the conversion and oxygen consumption in a reactor with bituminous coal and with lignite follow similar trends. Due to its higher

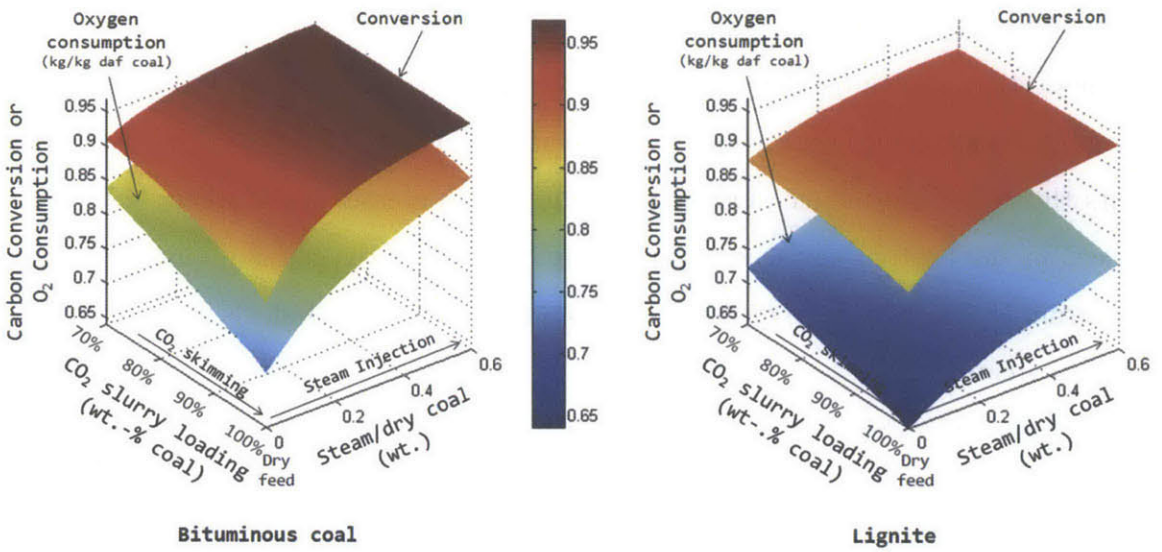

Figure 7-6: Specific oxygen consumption (bottom surface) and carbon conversion (top surface) for a PHICCOS-fed gasifier operating at its reference temperature with bituminous coal (left, 1,400°C) or lignite (right, 1,300°C).

reactivity, a gasifier operating on lignite at 1,300°C has a comparable -only slightly lower- carbon conversion than a bituminous coal-fed reactor operating at 1,400°C. Carbon conversion is incomplete for both feedstocks under these conditions and is in the range of 82%-96% for bituminous coal and 84%-93% for lignite.

Even though its conversion is comparable, the specific oxygen consumption in a gasifier operating on lignite is about 15% lower than for one with bituminous coal. Despite its higher moisture content, gasification of as-received low-rank coal is known to consume only slightly more oxygen than gasification of high-rank coal [154]. This is a result of the high oxygen content of this feedstock, see Table 2.1. For the same moisture and ash content, hence, the specific oxygen consumption of lignite is expected to be lower. This is the case in a PHICCOS-fed gasifier, where both coals are likely to have a comparable content of ash and moisture due to the upgrading effect of the feeding system [59].

Figure 7-6 shows that steam injection, which increases the reactant partial pressure in the gasifier, is an effective means of increasing carbon conversion at a given temperature. This is particularly true at low conversions, where the reaction rate is limited by the low reactant partial pressure. At higher conversions, the role of prod-

uct inhibition gains increasing importance and the kinetic benefits of steam injection are modest, as shown by the curvature of the conversion surfaces in the figure.

While beneficial for the gasifier kinetic performance, steam injection is detrimental to its thermal performance. Oxygen consumption increases when steam is injected, as seen in the bottom surfaces in Figure 7-6: additional oxygen is required not only to sustain the endothermic gasification of additional carbon, but also to heat up the injected steam.

Skimming the CO_2 from the slurry to achieve higher loadings is always beneficial for the thermal performance of the gasifier, as the bottom surfaces in Figure 7-6 show: O_2 consumption drops since CO_2 skimming reduces the thermal load of the slurrying medium in the reactor. At low steam injection ratios, however, increasing the slurry loading also reduces conversion: once again, under these conditions the conversion is limited by the low reactant partial pressure.

The overall tradeoff between the kinetic and thermal gasifier performance at different levels of steam injection and CO_2 skimming can be observed in Figure 7-7, which shows the gasifier cold gas efficiency.

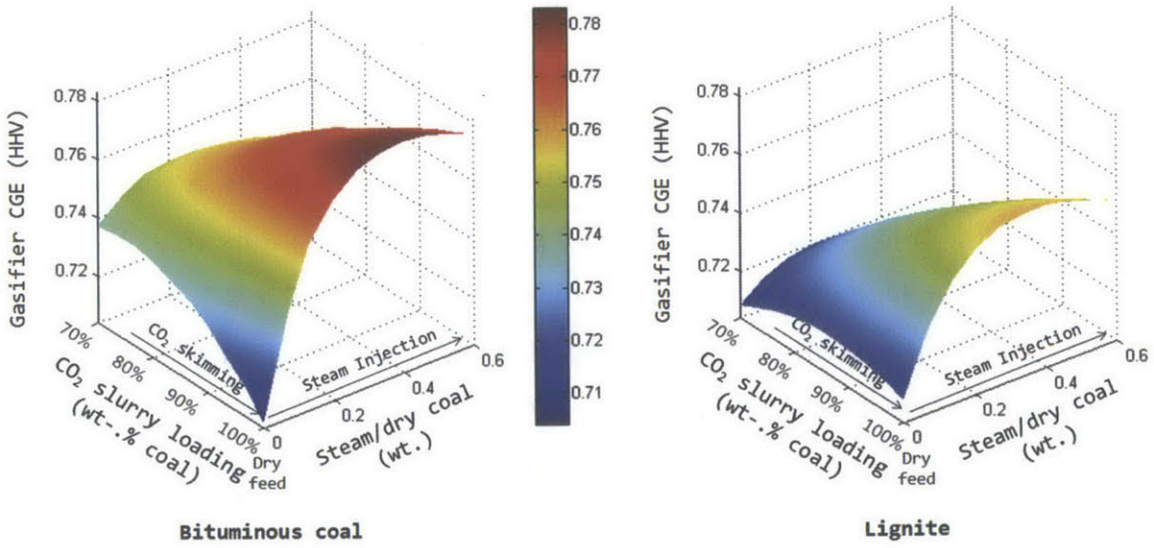

Figure 7-7: Gasifier cold gas efficiency as a function of coal-CO_2 slurry loading and steam/coal ratio for a gasifier operating at the reference temperature with bituminous coal (left, 1,400°C) and lignite (right, 1,300°C).

The results show that CO_2 skimming to loadings above an average of 80% is

detrimental to the gasifier efficiency when no steam is injected into the reactor. Under these conditions, the reactant partial pressure is very low so the oxygen savings arising from CO_2 skimming are over-weighed by the conversion reduction it causes, leading to a CGE decrease. As more steam is injected into the gasifier, however, the reactant partial pressure becomes high enough that the the thermal load of the injected CO_2 dominates. The latter is significantly less than that of steam, but must still be accounted for. As the figure shows, starting at a steam injection ratio of about 0.1, CO_2 skimming up to dry feed conditions (100% loading) always yields the highest cold gas efficiency for a given steam/coal ratio.

The curvature of the surfaces in Figure 7-7 shows that for any given slurry loading, an optimum steam injection ratio exists, i.e. that leading to a maximum CGE. It represents the best tradeoff between the kinetic benefits of steam and the thermal load it represents. The optimum steam/coal ratio increases with slurry loading: steam injection is especially beneficial when little CO_2 enters with the feed, in which case the gasification kinetics are limited by the low partial pressure of the gasification agents.

The maximum CGE of a PHICCOS-fed gasifier operating with bituminous coal at the reference outlet temperature of 1,400°C is 78.5%. For lignite, the maximum CGE at the reference temperature of 1,300°C is 75.9%. For both feedstocks, the efficiency optimum under these conditions is achieved when CO_2 is entirely skimmed out of the slurry (i.e. for 100% coal loading, dry feed conditions) and when steam is injected at a ratio of about 0.4 kg/kg dry coal.

The total cost of producing 1,000 normal cubic meters (kNm^3) of clean syngas with a H_2:CO ratio of 2:1 is presented in Figure 7-8 as a function of the coal-CO_2 slurry loading and of the steam injection ratio.

The cost of syngas production for a gasifier operating with no steam injection and a coal-CO_2 slurry loading of 80% is indicated in the figure. It corresponds to the conditions of the originally proposed PHICCOS design, see Chapter 5, in which the slurry is only skimmed up to the maximum loading at which it can still flow as a liquid [54, 59].

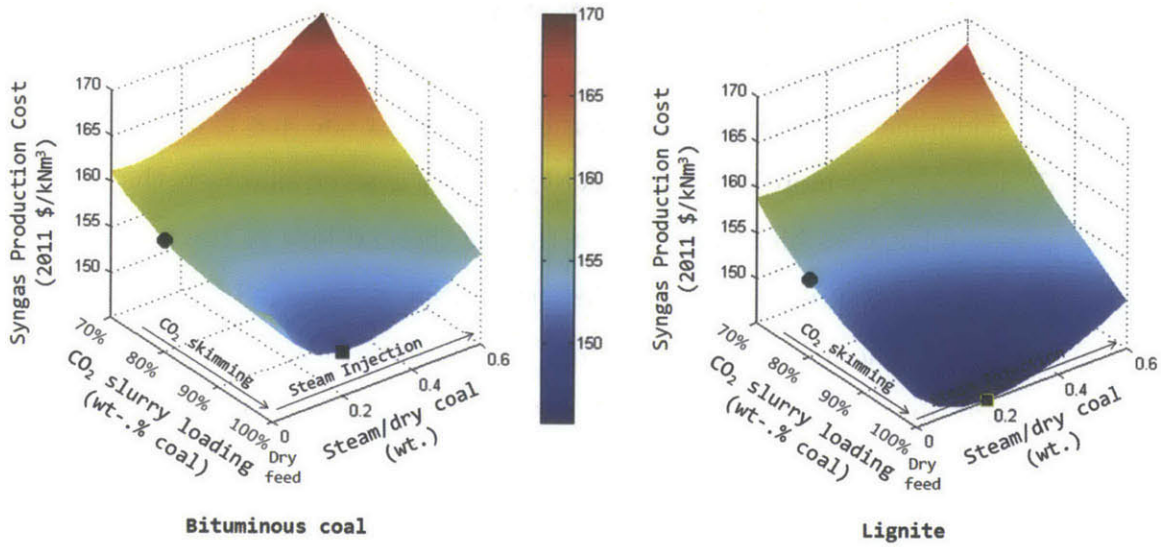

Figure 7-8: Syngas production cost as a function of coal-CO_2 slurry loading and steam/coal ratio for a gasifier operating at the reference temperature with bituminous coal (left, 1,400°C) and lignite (right, 1,300°C). The syngas cost at the originally proposed conditions (•) is compared with the achievable cost if CO_2 and H_2O flows are optimized (■).

The results show that, at the reference temperature, the syngas production cost can be reduced from \$157/kNm^3 to \$146/kNm^3 for bituminous coal and from \$154/kNm^3 to \$138/kNm^3 for lignite, if the flow of CO_2 and H_2O in the feed is optimized. For both feedstocks, the minimum syngas cost at the reference temperature is achieved when CO_2 is completely flashed out of the slurry and when steam is injected at a ratio of 0.2 kg/kg dry coal.

The minimum syngas production cost is located at a lower steam injection ratio than the maximum cold gas efficiency. This is predominantly due to the cost of producing additional oxygen when steam is added. Oxygen production consumes a large amount of electricity and, most importantly, is associated with very high capital costs. The latter is the dominating factor in the economics of a syngas production plant [155].

7.3.2 Influence of Temperature

The influence of the gasifier outlet temperature on carbon conversion at different steam/coal ratios is presented in Figure 7-9. The results in the figure are for a constant coal-CO_2 slurry loading of 100%, i.e. for dry feed conditions, as these led to the most favorable plant economics at the reference gasifier operating temperature, see Figure 7-8.

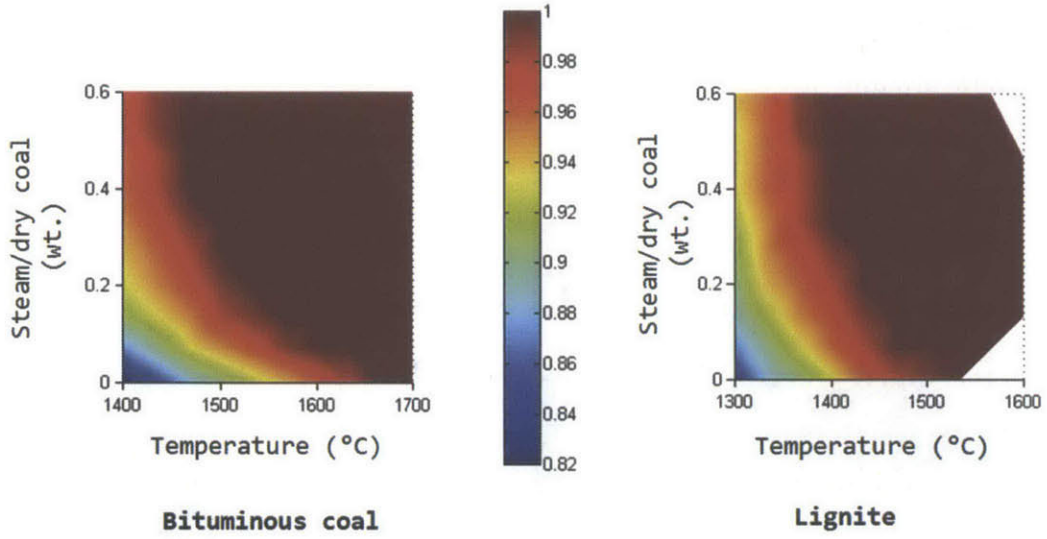

Figure 7-9: Carbon conversion as a function of gasifier outlet temperature and steam/coal ratio for a gasifier operating with full slurry skimming and with bituminous coal (left) or lignite (right).

The results show that carbon conversion increases with gasification temperature and with steam injection, both of which directly benefit the gasification kinetics. While raising the temperature is a very effective way of increasing conversion, the flow of oxygen required to operate under these conditions is high and costly. Furthermore, very high temperatures can compromise the lifetime and integrity of gasifier components.

The advantages of injecting steam into a PHICCOS-fed reactor are evident: if no steam is injected, the outlet temperature must be raised by about 200K, relative to the reference temperature of operation with CWS (1,400°C for bituminous coal and 1,300°C for lignite), in order to achieve full conversion under dry-feed conditions. On the other hand, if steam is injected into the reactor, a temperature increase as low as

50-100K is sufficient to achieve full conversion.

Very high steam injection ratios of about 0.25 and above have diminishing returns on conversion. As discussed earlier, this results from the effect of product inhibition on the reaction rate at high conversions. This, in conjunction with the thermal load of steam, makes large steam/coal ratios unattractive.

The latter can be observed in Figure 7-10, which presents the total syngas production cost for a system with full slurry skimming (i.e. no CO_2 injection) as a function of temperature and steam injection ratio.

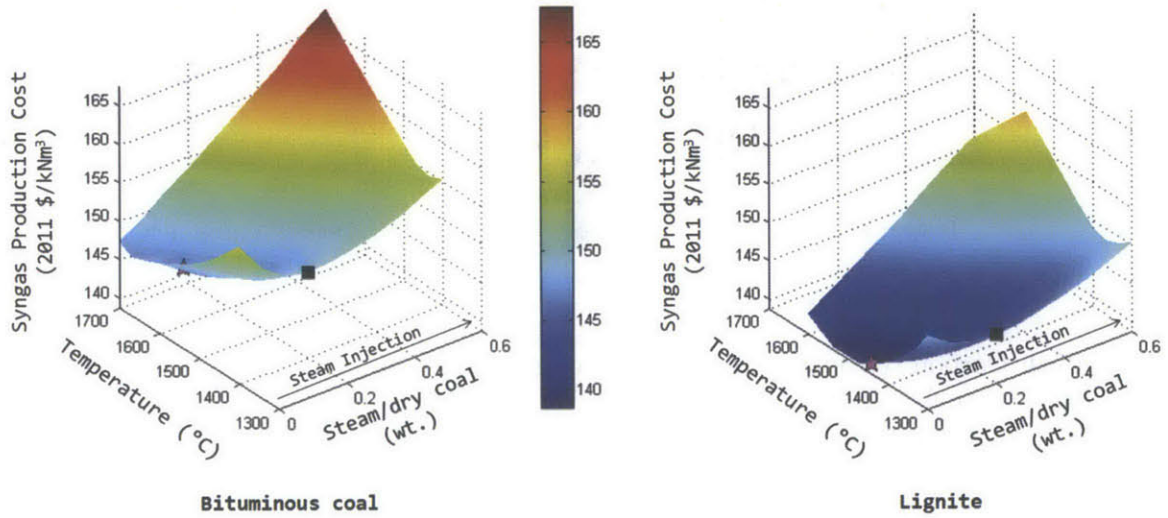

Figure 7-10: Syngas production cost as a function of gasifier outlet temperature and steam/coal ratio for a gasifier operating without CO_2 injection and with bituminous coal (left) or lignite (right). The optimum (★) corresponds to the overall economic optimum of the plant and is compared with the cost before optimizing the gasifier temperature (■).

The plant economics in the figure show that, for dry feed conditions, the syngas production costs are minimized when the gasifier is operated with an outlet temperature of 1,599°C and a steam/coal ratio of 0.06 for bituminous coal, and at 1,467°C and a steam/coal ratio of 0.03 in the case of lignite. A significant improvement in the plant economics is achieved by optimizing the temperature.

7.3.3 Overall Plant Economic Optimum

The coal-CO_2 slurry loading, steam/coal injection ratio, and gasifier outlet temperature were jointly optimized to find the lowest cost of producing clean, shifted syngas at a pressure of 52 bar, free of CO_2 and with a H_2:CO ratio of 2.0. The value of the gasifier operating conditions at the optimum is presented in Table 7.1, together with the main plant performance parameters for both feedstocks studied.

Table 7.1: Gasifier performance and plant technoeconomics at economic optimum for a syngas production plant with a gasifier operating at 55 bar. The product is clean syngas at 52 bar with a molar H_2:CO ratio of 2.0

		Bituminous	Lignite
Gasifier Operating Conditions			
CO_2 slurry loading	wt.% coal	100%	100%
Steam injection	kg/kg dry coal	0.06	0.03
Outlet temperature	°C	1,599	1,467
Gasifier Performance			
O_2 consumption	kg/kg daf coal	0.884	0.776
Carbon conversion		99.96%	99.84%
Cold gas efficiency	(HHV)	81.4%	81.8%
Plant Performance			
Coal feed (ar)	kg/h	238,783	402,705
Syngas product flow	kNm^3/h	394.2	396.6
Net plant efficiency	(HHV)	64.7%	63.6%
Optimized Syngas product cost	**$/kNm^3**	**$146.1**	**$138.7**
	($/GJ)	($12.3)	($11.7)

The results of the optimization show that, regardless of the feedstock, it is always desirable to skim the CO_2 from the coal slurry up to dry feed conditions, i.e. to 100% loading. Hence, the overall plant optima in Table 7.1 correspond to the cost minima from the sensitivity analysis in Figure 7-10, which were discussed in the previous section.

Accordingly, the minimum cost of syngas production is $\$146.1/kNm^3$ for bituminous coal and it is achieved when the gasifier is operated with an outlet temperature of 1,599°C and a steam/coal injection ratio of 0.06, by weight. When lignite is used as a feedstock, the cost of syngas production can be as low as $\$138.7/kNm^3$ if the gasifier operates at 1,467°C at the outlet and without steam injection at a ratio of 0.03. For both feedstocks, the plant economic optimum is achieved under conditions

at which the carbon conversion in the gasifier is complete (>99.8%).

Recall that the coal injected into the gasifier by the PHICCOS feeding system has a 10% moisture content for both feedstocks. For the more reactive lignite, this moisture content is enough to achieve a high enough conversions: the economic optimum is achieved without additional steam injection. This is not the case for bituminous coal, for which H_2O injection is required in order to minimize the cost of syngas production in the plant.

The optimum steam/coal ratio of only 0.03 estimated here for lignite agrees relatively well with that of a Shell gasifier, for which no steam injection is reported when operating with a similar coal dried to 12% moisture [11]. A Shell reactor is a good reference since it is dry-fed, like the PHICCOS-fed gasifier when operating under economically optimum conditions.

For bituminous coal, however, the optimum steam/coal injection ratio of 0.06 estimated here is lower than the value of 0.11 reported for a Shell gasifier. Nonetheless, the coal delivered by the PHICCOS feeding system has a moisture content which is twice as high as the 5% contained in the dried bituminous coal injected to a Shell reactor [19].

Furthermore, the steam injection values above are for a Shell gasifier operating with a temperature of 1,427°C [11, 19], for both coals, which is somewhat lower than the optimum temperature of a PHICCOS-fed reactor. As the results in Figure 7-10 showed, the optimum steam/coal ratio increases with decreasing temperature, which partly explains the deviation from our results.

In practice, the gasifier operating temperature is not only very hard to measure but is also very feedstock-dependent. Approximate ranges, rather than a single value, are typically given by manufacturers. A Shell reactor, for example, is generally reported to operate at 1,400-1500°C for both bituminous coal and lignite [156]. Furthermore, the operating temperature is strongly affected by practical considerations beyond the aspects considered here, such as the ash characteristics of the coal, as well as the lifetime of the gasifier parts.

For operation of the gasifier at temperatures other than the optimum, the cost of

syngas production increases according to the results in Figure 7-11, which corresponds to the top view of Figure 7-8. It is a gasifier operating map showing how much steam should be injected at any given temperature in order to achieve the best possible plant economics.

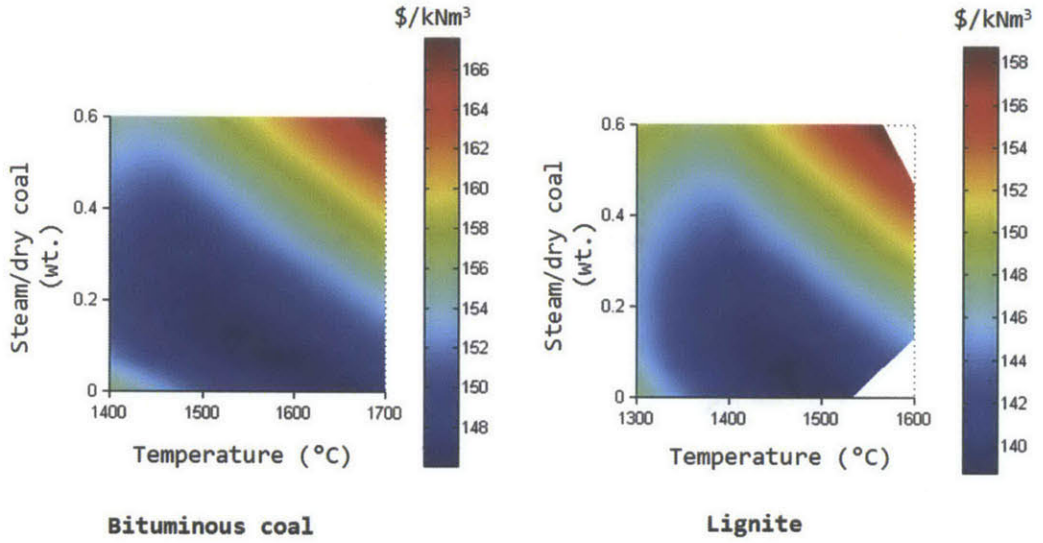

Figure 7-11: Operating maps for a dry-fed gasifier with bituminous coal (left) and lignite(right). The resulting cost of clean syngas production is indicated as a function of the gasifier outlet temperature and steam injection ratio.

7.3.4 Comparison with Commercial Technologies

The technoeconomics of syngas production in a plant with PHICCOS feed operating at its economic optimum are summarized in Figure 7-12 and compared with estimates for competing commercial technologies based on EFGs. The figure shows the total cost of producing a unit of clean syngas at a final pressure of 52 bar, which is the figure of merit used in this study, together with the overnight capital costs of the plant, and the net plant cold gas efficiency.

The net plant efficiency in the figure is the chemical energy contained in the clean, shifted syngas product as a fraction of the total energy input to the plant in the form of coal, electricity, and steam. The two latter were converted to fuel-equivalent by assuming a power generation efficiency of 33% and a boiler efficiency of 90%, respectively [75, 157].

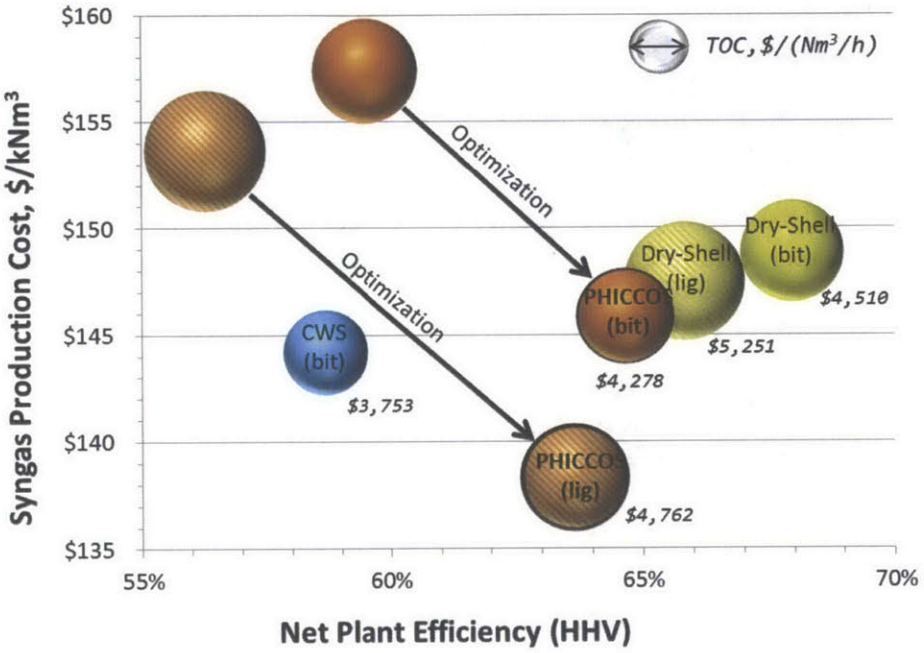

Figure 7-12: Summary of PHICCOS technoeconomics at optimum and comparison with competing commercial technologies for bituminous coal (bit) and lignite(lig). The arrows indicate the improvement achieved through optimization. The cost of syngas production from lignite in a CWS-fed gasifier is outside the range shown in the figure.

The results show that the cost of syngas production was reduced by an average of 10% through the optimization of gasifier operating conditions conducted in this study. The improvement presented is relative to the initially proposed PHICCOS feeding system [59, 125], i.e. relative to a plant operating at the reference gasifier temperature, without steam injection, and with a coal-CO_2 slurry loading of 80%.

A plant with PHICCOS feed and a full-quench gasifier can produce clean syngas from bituminous coal at almost the same cost as one with conventional CWS feed, which is the cheapest EFG-based commercial technology for this feedstock [19]. For lignite, the PHICCOS feeding system leads to the lowest cost of syngas production and is hence more economic than a system based on a dry-fed Shell gasifier.

The clean syngas production cost from an optimized, PHICCOS-fed gasifier is also lower than the \$160-200/kNm^3 (\$15-19/GJ, 2010 cost basis) reported in the literature for a plant based on a fluidized bed gasifier with post-gasification tar removal [155]. This comparison should be treated with caution, however, since the estimates not only contain uncertain parameters, whose effect is being studied, but they also originate from different cost sources.

The economic attractiveness of a syngas production plant with PHICCOS feed and a full-quench gasifier, relative to competing technologies, can be attributed to the combination of an intermediate plant efficiency and intermediate capital costs. The latter dominate the total cost of syngas production and have been presented in more detail in Chapter 6 for IGCC.

Interestingly, the results of this work showed that the most economic way of producing clean syngas from coal with an EFG is by using the PHICCOS feeding system and skimming out all the CO_2 from the coal-CO_2 slurry prior to gasification, achieving dry feed conditions. Hence, the role of CO_2 in an optimized PHICCOS-fed system is to help remove the water content from a pressurized coal-water slurry before being flashed out of the feed prior to the reactor.

Operating the system under optimum, dry feed conditions implies that the coal is no longer injected into the gasifier as a liquid but is rather fed in its dense state. As discussed in Section 7.1.1, a screw conveyor is required for evaporating the CO_2

and transporting the pressurized, dense solids to the gasifier after phase inversion with CO_2. This resembles the transport of solids between a lock hopper system and a dry-fed gasifier such as Shell's.

In the case of PHICCOS, the screw must be internally heated to 20-30°C with warm water in order to skim out the CO_2. The moisture content of the coal delivered by the PHICCOS feeding system is about 10%. This is within the range of 5-12% used in lock hopper-based dry feeding systems [11, 19] in order to ensure proper flow behavior of the dense solid stream.

While this study shows that dry feed conditions lead to the lowest cost of syngas production, dry solids handling adds complexity to the plant and may compromise its reliability. Hence, it may be preferable to operate at the maximum slurry loading of 80% and avoid the need for such. The operational aspects of the PHICCOS feeding system are the topic of future work.

7.4 Chapter Summary

Multiscale analysis was used to study the technoeconomics of CO_2 skimming and steam injection as ways to control the flow of CO_2 and H_2O injected into a PHICCOS-fed full-quench gasifier and, in combination with a temperature increase, help improve carbon conversion. The CO_2 and H_2O flow in the feed were optimized, together with the gasifier temperature, in order to achieve the lowest cost of syngas production in a plant producing clean, shifted syngas at a pressure of 52 bar and with a H_2:CO ratio of 2.0, as appropriate for synthetic fuel production. Both as-received bituminous coal and as-received lignite were considered; their moisture and ash content are reduced to 10% each through the inherent upgrading occurring in the PHICCOS feeding system [59].

The syngas production cost in the plant was reduced by an average of 10% through optimization of the gasifier operation conditions. The minimum cost is \$146.1/kNm^3 for bituminous coal and \$138.7/kNm^3 for lignite. This optimum is achieved when the gasifier is operated without CO_2 injection (i.e. full coal-CO_2 slurry skimming),

with an outlet temperature of 1,599°C for bituminous coal and 1,467°C for lignite, and with a steam/coal ratio of 0.06 and 0.03, respectively. The carbon conversion in the gasifier is complete for both feedstocks when operating under optimum conditions.

Gasifier operating maps were generated, which can be used as a guideline to determine the optimum steam/coal ratio for dry-fed gasification at temperatures other than the optimum, which may be desirable due to practical constraints.

Compared to competing commercial technologies based on entrained flow gasification of coal, a PHICCOS-fed plant with a full-quench gasifier offers the lowest cost of clean syngas production from lignite and a similar cost as the cheapest commercial technology for bituminous coal.

Chapter 8

Sensitivity and Uncertainty Quantification

The experimental observations of phase inversion of coal with CO_2 from the LICADO project are a good indication of the feasibility of the process, as well as of its expected performance. However, a significant degree of uncertainty still exists: the data collected is limited in number, originates from a small-scale experimental set-up, and corresponds to operation of the process for the purpose of beneficiation, rather than for slurry preparation.

This chapter studies the impact of the uncertainty in the PHICCOS feeding system performance and economics on the cost of syngas production in the plant. The coupled multiscale model presented in Section 2.4.2 is used for this purpose.

First, the main uncertain variables in the PHICCOS system are identified and the range within which these are expected to lie is discussed. Experimental measurements of phase inversion of coal with CO_2, data from the literature, and recommendations from experts are used to define these ranges.

Next, a deterministic sensitivity analysis is conducted in order to study the effect of the individual uncertain variables on the plant technoeconomics. A probability distribution function is then used to describe each of the uncertain variables and Monte Carlo simulations are conducted to quantify the propagation of PHICCOS uncertainty to the syngas production cost.

Finally, the resulting probability distribution function of the syngas cost is presented. Its mean value is compared with that resulting from commercial feeding systems, as well as with the cost estimates presented earlier in this work, which did not consider process uncertainty.

8.1 Uncertain Variables and Uncertainty Range

The uncertain parameters in the PHICCOS feeding system can be classified as performance or economic variables.

The performance uncertainty arises from the variability of the PHICCOS performance for a given set of operating conditions. The enthalpy recovery, and the ash and moisture content of the product coal have been observed to vary under otherwise identical conditions [56]. The variable characteristics of the feedstock, together with the complex interactions involved in the phase inversion process, are responsible for this.

Furthermore, the economics of the plant depend strongly on the reactivity of the feedstock. The latter also varies significantly from coal to coal, even within the same rank, and is hence an important uncertain variable that must be accounted for.

The main uncertain economic parameters are the capital costs of PHICCOS and its availability, or capacity factor. The latter is an indication of how reliable this technology is. It affects the capacity factor of the overall plant directly, and hence the cost of syngas production.

The range within which each of the uncertain variable considered is expected to lie is presented in Table 8.1. It is characterized by a maximum and a minimum, which were estimated either from experimental data from the literature or from personal communication with experts in the field. The mean reported in the table is the base-case value, i.e. it corresponds to the optimum conditions identified in Chapter 7.

With the exception of the feedstock reactivity factor, the uncertain variables have the same mean value for both lignite and bituminous coal. Hence, the uncertainty range was also assumed to be the same. This assumption may have to be revisited

Table 8.1: Uncertain variables and uncertainty range considered.

Variable	*Lower Limit*	**Mean**	*Upper Limit*
PHICCOS performance			
Enthalpy recovery	*91%*	**95%**	*99%*
Product ash (daf)	*9.2%*	**10%**	*10.8%*
Product moisture	*5%*	**10%**	*15%*
PHICCOS bare erected costs	*70%*	**100%**	*150%*
PHICCOS yearly outage days	*0*	**2**	*7*
Feedstock Reactivity Factor			
Bituminous coal	*0.6*	**8.3**	*11.9*
Lignite	*3.7*	**9.8**	*71.8*

as more experimental evidence of phase inversion of lignite becomes available.

Furthermore, the uncertain variables in the PHICCOS performance were assumed to be independent of each other. In reality, enthalpy recovery, ash and moisture content are correlated, however, more experimental data at the conditions of interest is necessary to be able to establish this correlation.

8.1.1 PHICCOS Performance

The performance of the PHICCOS feeding system is characterized by its enthalpy recovery and by the ash and moisture content of the product it delivers to the gasifier.

The upper and lower uncertainty limits for the PHICCOS performance in Table 8.1 were estimated from experimental observations of phase inversion of coal with CO_2 in the LICADO project (see Section 5.3). These limits were assumed to be the same for bituminous coal and lignite. This is consistent with the LICADO results, which showed that the phase inversion performance was similar for different coals ranging from fully hydrophobic to fully hydrophilic, as long as 1-Octanol is added in the latter case in very small quantities (parts per million) [56].

The raw experimental data from the LICADO project contains enthalpy recovery and product ash results for a large number of experimental runs. Their variability from run to run under a given set of operating conditions can hence be used to define the uncertainty range in Table 8.1.

However, the raw data shows that most runs were conducted under different operating conditions or for different coals, making it difficult to quantify variability. Still, 15 sets of runs could be identified for which more than one experiment was conducted without changing the operating conditions or feedstock. The mean enthalpy recovery and product ash content in each of these sets of runs is presented in Figure 8-1. Every data point in the figure represents an average of 2-3 runs (maximum 6) for a given coal and under a given set of conditions.

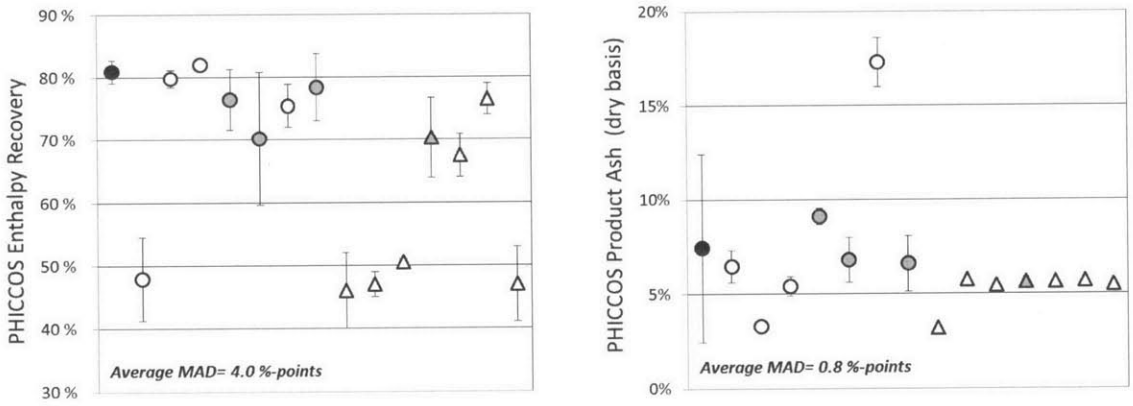

(a) Enthalpy recovery

(b) Product ash content

Figure 8-1: Variability of PHICCOS performance estimated from raw experimental data from LICADO project [56]. Each data point represents the mean of two or more runs for a given feedstock and under a given set of experimental conditions. The error bars show the mean absolute deviation.

The error bars in the figure show the mean absolute deviation (MAD) in each case. The MAD is the mean of the absolute deviations of a set of data about the data's average. It is a more robust measure of statistical dispersion than the standard deviation for cases with outliars [158, 159].

Given the limited data available for every set of operating conditions, there is indeed a high risk of overweighing outliars if the standard deviation is used as a measure of variability in this case. Hence, the average MAD of the 15 sets of runs in the figure was used instead. It is 4.0%-pt. for the enthalpy recovery and 0.8%-pt. for the ash content of the product. The uncertainty of these variables is hence assumed to be limited to values ±4%-pt. and ±0.8%-pt. away from the mean, respectively, see

Table 8.1.

The moisture content of the PHICCOS product is not tabulated in the raw experimental data from the LICADO project. A range of 5-15% moisture is reported as typical for all coals studied [56] and was assumed here.

8.1.2 PHICCOS Capital Costs

The accuracy in the capital costs estimates for the PHICCOS feeding system is expected to be about -30% to +50%. These limits correspond to those defined by AACE for Class 4, i.e. feasibility-stage, cost estimates [11], and were used to define the uncertainty range for this variable.

The lower and upper limit of the uncertainty range of the bare erected capital costs of PHICCOS is thus 70% and 150% of the mean value, respectively. The mean is the estimate resulting from the cost model described in Section 2.3.5.

8.1.3 PHICCOS Yearly Outage Days

A similar pump as that used for CWS feed is required in the PHICCOS feeding system in order to pump CWS to the phase-inversion vessel, where it is put in contact with CO_2.

The CWS feeding system at the Tampa IGCC Polk power station reports about 2 days of unplanned outages per year. These are typically due to problems with the slurry pump, which require the replacement of diaphragms and check valves [49, 71].

Since rotating equipment tends to be the largest source of outages and a similar pump is used, a mean of 2 yearly outage days was also assumed for PHICCOS. This is included in the 86% mean plant availability discussed in Section 2.3.5.

The number of unplanned outage days of PHICCOS is expected to vary within the range of 0 to 7 per year. The lower limit indicates that the feeding system runs smoothly. The upper limit considers the operational risks of adding additional equipment to the plant beyond the CWS pump. It was selected based on recommendations from experts operating existing slurry-fed gasification-based units [71]. The

overall plant availability changes by about ±1%-pt. when the number of outage days of PHICCOS varies within the specified range.

8.1.4 Feedstock Reactivity Factor

The relative reactivity factor of the feedstock, ψ, was introduced in Chapter 4. It is an adjustment parameter which accounts for the difference in the reactivity between coals with different physico-chemical characteristics. The intrinsic gasification rate increases proportionally with ψ, see eq. 4.5, so it affects carbon conversion directly, and thus plant economics.

The value of ψ is strongly rank-dependent and can differ by orders of magnitude even between coals of similar rank. This is illustrated in Figure 8-2, which shows the value of ψ for coals with increasing carbon content (i.e. increasing rank), as calculated from reaction rates measurements from the literature [66].

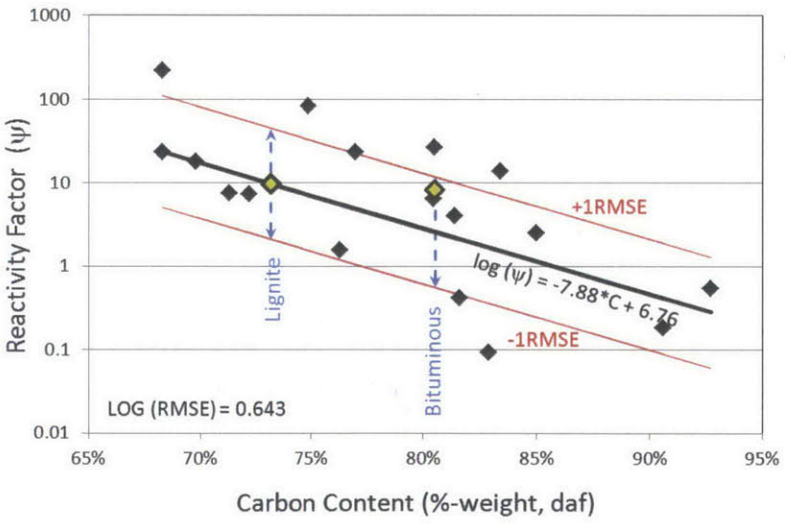

Figure 8-2: Reactivity factor for coals of different ranks. The RMSE is used as a measure of variability to define uncertainty range. The data points highlighted indicate the values used throughout this work for each feedstock.

The data points in the figure are identical to those in Figure 4-2. The values of ψ used throughout this study for bituminous coal and lignite are highlighted, see Chapter 4 for more details on their estimation.

In addition, the figure shows the root mean square error (RMSE) of the data

relative to the correlation. The RMSE was used as an estimate of the lower and upper limits within which the reactivity factor is expected to lie for each feedstock. The value of ψ for bituminous coal is close to the upper limit of the defined range. Lignite lies in the middle given that it was estimated with the correlation.

8.2 Sensitivity to Uncertain Variables

The relative importance of the variables in Table 8.1 was assessed by studying the sensitivity of the syngas production cost to each of them, individually, within its uncertainty range.

The results of the sensitivity analysis are presented in Figure 8-3. The uncertainty range of each variable has been normalized between its lower limit (0%) and its upper limit (100%).

The results in the figure show that, within the uncertainty range studied, the feedstock reactivity factor has the highest impact on the syngas cost. This reflects one of the challenges of coal as a feedstock and is a result of its variable and inhomogeneous composition.

Feedstock reactivities on the low-end of the uncertainty range affect plants with bituminous coal more than they affect plants with lignite. This is due to the lower reactivity and over three times higher price of the former. While lignite has a higher variability in its reactivity factor, it is almost always completely converted under the conditions studied. In either case, once the reactivity is high enough to achieve complete conversion, this variable no longer plays a role.

The sensitivity of the syngas production cost to the other variables in Figure 8-3 is very modest, when considered individually and within the range in Table 8.1. The PHICCOS capital costs, which play the most important role after the reactivity factor, impact the syngas production cost by a maximum of 5%, relative to the base-case value.

Finally, note that moisture contents lower than the nominal 10% assumed in the base case (50% in the normalized uncertainty scale) are not beneficial for the

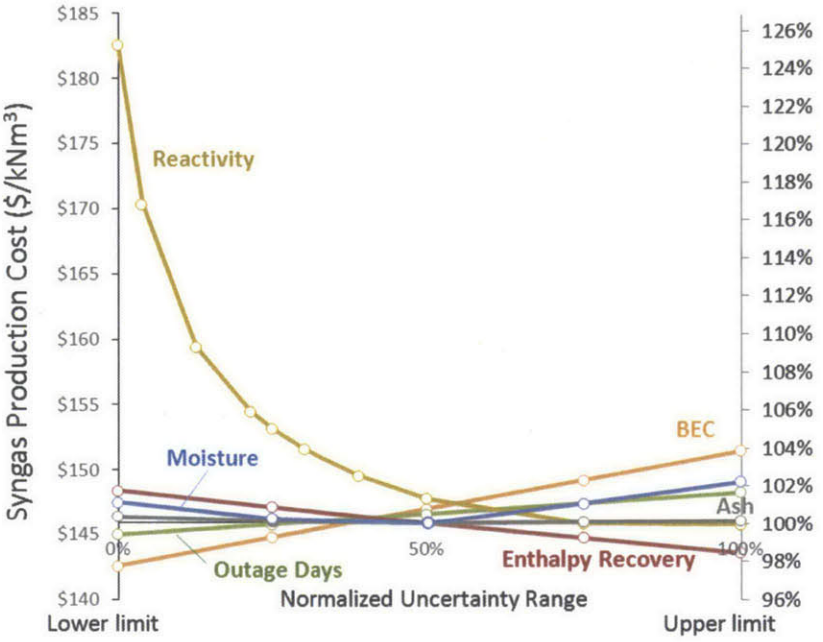

(a) Bituminous coal

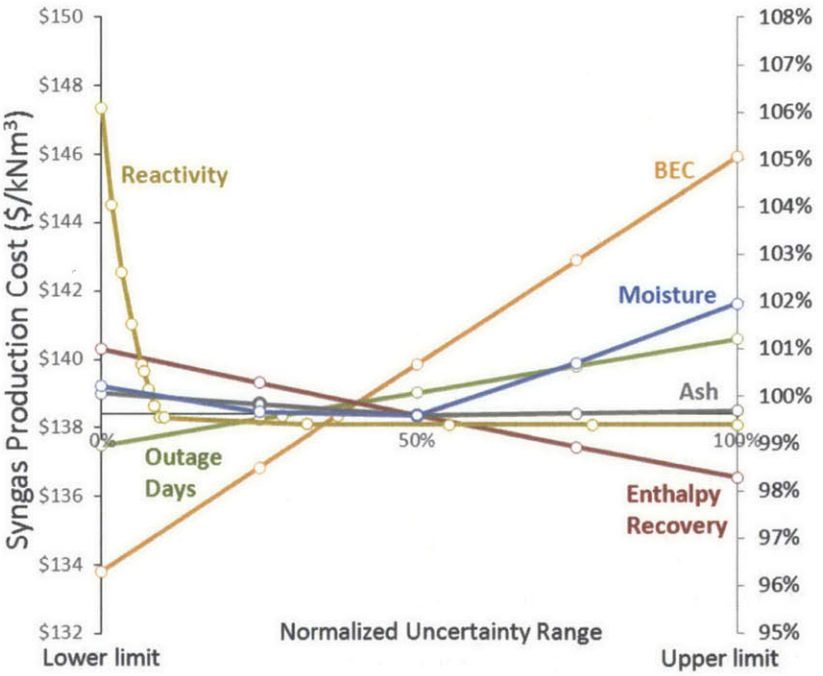

(b) Lignite

Figure 8-3: Sensitivity of syngas production cost to variation of the individual uncertain variables within their normalized uncertainty range.

plant economics. This is because gasification kinetics, and with them conversion, are negatively affected when the partial pressure of water in the gasifier is too low, see Chapter 4.

8.3 Propagation of Uncertainty

The propagation of uncertainty in the input variables in Table 8.1 to the overall plant technoeconomics was studied using the Monte Carlo method.

This method is a combinatorial uncertainty propagation technique that can provide estimates of full probability distribution functions (PDF) for the model outputs and accurately reflect any nonlinearity in the model. It relies on repeated random sampling of the PDFs of input variables, followed by recording of the model output [160].

8.3.1 Probability Distribution of Uncertain Variables

The PDF assumed for each of each of the uncertain variables considered is presented in Figure 8-4. A BetaPert distribution around the mean was used in all cases. It is characterized by the mean, minimum, and maximum in Table 8.1. This type of distribution is a smoother alternative to the triangular distribution, which is commonly used to describe the PDF of a variable for which little information is available except for expected maximum, minimum, and most likely values [76].

8.3.2 Probability Distribution of Syngas Production Cost

Monte Carlo simulations were conducted until the precision of the standard deviation was less than 5%, with 95% confidence. The number of runs required to achieve this is was close to 600.

The probability distribution of the syngas production cost obtained from the Monte Carlo simulations is presented in Figure 8-5. Its main statistics are summarized in Table 8.2. Furthermore, the mean value of other performance and cost

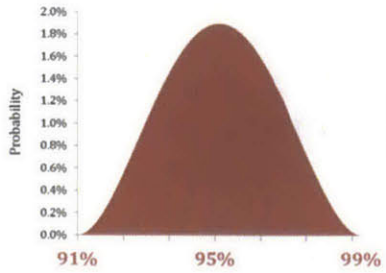

(a) PHICCOS enthalpy recovery

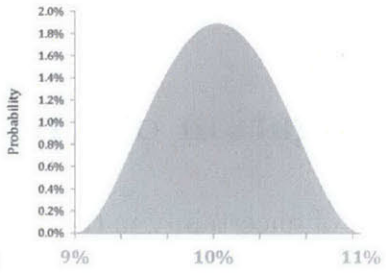

(b) PHICCOS product ash

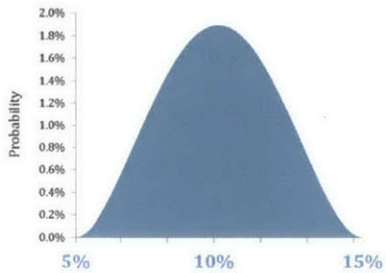

(c) PHICCOS product moisture

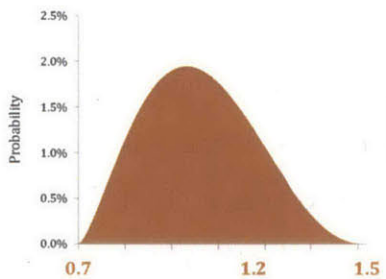

(d) PHICCOS BEC

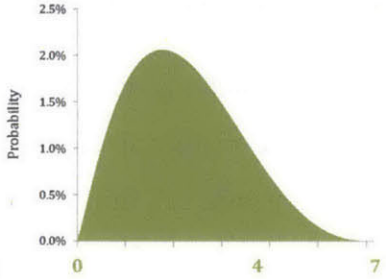

(e) PHICCOS yearly outage days

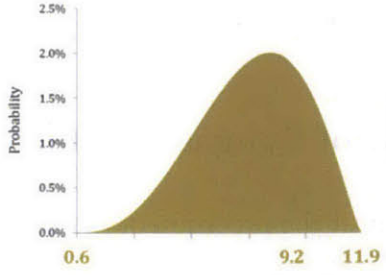

(f) Reactivity factor - bituminous

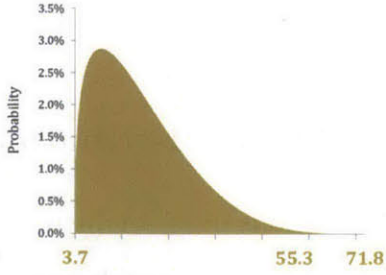

(g) Reactivity factor -lignite

Figure 8-4: Probability distribution of uncertain variables considered. The PDFs apply to both bituminous coal and lignite, unless otherwise indicated.

variables in the plant is summarized in Table 8.3.

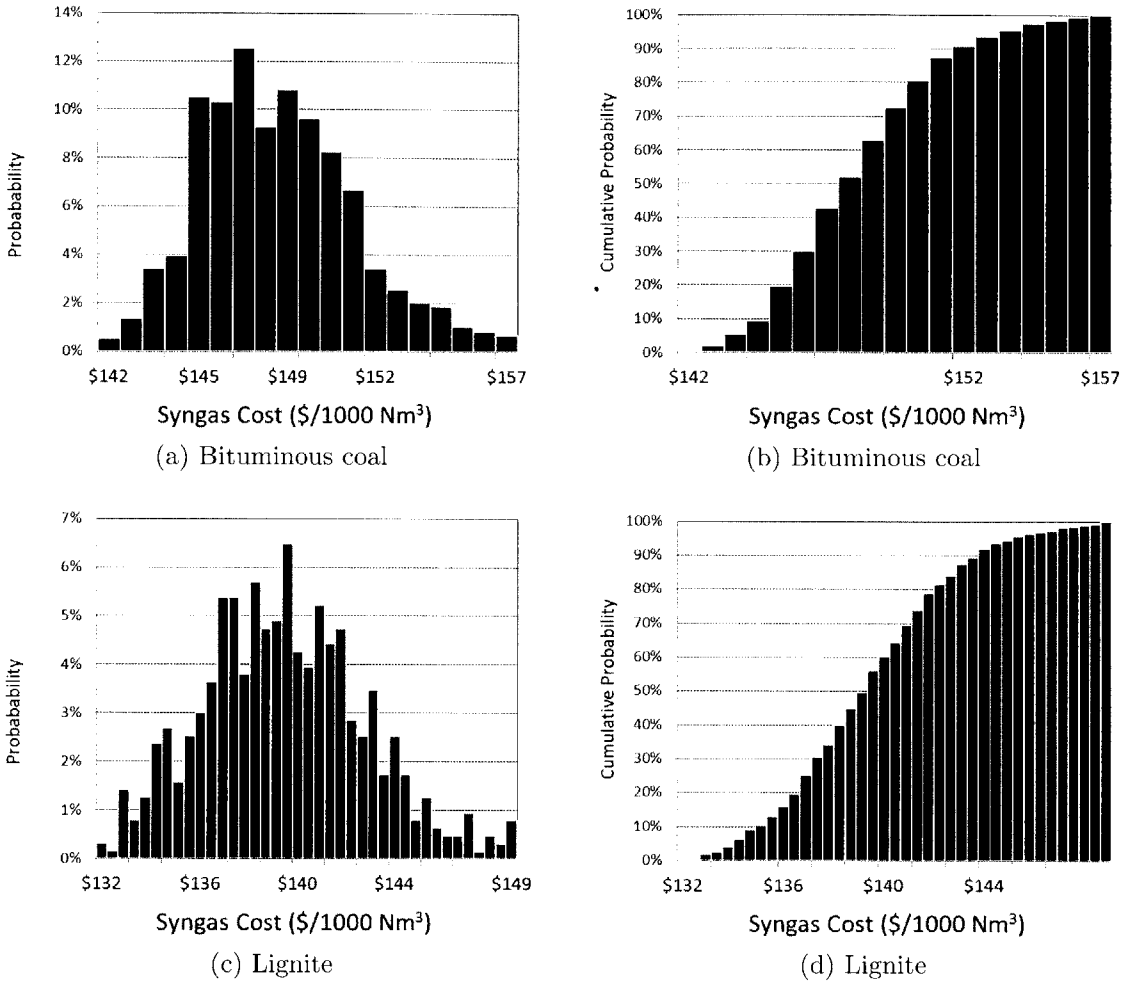

(a) Bituminous coal

(b) Bituminous coal

(c) Lignite

(d) Lignite

Figure 8-5: PDF of syngas cost for bituminous coal and lignite, from Monte Carlo simulations.

The results of the uncertainty propagation analysis show that, once the process uncertainties are considered, the mean cost of syngas production per kNm^3 in a plant with PHICCOS feed is \$148.4 for bituminous coal and \$139.7 for lignite. This is only modestly higher than the deterministic optimum presented in Table 7.1, which did not consider uncertainty.

The PDFs are skewed towards higher syngas costs. This reflects the influence of the feedstock reactivity discussed in Section 8.2.

Figure 8.3 compares the mean syngas production cost in a PHICCOS-fed plant, considering uncertainty, with that of plants based on commercial technologies and

Table 8.2: Syngas production cost: Main statistics from Monte Carlo simulations.

	Bituminous	**Lignite**
Number of runs	592	635
Mean	\$148.4	\$139.7
Median	\$148.1	\$139.6
Standard Deviation	\$3.1	\$3.3
Minimum	\$141.8	\$132.2
Maximum	\$164.2	\$151.4

Table 8.3: Plant performance and economics: mean from uncertainty analysis.

		Bituminous	Lignite
Gasifier Performance			
Carbon conversion		98.4%	99.3%
Cold gas efficiency	(HHV)	80.1%	81.3%
Plant Technoeconomics			
Coal feed (ar)	tonne/h	238.8	402.9
Syngas product flow	kNm^3/h	388.2	394.1
Net plant efficiency	(HHV)	63.7%	63.2%
Total owners cost	($/Nm^3/h$)	4,348	4,816
Syngas product cost	**$/kNm^3**	**\$148.4**	**\$139.7**
	(\$/GJ)	(\$12.5)	(\$11.8)

with previous estimates that did not consider uncertainty. The standard deviation of the syngas cost is used to indicate the uncertainty range.

The results in the figure show that, once the PHICCOS process uncertainties are considered, the mean cost of producing syngas is higher than previously estimated, but the trends relative to commercial technologies remain the same: a PHICCOS-fed plant is competitive (somewhat more expensive) with commercial technologies for bituminous coal. For lignite, PHICCOS is the most economic solution. The cost advantage of lignite, relative to commercial technologies, is outside the uncertainty range.

8.4 Chapter Summary

This chapter identified the main uncertain variables in the PHICCOS feeding system and used Monte Carlo simulations to quantify the propagation of these uncertainties

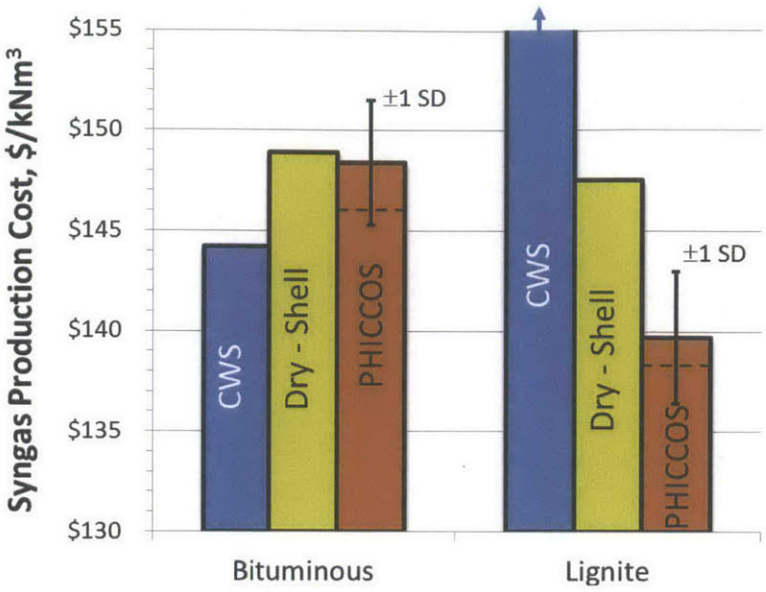

Figure 8-6: Syngas production cost: comparison with commercial technologies under consideration of PHICCOS uncertainties. The error bars indicate the cost one standard deviation away from the mean and the dotted line is the cost estimate before considering PHICCOS uncertainty.

to the syngas production costs.

The uncertain variables considered were the enthalpy recovery of the PHICCOS feeding system, the ash and moisture content of the product it delivers to the gasifier, the feedstock reactivity, the PHICCOS capital costs, and its yearly number of unplanned outages. Experimental data from the literature and recommendations from experts were used to estimate the uncertainty range for each variable.

The results show that, within the range of uncertainties studied, the feedstock reactivity is the variable that most affects plant economics. Once the process uncertainties are accounted for, the mean cost of syngas production is only modestly higher than previously estimated and does not affect the previously discussed trends, relative to commercial technologies. The cost advantage of PHICCOS for low-rank coal is outside the uncertainty range of the feeding system performance and economics.

Chapter 9

Conclusions and Outlook

Coal-CO_2 slurry was studied in this work as an alternative to commercial technologies for feeding pulverized coal to pressurized entrained flow gasifiers in plants with carbon capture. A multiscale approach was used, which couples system-level technoeconomic analysis with component-level modeling and particle-scale phenomena. Both bituminous coal and lignite feedstocks were studied in order to cover a broad range of coal ranks. Furthermore, two example applications were considered: an Integrated Gasification Combined Cycle (IGCC) power plant and a plant producing clean shifted syngas ready for synthetic fuel production via Fischer Tropsch.

Liquid CO_2 - or supercritical CO_2 with liquid-like density - is available in plants with carbon capture. When mixed with coal, it yields a suspension, or slurry, that can be pumped to a high-pressure. This is the same principle used in commercial coal-water slurry (CWS) feeding systems. The lower enthalpy of vaporization and viscosity of CO_2 make it a potentially more attractive slurrying medium than water.

The preliminary feasibility of the coal-CO_2 slurry feeding system was studied through system-level modeling in an IGCC plant. The results showed that the thermodynamic benefits of this feeding system are significant: an up to 12%-pt. higher gasifier cold gas efficiency and up to 5%-pt. higher net IGCC plant efficiency are achieved, when compared with a similar plant with CWS feed, assuming complete carbon conversion. Low-rank coal benefits the most.

Simulations with a 1-D reduced order model (ROM) of the gasifier including high-

pressure chemical kinetics showed that the assumption of complete conversion in a gasifier with coal-CO_2 slurry feed is inaccurate. Injecting CO_2 with the feed, instead of H_2O, leads to the production of raw syngas with a lower H_2:CO ratio of about 0.4-0.5, when compared to the 0.7-0.9 typical of a gasifier with CWS feed. The high partial pressure of CO slows down the heterogeneous gasification kinetics directly, through inhibition of the steam and CO_2 gasification reactions, as well as indirectly, through a slower diffusion of reactants and products in the pores of the pulverized coal particles. Once this is accounted for, an up to 13%-pt. reduction in the carbon conversion is predicted in a gasifier operating with CO_2 slurry, relative to a reactor with CWS feed and the same feedstock and outlet temperature.

Preparation of coal-CO_2 slurry was found to be the most challenging aspect of this feeding system: the triple point pressure of CO_2 is about 5 bar, so liquid CO_2 does not exist at ambient pressure. A novel coal-CO_2 slurry preparation and feeding system was proposed in this work which, unlike other solutions, does not require cryogenic cooling or lock-hoppers. The Phase Inversion-based Coal-CO_2 Slurry (PHICCOS) feeding system introduced here takes advantage of a physical phenomenon known as phase inversion, whereby the hydrophobic surface of coal is selectively wetted by CO_2 and its mineral particles are selectively wetted by water. The PHICCOS feeding system operates at ambient temperature, without lock-hoppers, and inherently reduces the ash and moisture content of the feedstock . Experimental results of phase inversion of coal with CO_2 for coal beneficiation were used as a basis for the design and analysis of PHICCOS.

Coupled multiscale modeling was used to study the overall technoeconomics of the PHICCOS feeding system under consideration of the thermodynamic, kinetic, and slurry preparation aspects individually addressed before. Furthermore, slurry skimming and steam injection were proposed as a way to achieve an optimum tradeoff between the thermal benefits of CO_2 and the kinetic benefits of H_2O in the feed.

The most favorable plant economics in a plant with PHICCOS feed are achieved for conditions under which carbon conversion in the gasifier is complete. This requires full CO_2 slurry skimming (i.e. flashing to dry feed conditions), an about 100K higher

gasifier outlet temperature than that used for CWS gasification, and the injection of small quantities of steam into the reactor.

A PHICCOS-fed plant with optimized gasifier operating conditions produces clean, shifted-syngas at a cost of \$146.1/kNm^3 for bituminous coal and \$138.7/kNm^3 for lignite. Monte Carlo simulations showed that, once the key uncertainties of the process are accounted for, the mean cost of syngas production increases by only 2-3%, relative to the deterministic optimum. The feedstock reactivity is the most influencing variable, within the uncertainty range considered.

The economics of the PHICCOS feeding system are competitive with the cheapest commercial technology for bituminous coal (CWS) are more attractive than those of the most economic commercial feeding system for lignite (dry feed based on lock hoppers). The cost advantage of PHICCOS is outside the uncertainty range associated with the performance and economics of this technology.

While the cost advantage of PHICCOS is a modest 5-10%, this feeding system offers a unique combination of operational advantages: it can achieve very high feed pressures and has a good fuel flexibility. The earlier can be attributed to the use of a pump, rather than a lock hopper, for building pressure in the system. The fuel flexibility is due to the inherent feedstock upgrading occurring in the phase-inversion step of a PHICCOS system: the moisture and ash content of the incoming coal are reduced, so a PHICCOS-fed plant can efficiently process low-quality feedstocks with a high moisture or a high-ash content, which are cheap and widely available.

Outlook

Fundamental theoretical and experimental studies at the particle-scale are required in order to gain a better understanding of the physics underlying phase inversion of coal with CO_2. In addition, further experimental investigation of phase inversion at the lab and pilot scales is necessary for quantifying the influence of operating conditions on process performance, especially under high enthalpy recovery conditions. Furthermore, it is important to study how the ash content reduction inherent to the PHICCOS feeding system affects the high reactivity of low-rank coal, which is known

to be influenced by the catalytic activity of some of its inorganic constituents.

The PHICCOS feeding system is not limited to gasification-based systems but is applicable to any plant based on pulverized coal and where CO_2 is or can be made available. The PHICCOS feeding system could prove especially attractive in high pressure oxyfuel plants, where CO_2 is required as a diluent in the combustor. Furthermore, future work should focus on high-ash coal, for which this feeding system is especially promising.

Finally, operational aspects of the PHICCOS feed should be considered in more detail. Startup considerations, for example, are important, since more CO_2 is required in the PHICCOS recirculation loop than what is captured in the plant (see Figure 6-6). Hence, it may be necessary to start up with CWS while enough CO_2 is accumulated. Furthermore, it is important to study the effect of coal deashing on the thickness of the protective slag layer forming on the wall of the gasifier. Lastly, while optimization showed that the best plant economics are achieved with full CO_2 slurry skimming to dry feed conditions, the operational complexity and economics of this option must be assessed in more detail.

Bibliography

[1] Breault R. W., Gasification processes old and new: A basic review of the major technologies, Energies 3 (2010) 216–240.

[2] Weil K. S., Coal gasification and IGCC technology: a brief primer, Proceedings of the ICE - Energy 163 (1) (2010) 7–16.

[3] Higman C., van der Burgt M., Gasification, 2nd Edition, Elsevier, 2008.

[4] Littlewood K., Gasification: Theory and application, Progress in Energy and Combustion Science 3 (1) (1977) 35–71.

[5] Tampa Electric, Polk Power Station , `http://www.tampaelectric.com/company/ourpowersystem/powerstations/polk/` (Accessed August 1, 2013).

[6] National Energy Technology Laboratory , Worldwide gasification database (2010).

[7] British Petroleum , BP Statistical Review of World Energy, 2013.

[8] Anantharaman B., Chatterjee D., Ariyapadi S., Gualy R., Economics of coal to liquids plants in Asia, in: Chemical Engineering World (73), 2012.

[9] International Energy Agency (IEA), Clean Coal Centre , Utilisation of low rank coals, in: Profiles (11/4), 2011.

[10] Basu P., Biomass Gasification, Pyrolysis and Torrefaction: Practical Design and Theory, Elsevier Science, 2013.

[11] National Energy Technology Laboratory , Cost and performance baseline for fossil energy plants, volume 3a: Low rank coal to electricity: IGCC cases, Technical Report DOE/NETL-2010/1399 (2011).

[12] Rubin E. S., Mantripragada H., Marks A., Versteeg P., Kitchin J., The outlook for improved carbon capture technology, Progress in Energy and Combustion Science 38 (5) (2012) 630–671.

[13] Holt N., Integrated gasification combined cycle power plants, in: Encyclopedia of Physical Science and Technology, 3rd Edition, Academic Press, 2001.

[14] Simbeck D. R., Korens N., Biasca F. E., Vejtasa S., Dickenson R. L., Coal gasification guidebook: Status, applications, and technologies, Technical Report TR-102034, Electric Power Research Institute (EPRI) (1993).

[15] Collot A.-G., Matching gasification technologies to coal properties, International Journal of Coal Geology 65 (3-4) (2006) 191–212.

[16] Simbeck D., SFA Pacific Inc., personal communication (2013).

[17] McHale E. T., Coal-water fuel combustion, Symposium (International) on Combustion 21 (1) (1988) 159–171.

[18] Botero C., Field R. P., Herzog H., Ghoniem A. F., Performance of an IGCC plant with carbon capture and coal-CO_2-slurry feed: Impact of coal rank, slurry loading, and syngas cooling technology, Industrial & Engineering Chemistry Research 51 (36) (2012) 11778–11790.

[19] National Energy Technology Laboratory , Cost and performance baseline for fossil energy plants, revision 2, Technical Report DOE/NETL-2010/1397 (2010).

[20] Netzsch Group , `http://www.netzsch.com` (Accessed 2010).

[21] Atesok G., Boylu F., Sirkeci A. A., Dincer H., The effect of coal properties on the viscosity of coal-water slurries, Fuel 81 (14) (2002) 1855–1858.

[22] Black & Veatch , Holcomb generation expansion project: Coal technology selection study, Technical Report 144102 (2006).

[23] National Energy Technology Laboratory , Development of a high-pressure dry feed pump for gasification systems, Project Fact Sheet (2008-2012).

[24] National Energy Technology Laboratory , Evaluation of the benefits of advanced dry feed systems for low rank coal, Project No. DE-FE0007902 (2011-2012).

[25] Darby A., Dry solids pump development status, in: Gasification Technologies Conference, Washington, D.C., 2012.

[26] Holt N., Maxson A., Parkes J., Phillips J., Trautz R., Wheeldon J., Advanced Coal Power Systems with CO_2 Capture: EPRI's CoalFleet for Tomorrow Vision, EPRI, Report 1016877 (2008).

[27] Holt N., Gasification process selection - trade-offs and ironies, in: Gasification Technologies Conference, Washington, DC (USA), 2004.

[28] Span R., Wagner W., A new equation of state for carbon dioxide covering the fluid region form the triple-point temperature to 1100 K at pressures up to 800 MPa, J. Phys. Chem, Ref. Data 25 (6) (1996) 1509–1596.

[29] Vesovic V., Wakeham W. A., Olchowy G. A., Sengers J. V., Watson J. T. R., Millat J., The transport properties of carbon dioxide, J. Phys. Chem. Ref. Data 19 (3) (1990) 763–809.

[30] Somayajulu G. R., A generalized equation for surface tension from the triple point to the critical point, International Journal of Thermophysics 9 (4) (1988) 559–566.

[31] Electrical Research Association , Steam Tables, Edward Arnold Publishers, London, 1967.

[32] Haar L., Gallagher J. S., Kell G. S., NBS/NRC Steam Tables, Hemisphere Publishing Co., 1984.

[33] Peirson J. F. J., Burje W. J., Santhanam C. J., Investigation of low-rank-coal-liquid carbon dioxide slurries, Technical Report EPRI AP-4849, Prepared by Arthur D. Little, Inc. for Electric Power Research Institute (1986).

[34] Dooher J., Phillips J., Program on technology innovation: Advanced concepts in slurry-fed low-rank coal gasification. liquid CO_2/coal slurries and hot water drying, Technical Report 1014432, Prepared by Dooher Institute of Physics and Energy for the Electric Power Research Institute (2006).

[35] Cho S. Y., Takahashi F., Dryer F. L., Some theoretical considerations on the combustion and disruption of free slurry droplets, Combustion Science and Technology 67 (1) (1989) 37 – 57.

[36] Holve D. J., Fletcher T. H., Gomi K., Comparative combustion studies of ultra-fine coal/water slurries and pulverized coal, Combustion Science and Technology 52 (4) (1987) 269 – 291, 3.

[37] Yu T. U., Kang S. W., Toqan M. A., Walsh P. M., Teare J. D., Beer J. M., et al., Effect of fuel treatment on coal-water fuel combustion, Symposium (International) on Combustion 21 (1) (1988) 369 378.

[38] Santhanam C. J., Dale S. E., Nadkarni R. M., Non-water slurry pipelines - potential techniques, in: 5th International Technical Conference on Slurry Transportation, Lake Tahoe, Nevada (USA), 1980.

[39] Santhanam C. J., Development of coal/liquid CO_2 slurry transportation - current status, in: 7th International Technical Conference on Slurry Transportation, Lake Tahoe, Nevada (USA), 1982.

[40] Santhanam C. J., Dale S. E., Peirson J. F., Burke W. J., Hanks R. W., Coal-liquid CO_2 slurry pipeline technology, in: 9th International Technical Conference on Slurry Transportation, Lake Tahoe, Nevada (USA), 1984.

[41] Aude T. C., Thompson T. L., Alternative coal systems (CWM, CO_2, or Black Mesa Technology), in: 10th International Conference on Slurry Technology, Lake Tahoe, Nevada (USA), 1985.

[42] McNamee G. P., White G. A., Use of lignite in texaco gasification-based-combined-cycle power plants, Technical Report AP-4509, Prepared by Energy Conversion Systems, Inc. for Electric Power Research Institute (1986).

[43] Ansolabehere S., Beer J., Deutch J., Ellerman A. D., Friedmann J., Herzog H., et al., The future of coal, Technical report, Massachusetts Institute of Technology (2007).

[44] Phillips J., Electric Power Research Institute, personal communication (2010).

[45] Dooher J. P., Physio-chemical properties of low rank coal/liquid CO_2 slurries as gasifier feedstocks, in: 34th International Technical Conference of Coal Utilization and Fuel Systems, Clearwater, Florida (USA), 2009.

[46] Dooher J. P., Castaldi M. J., Rubin D., Phillips J. N., Schoff R., Evaluation of low rank coal/liquid CO_2 slurries for generic, single-stage, slurry-fed gasifiers, in: 35th International Technical Conference of Coal Utilization and Fuel Systems, Clearwater, Florida (USA), 2010.

[47] Dooher J., Marasigan J., Goldstein H. N., Liquid CO2 slurry (LCO2) for feeding low rank coal (LRC) to gasifiers, in: 37th International Technical Conference on Clean Coal and Fuel Systems, Clearwater, FL (USA), 2012.

[48] McGurl G. V., James R. E., Parsons E. L., Ruether J. A., Wimer J. G., Quality guidelines for energy system studies, Technical report, U.S. Department of Energy (DOE), National Energy Technology Laboratory (NETL) (2004).

[49] Mc.Daniel J. E., Tampa Electric Polk Power Station Integrated Gasification Combined Cycle Project, Technical report, Prepared by Tampa Electric Company for The U.S. Department of Energy (2002).

[50] Breton D. L., Keeler C. G., Comparative IGCC performance and cost for domestic coals, in: Gasification Technologies Conference, San Francisco, California (USA), 2005.

[51] Breton D. L., Amick P., Comparative IGCC cost and performance for domestic coals, in: Gasification Technologies Conference, San Francisco, California (USA), 2002.

[52] Electric Power Research Institute , Cool Water coal gasification program: Final report, Technical Report GS-6805 (1990).

[53] Chinese Academy of Sciences (CAS) and U.S. Department of Energy (DOE) , The United States of America and the People's Republic of China experts report on integrated gasification combined cycle technology, Technical Report DOE/FE-0357 (1996).

[54] Botero C., Field R. P., Herzog H. J., Ghoniem A. F., The Phase Inversion-based Coal-CO_2 Slurry (PHICCOS) feeding system: Technoeconomic assessment using coupled multiscale analysis, International Journal of Greenhouse Gas Control 18 (2013) 150–164.

[55] Moss D. R., Pressure Vessel Design Manual (3rd Edition), Elsevier, 2004.

[56] Westinghouse Electric Corporation , Development of the LICADO coal cleaning process, Technical Report DOE/PC/79873-T1; (1990).

[57] Aspen Technology, Inc. , Aspen Plus, Version 7.3.

[58] Field R. P., Brasington R., Baseline flowsheet model for IGCC with carbon capture, Industrial & Engineering Chemistry Research 50 (19) (2011) 11306–11312.

[59] Botero C., Field R., Herzog H., Ghoniem A., Coal-CO_2 slurry feed for pressurized gasifiers: Slurry preparation system characterization and economics, in: Energy Procedia, Vol. 37, 2013.

[60] Wallrnan P. H., Richardson J. H., Thorsness C. B., Leininger T. F., Klein J. D., Winter J. D., et al., Hydrogen production from municipal solid waste, Technical report, Lawrence Livermore National Laboratory (1996).

[61] Monaghan R. F. D., Ghoniem A. F., A dynamic reduced order model for simulating entrained flow gasifiers: Part I: Model development and description, Fuel 91 (1) (2012) 61–80.

[62] Monaghan R. F. D., Ghoniem A. F., A dynamic reduced order model for simulating entrained flow gasifiers: Part II: Model validation and sensitivity analysis, Fuel 94 (0) (2012) 280–297.

[63] Monaghan R. F. D., Ghoniem A. F., Simulation of a commercial-scale entrained flow gasifier using a dynamic reduced order model, Energy & Fuels 26 (2) (2011) 1089–1106.

[64] Monaghan R. F. D., Dynamic reduced order modeling of entrained flow gasifiers, PhD thesis, Massachusetts Institute of Technology (2010).

[65] Muchlen H. J., van Heek K. H., Juentgen H., Kinetic studies of steam gasification of char in the presence of H_2, CO_2 and CO, Fuel 64 (7) (1985) 944–949.

[66] Botero C., Field R. P., Herzog H. J., Ghoniem A. F., Impact of finite-rate kinetics on carbon conversion in a high-pressure, single-stage entrained flow gasifier with coal-CO_2 slurry feed, Applied Energy 104 (0) (2013) 408–417.

[67] Aspen Technology, Inc. , Aspen Properties Excel Calculator, Version 7.3 (2011).

[68] National Energy Technology Laboratory , Quality guidelines for energy system studies: Cost estimation methodology for NETL assessments of power plant performance, Technical Report DOE/NETL-2011/1455, NETL (2011).

[69] U.S. Department of Energy, National Energy Technology Laboratory (NETL) , Industrial size gasification for syngas, substitute natural gas and power production, Technical Report DOE/NETL-401/040607, U.S. Department of Energy, National Energy Technology Laboratory (2007).

[70] U.S. Energy Information Administration , Annual coal report 2011 (2012).

[71] Linjewile T., TECO Energy, personal communication (2013).

[72] Lozowski D., Economic indicators, Chemical Engineering 120 (1) (2013) 63–64.

[73] Peters M. S., Timmerhaus K. D., West R. E., Plant Design and economics for chemical engineers, 5th Edition, McGraw-Hill, 2003.

[74] U.S. Energy Information Administration , Electric power monthly (January 2013).

[75] U.S. Department of Energy , Energy efficiency and renewable energy, advanced manufacturing office: Benchmark the fuel cost of steam generation (2012).

[76] Oracle , Oracle Crystal Ball Clasroom Edition, Release 11.1.2.2.000 (2012).

[77] Oracle , Oracle Crystal Ball Decision Optimizer, Release 11.1.2.2: OptQuest User's Guide (2012).

[78] Glover F., Kelly J. P., Laguna M., The OptQuest approach to Crystal Ball simulation optimization, University of Colorado (1998).

[79] Microsoft Corporation , Microsoft Visual Basic for Applications, Version 7.0 (2010).

[80] Maurstad O., An overview of coal based integrated gasification combined cycle (IGCC) technology, Technical Report MIT LFEE 2005-002 WP, Massachusetts Institute of Technology (2005).

[81] Hurt R., Calo J., Fletcher T. H., Sayre A., Fundamental investigation of fuel transformations in pulverized coal combustion and gasification technologies, Technical Report DE-FG26-OONT40815, Prepared by Brown University for the U.S. Department of Energy (2005).

[82] Roberts D. G., Harris D. J., Char reactivity in gas mixtures: Towards an understanding of the C-CO-CO_2 reaction system, Technical Report TN35, CSIRO Energy Technology (2008).

[83] Roberts D. G., Harris D. J., A kinetic analysis of coal char gasification reactions at high pressures, Energy & Fuels 20 (6) (2006) 2314 2320.

[84] Gadsby J., Long F. J., Sleightholm P., Sykes K. W., The mechanism of the carbon dioxide-carbon reaction, Proceedings of the Royal Society of London. Series A. Mathematical and Physical Sciences 193 (1034) (1948) 357–376.

[85] Blackwood J. D., Ingeme A. J., The reaction of carbon with carbon dioxide at high pressure, Australian Journal of Chemistry 13 (2) (1960) 194–209.

[86] Liu G.-s., Tate A. G., Bryant G. W., Wall T. F., Mathematical modeling of coal char reactivity with CO_2 at high pressures and temperatures, Fuel 79 (10) (2000) 1145–1154.

[87] Huettinger K. J., Merdes W. F., The carbon-steam reaction at elevated pressure: Formations of product gases and hydrogen inhibitions, Carbon 30 (6) (1992) 883–894.

[88] Blackwood J., McGrory F., The carbon-steam reaction at high pressure, Australian Journal of Chemistry 11 (1) (1958) 16–33.

[89] Harris D. J., Smith I. W., Intrinsic reactivity of petroleum coke and brown coal char to carbon dioxide, steam and oxygen, Symposium (International) on Combustion 23 (1) (1991) 1185–1190.

[90] Roberts D. G., Intrinsic reaction kinetics of coal chars with oxygen, carbon dioxide and steam at elevated pressures, Ph.D. thesis, University of Newcastle (2000).

[91] Gadsby J., Hinshelwood C. N., Sykes K. W., The kinetics of the reactions of the steam-carbon system, Proceedings of the Royal Society of London. Series A. Mathematical and Physical Sciences 187 (1009) (1946) 129–151.

[92] Huang Z., Zhang J., Zhao Y., Zhang H., Yue G., Suda T., et al., Kinetic studies of char gasification by steam and CO_2 in the presence of H_2 and CO, Fuel Processing Technology 91 (8) (2010) 843–847.

[93] Roberts D. G., Harris D. J., Char gasification in mixtures of CO_2 and H_2O: Competition and inhibition, Fuel 86 (17-18) (2007) 2672–2678.

[94] Irfan M. F., Usman M. R., Kusakabe K., Coal gasification in a CO_2 atmosphere and its kinetics since 1948: A brief review, Energy 36 (1) (2011) 12–40.

[95] Bliek A., Mathematical modeling of a concurrent fixed bed coal gasifier, Ph.D. thesis, Twente University of Technology, The Netherlands (1984).

[96] Everson R. C., Neomagus H. W. J. P., Kasaini H., Njapha D., Reaction kinetics of pulverized coal-chars derived from inertinite-rich coal discards: Gasification with carbon dioxide and steam, Fuel 85 (7-8) (2006) 1076–1082.

[97] Muchlen H. J., Zum Einfluss der Produktgasse auf die Kinetik der Wasserdampfvergasung in Abhaengigkeit von Druck und Temperatur (*Influence of product gases on the kinetics of steam gasification as a function of pressure and temperature*), PhD thesis, University of Essen (1983).

[98] Liu G.-S., Niksa S., Coal conversion submodels for design applications at elevated pressures. Part II. Char gasification, Progress in Energy and Combustion Science 30 (6) (2004) 679–717.

[99] Walker Jr P. L., Rusinko Jr F., Austin L. G., Gas reactions of carbon, in: D.D. Eley P. W. S., Paul B. W. (Eds.), Advances in Catalysis, Vol. Volume 11, Academic Press, 1959, pp. 133–221.

[100] Liu G.-S., Mathematical modelling of coal char reactivity in a pressurised entrained flow gasifier, Ph.D. thesis, The University of Newcastle, Australia (1999).

[101] Goyal A., Zabransky R. F., Rehmat A., Gasification kinetics of western kentucky bituminous coal char, Industrial & Engineering Chemistry Research 28 (12) (1989) 1767 1778.

[102] Umemoto S., Kajitani S., Hara S., Modeling of coal char gasification in coexistence of CO_2 and H_2O considering sharing of active sites, Fuel 103 (2011) 14 21.

[103] Miura K., Hashimoto K., Silveston P. L., Factors affecting the reactivity of coal chars during gasification, and indices representing reactivity, Fuel 68 (11) (1989) 1461–1475.

[104] Johnson J. L., Kinetics of Coal Gasification, John Wiley & Sons, Inc. 1979.

[105] Tremel A., Haselsteiner T., Kunze C., Spliethoff H., Experimental investigation of high temperature and high pressure coal gasification, Applied Energy 92 (0) (2012) 279–285.

[106] Sha X.-Z., Chen Y.-G., Cao J., Yang Y.-M., Ren D.-Q., Effects of operating pressure on coal gasification, Fuel 69 (5) (1990) 656–659.

[107] Adanez J., Miranda J., GavilÃ¡n J., Kinetics of a lignite-char gasification by CO_2, Fuel 64 (6) (1985) 801–804.

[108] Zevenhoven R., Hupa M., Characterization of solid fuel at pressurized fluidized bed gasification conditions, in: 23rd international technical conference on coal utilization and fuel systems, Clearwater, FL, USA, 1998.

[109] Kajitani S., Hara S., Matsuda H., Gasification rate analysis of coal char with a pressurized drop tube furnace, Fuel 81 (5) (2002) 539–546.

[110] Nozaki T., Adschiri T., Fujimoto K., Coal char gasification under pressurized CO_2 atmosphere, Fuel 71 (3) (1992) 349–350.

[111] Roberts D. G., Harris D. J., Char gasification with O_2, CO_2, and H_2O: Effects of pressure on intrinsic reaction kinetics, Energy & Fuels 14 (2) (2000) 483–489.

[112] Radovic L. R., Steczko K., Walker Jr P. L., Jenkins R. G., Combined effects of inorganic constituents and pyrolysis conditions on the gasification reactivity of coal chars, Fuel Processing Technology 10 (3) (1985) 311–326.

[113] Thiele E. W., Relation between catalytic activity and size of particle, Industrial & Engineering Chemistry 31 (7) (1939) 916–920.

[114] Bischoff K. B., Effectiveness factors for general reaction rate forms, AIChE Journal 11 (2) (1965) 351–355.

[115] Hong J., Hecker W. C., Fletcher T. H., Improving the accuracy of predicting effectiveness factors for mth order and langmuir rate equations in spherical coordinates, Energy & Fuels 14 (3) (2000) 663–670.

[116] Roberts G. W., Satterfield C. N., Effectiveness factor for porous catalysts. Langmuir-Hinshelwood kinetic expressions, Industrial & Engineering Chemistry Fundamentals 4 (3) (1965) 288–293.

[117] Harris D. J., Coal gasification reactivity: Measurement and application, in: Pittsburgh Coal Conference, Johannesburg, South Africa, 2007.

[118] Valix M. G., Harris D. J., Smith I. W., Trimm D. L., The intrinsic combustion reactivity of pulverised coal chars: The use of experimental pore diffusion coefficients, Symposium (International) on Combustion 24 (1) (1992) 1217–1223.

[119] van Heek K. H., Muehlen H.-J., Juentgen H., Progress in the kinetics of coal and char gasification, Chemical Engineering & Technology 10 (1) (1987) 411–419.

[120] Wall T. F., Liu G.-s., Wu H.-w., Roberts D. G., Benfell K. E., Gupta S., et al., The effects of pressure on coal reactions during pulverised coal combustion and gasification, Progress in Energy and Combustion Science 28 (5) (2002) 405–433.

[121] Kajitani S., Suzuki N., Ashizawa M., Hara S., CO_2 gasification rate analysis of coal char in entrained flow coal gasifier, Fuel 85 (2) (2006) 163–169.

[122] The University of Toronto , Physics of carbon dioxide, `http://www.physics.utoronto.ca/~exploration/UofT-mentorship/Physics_CO2.html` (Accessed February 18, 2013).

[123] Paull P. L., Schlinger W. G., Synthesis gas from solid carbonaceous fuel (1976).

[124] Santhanam C. J., Method and apparatus for transporting coal as a coal/liquid carbon dioxide slurry (1980).

[125] Botero C., Field R., Herzog H., Ghoniem A., Method for preparing a slurry of pulverized solid material in liquid or supercritical carbon dioxide, U.S. Patent Application No.: 61/712954 (2012).

[126] Cooper M., Muenchow H. O., Chiang S. H., Klinzing G. E., Morsi S., Venkatadri R., The licado coal cleaning process: A strategy for reducing SO_2 emissions from fossil-fueled power plants, in: Energy Conversion Engineering Conference, 1990. IECEC-90. Proceedings of the 25th Intersociety, Vol. 4, 1990, pp. 137–142.

[127] Darcovich K. P., Hydrodynamic and surface chemistry effects in coal-oil agglomerate flotation, PhD Thesis, University of Ottawa (1993).

[128] Keller D. V., Burry W. M., The demineralization of coal using selective agglomeration by the t-process, Coal Preparation 8 (1-2) (1990) 1–17.

[129] Kawatra K., Coal Desulfurization: High Efficiency Preparation Methods, Taylor & Francis, 2001.

[130] Botsaris G. D., Glazman Y. M., Interfacial Phenomena in Coal Technology, Vol. 32, Marcel Dekker, Inc., 1989.

[131] Smith K. E., Cleaning and dewatering fine coal using hydrophobic displacement, Ph.D. thesis, Virginia Polytechnic Institute and State University (2008).

[132] Osman H., Jangam S. V., Lease J. D., Mujumdar A. S., Drying of low-rank coal (LRC) - a review of recent patents and innovations, Technical Report M3TC/TPR/2011/02, National University of Singapore (2011).

[133] Chiang S., Cobb J. T., Coal Conversion Processes, Cleaning and Desulfurization, Kirk-Othmer Encyclopedia of Chemical Technology, John Wiley & Sons, Inc., 2000.

[134] Yoon R. H., Luttrell G. H., Method for dewatering fine coal, Patent US 5,458,786 (1995).

[135] Good R. J., Islam M., Liquid bridges and the oil agglomeration method of coal beneficiation: an elementary theory of stability, Langmuir 7 (12) (1991) 3219–3221.

[136] National Energy Technology Laboratory , NETL Multimedia, Historical Images, Print 85-546 `http://www.flickr.com/photos/netlmultimedia` (Accessed August, 2013).

[137] Chi S. M., Morsi B. I., Klinzing G. E., Chiang S. H., Licado process for fine coal cleaning - mechanism, Coal Preparation 6 (3-4) (1989) 241–263.

[138] Araujo G., He D. X., Chi S. M., Morsi B. I., Klinzing G. E., Use of liquid CO_2 for fine coal cleaning, Energy Progress 7 (2) (1987) 72–76.

[139] Chi S. M., Interfacial properties and coal cleaning in the licado process, Ph.D. thesis, University of Pittsburgh (1986).

[140] Chiang S.-H., Klinzing G. E., HE D.-X., Feng Y.-R., Yu S.-N., Jenkins K., et al., Update of the LICADO coal cleaning process, in: 10th Annual Coal Preparation, Utilization, and Environmental Control Contractors Conference, Pittsburgh (PA), USA, 1994, pp. 67–74.

[141] Araujo G., Feng Y., Chiang S.-H., Klinzing G. E., Development of a computer controlled continuous system for the licado process, International Journal of Coal Preparation and Utilization 11 (1) (1992) 21 – 33.

[142] Hardesty D. E., Buchholz H. F., Solvent dewatering coal, Patent US 4,459,762 (1984).

[143] Jha M. C., Smit F. J., Shields G. L., Moro N., Engineering development of advanced physical fine coal cleaning for premium fuel applications, Technical Report DE-AC22-92PC92208, Prepared for the U.S. Department of Energy by Amax Research & Development Center (1997).

[144] Miller J. D., Misra M., Coal cleaning by gaseous carbon dioxide conditioning and froth flotation, U.S. Patent No.: 4,676,804 (1987).

[145] Walters A. B., Chemical treatment prior to physical coal beneficiation, in: Symposium on Chemistry of Mineral Matter and Ash in Coal, Vol. 29(4), American Chemical Society, Division of Fuel Chemistry, Philadelphia, 1984.

[146] Jin R., Ye Y., Miller J., The hydrophobic character of pretreated coal surfaces, American Chemical Society, Division of Fuel Chemistry 33 (4) (1988) 811–817.

[147] Robbins G. A., Winschel R. A., Amos C. L., Burke F. P., Agglomeration of low-rank coal as a pretreatment for direct coal liquefaction, Fuel 71 (9) (1992) 1039–1046.

[148] Musich M. A., R.A. D., Timpe R. C., Oil agglomeration of low-rank coals, in: Eight annual coal preparation, utilization and environmental control contractors conference, Pittsburgh (USA), 1992.

[149] Gray M. L., Champagne K. J., Soong Y., Finseth D. H., Parametric study of the column oil agglomeration of fly ash, Fuel 80 (6) (2001) 867–871.

[150] Siemens A.G. , Integrated Gasification Combined Cycle (IGCC) industry study (2008).

[151] Dooher J. P., Marasigan J., Goldstein H., Liquid CO_2 slurry (LCO2) for feeding low rank coal (LRC) to gasifiers, in: 37th International Technical Conference on Clean Coal and Fuel Systems, Clearwater, Florida (USA), 2012.

[152] Diamond L. W., Akinfiev N. N., Solubility of CO_2 in water from -1.5 to 100°C and from 0.1 to 100 MPa: evaluation of literature data and thermodynamic modelling, Fluid Phase Equilibria 208 (1-2) (2003) 265–290.

[153] Botero C., Field R., Herzog H., Ghoniem A., Method for conveying a solid to a dense, high pressure state via phase inversion with CO_2, U.S. Patent Application No.: 61/829321 (2013).

[154] Klosek J., Smith A. R., Solomon P. R., The role of oxygen in coal gasification, in: Eighth Annual Industrial Energy Technology Conference, Houston, TX, 1986.

[155] International Energy Agency , Energy Technology Systems Analysis Program, technology brief s01: Syngas production from coal (2010).

[156] De Graaf J. D., Shell coal gasification technology (2008).

[157] United States Environmental Protection Agency (EPA) , Available and emerging technologies for reducing greenhouse gas emissions from coal-fired electric generating units, Technical report (2010).

[158] Weisstein E. W., Mean deviation. From MathWorld–A Wolfram Web Resource. `http://mathworld.wolfram.com/FibonacciNumber.html` (Accessed July 15, 2013).

[159] Gorard S., Revisiting a 90-year-old debate: the advantages of the mean deviation, in: British Educational Research Association Annual Conference, University of Manchester, 16-18 September, 2004.

[160] Ramaswami A., Milford J. B., Small M. J., Integrated Environmental Modeling - Pollutant Transport, Fate, and Risk in the Environment, John Wiley & Sons, 2005.

List of Publications Based on this Thesis

1. Botero C., Field R.P., Brasington R.D., Herzog H.J. and Ghoniem, A.F., Performance of an IGCC Plant with Carbon Capture and Coal-CO_2-Slurry Feed: Impact of Coal Rank, Slurry Loading, and Syngas Cooling Technology. *Industrial & Engineering Chemistry Research*, 51 (36), 2012.

2. Botero C., Field R.P., Brasington R.D., Herzog H.J. and Ghoniem, A.F. , Impact of Finite-Rate Kinetics on Carbon Conversion in a Single-Stage Entrained Flow Gasifier with Coal-CO_2 Slurry Feed. *37th International Technical Conference on Clean Coal and Fuel Systems*, Clearwater, FL. USA, June 3-7, 2012.

3. Botero C., Field R.P., Herzog H.J. and Ghoniem, A.F. , Coal-CO_2 Slurry Feed for Pressurized Gasifiers: Slurry Preparation System Characterization and Economics. *Energy Procedia*, Volume 37, 2013.

4. Botero C., Field R.P., Herzog H.J. and Ghoniem, A.F., Impact of Finite-Rate Kinetics on Carbon Conversion in a Single-Stage Entrained Flow Gasifier with Coal-CO_2 Slurry Feed. *Applied Energy*, Volume 104, 2013.

5. Botero C., Field R.P., Herzog H.J. and Ghoniem, A.F. , On the Thermal and Kinetic Performance of a Coal-CO_2 Slurry-fed Gasifier: Optimization of CO_2 and H_2O Flow using CO_2 Skimming and Steam Injection. *38th International Technical Conference on Clean Coal and Fuel Systems*, Clearwater (FL), USA, June 2-6, 2013.

6. Botero C., Field R.P., Herzog H.J. and Ghoniem, A.F., The Phase Inversion-based Coal-CO_2 Slurry (PHICCOS) Feeding System: Technoeconomic Assessment using Coupled Multiscale Analysis. *International Journal of Greenhouse Gas Control*, Volume 18, 2013.

7. Botero C., Field R.P., Herzog H.J. and Ghoniem, A.F., Clean Syngas Production from Coal in a Plant with Coal-CO_2 Slurry Feed Based on the PHICCOS Feeding System: Effect of Process Uncertainty and Comparison with Commercial Technologies. *Manuscript in Preparation*, 2013.

List of Patents Based on this Thesis

1. Botero, C., Field, R. P., Herzog, H. J., Ghoniem, A. F., *Method for Preparing a Slurry of Pulverized Solid Material in Liquid or Supercritical Carbon Dioxide.* U.S. Patent Application No.: 61/712954, Filing Date: October, 2012

2. Botero, C., Field, R. P., Herzog, H. J., Ghoniem, A. F., *Method for Conveying a Solid to a Dense, High Pressure State via Phase Inversion with Carbon Dioxide* U.S. Patent Application No.: 61/829321, Filing Date: June, 2013